(2)

NAVAL POSTGRADUATE SCHOOL

Monterey, California

THESIS

APPLICATIONS OF MODERN CONTROL THEORY SYNTHESIS TO A SUPER-AUGMENTED AIRCRAFT

by

Walter L. Rogers

June 1989

Thesis Advisor: Prof. D. J. Collins

UNCLASSIFIED
SECURITY CLASSIFICATION OF THIS PAGE

REPORT DOCUMENTATION PAGE

1a. REPORT SECURITY CLASSIFICATION Unclassified	1b RESTRICTIVE MARKINGS
2a. SECURITY CLASSIFICATION AUTHORITY	3. DISTRIBUTION/AVAILABILITY OF REPORT Approved for public release; distribution is unlimited.
2b. DECLASSIFICATION/DOWNGRADING SCHEDULE	
4. PERFORMING ORGANIZATION REPORT NUMBER(S)	5. MONITORING ORGANIZATION REPORT NUMBER(S)
6a NAME OF PERFORMING ORGANIZATION Naval Postgraduate School 6b OFFICE SYMBOL (If applicable) 31	7a NAME OF MONITORING ORGANIZATION Naval Postgraduate School
6c. ADDRESS (City, State, and ZIP Code) Monterey, CA 93943-5000	7b. ADDRESS (City, State, and ZIP Code) Monterey, CA 93943-5000
8a. NAME OF FUNDING/SPONSORING ORGANIZATION 8b OFFICE SYMBOL (If applicable)	9. PROCUREMENT INSTRUMENT IDENTIFICATION NUMBER
8c. ADDRESS (City, State, and ZIP Code)	10. SOURCE OF FUNDING NUMBERS PROGRAM ELEMENT NO. / PROJECT NO. / TASK NO / WORK UNIT ACCESSION NO.

11. TITLE (Include Security Classification)
Applications of Modern Control Theory Synthesis to a Super-Augmented Aircraft

12. PERSONAL AUTHOR(S)
Rogers, Walter L.

13a. TYPE OF REPORT	13b TIME COVERED	14 DATE OF REPORT (Year, Month, Day)	15 PAGE COUNT
Master's Thesis	FROM _____ TO _____	1989, June	167

16 SUPPLEMENTARY NOTATION The views expressed in this thesis are those of the author and do not reflect the official policy or position of the Department of Defense or the U.S. Government.

17 COSATI CODES		
FIELD	GROUP	SUB-GROUP

18. SUBJECT TERMS (Continue on reverse if necessary and identify by block number)
Modern Control Theory, H infinity Control Theory, H2 Control Theory, Multivariable Robustness, X-29 Controller Synthesis, Super-Augmented Aircraft,

19 ABSTRACT (Continue on reverse if necessary and identify by block number)

The singular value Bode plot of return difference and loop gain matrices have emerged as useful indicators of multivariable robustness. The H_∞ and H_2 control theories provide a systematic procedure for shaping the singular value loop gains of a multivariable feedback control system.

It is shown that H_∞ control theory, using specified performance objectives and stability constraints, is effective in synthesizing a stabilizing controller for the statically unstable longitudinal dynamics of the X-29. H_∞ control synthesis also demonstrates a good ability to cope with a true multivariable design problem such as the multiple, independently controlled surfaces of a super-maneuverable aircraft. However, it is also shown that the control surface deflections and control rates necessary to effect the

20 DISTRIBUTION/AVAILABILITY OF ABSTRACT	21. ABSTRACT SECURITY CLASSIFICATION
☒ UNCLASSIFIED/UNLIMITED ☐ SAME AS RPT ☐ DTIC USERS	Unclassified
22a NAME OF RESPONSIBLE INDIVIDUAL Dr. D. J. Collins	22b TELEPHONE (Include Area Code) (408) 646-2628 / 22c. OFFICE SYMBOL 67Co

DD FORM 1473, 84 MAR 83 APR edition may be used until exhausted
All other editions are obsolete

SECURITY CLASSIFICATION OF THIS PAGE
UNCLASSIFIED

BLOCK #18 (CONT)

Feedback Properties of a Multivariable Feedback Control System, H infinity Small Gain Problem

BLOCK #19 (CONT)

specified performance levels exceed the performance capabilities of the X-29's actuators.

A work-around to the limited actuator performance is provided by penalizing the control input vector more heavily during the problem formulation. This approach, while reducing the actuator performance requirements, results in a limited-performance X-29.

Approved for public release; distribution is unlimited.

APPLICATIONS OF MODERN CONTROL THEORY SYNTHESIS TO A SUPER-AUGMENTED AIRCRAFT

by

Walter L. Rogers
Lieutenant Commander, United States Navy
B.S., Florida Institute of Technology, 1973

Submitted in partial fulfillment of the requirements for the degree of

MASTER OF SCIENCE IN AERONAUTICAL ENGINEERING

from the

NAVAL POSTGRADUATE SCHOOL
June 1989

Author: _____
Walter L. Rogers

Approved by: _____
D. J. Collins, Thesis Advisor

_____
J. P. Hauser, Second Reader

_____
E. Roberts Wood, Chairman, Department of Aeronautics and Astronautics

_____
Gordon E. Schacher, Dean of Science and Engineering

ABSTRACT

The singular value Bode plot of return difference and loop gain matrices have emerged as useful indicators of multivariable robustness. The H_∞ and H_2 control theories provide a systematic procedure for shaping the singular value loop gains of a multivariable feedback control system.

It is shown that H_∞ control theory, using specified performance objectives and stability constraints, is effective in synthesizing a stabilizing controller for the statically unstable longitudinal dynamics of the X-29. H_∞ control synthesis also demonstrates a good ability to cope with a true multivariable design problem such as the multiple, independently controlled surfaces of a super-maneuverable aircraft. However, it is also shown that the control surface deflections and control rates necessary to effect the specified performance levels exceed the performance capabilities of the X-29's actuators.

A work-around to the limited actuator performance is provided by penalizing the control input vector more heavily during the problem formulation. This approach, while reducing the actuator performance requirements, results in a limited-performance X-29.

TABLE OF CONTENTS

LIST OF TABLES

LIST OF FIGURES

ACKNOWLEDGMENTS

One justifiably experiences considerable satisfaction, as well as a tremendous relief, upon the completion of a thesis. Unfortunately, one is often too busy or too involved during the course of the thesis to thank those who contributed. But now as the pace slows and the final signatures are collected, it is time that I give the proper recognition and express my appreciation to the friends and associates who have provided advice, assistance, and direction.

A special thank you goes to Professor Dan Collins, my thesis advisor, who suggested the topic of this thesis and provided the right amount of guidance and direction. His support was a key to its successful completion.

A thank you is also extended to Professor Jim Hauser who served as the second reader to this document, and to Professor Art Schoenstadt of the NPS Mathematics Department. Professor Schoenstadt's generous help provided me an understanding of the mathematical theory underlying H_∞ control synthesis.

I also wish to express my gratitude to LCDR Tom McKannon who dealt with the "system" in procuring the computer hardware needed for this study, and to LT Russ Scott who unwittingly became a sounding board for my thoughts and ideas. Russ's only mistake was to occupy an adjacent computer work station throughout the course of this study.

A most sincere thank you must go to June Melody, my friend, my love, my wife. Without her constant support, encouragement, and love this thesis could not have been realized.

I. INTRODUCTION

System performance, specifically a system's response to input commands, is of primary concern in the design of a feedback controller. Of equal importance in controller synthesis are stability margin and the remaining performance characterizations such as disturbance attenuation and sensitivity. Stability margin is a relative measure of a control system's stability, i.e., defining the smallest perturbation or modeling error that will cause the control system to become unstable. Disturbance attenuation and sensitivity refer to a control system's ability to reduce or limit the effects of disturbances and plant variation, respectively, on the plant outputs. The analysis of single-input single-output (SISO) systems has the advantage of classical techniques, including Nyquist diagrams, Bode plots, and root locus plots, to measure the gain and phase margins and system performance. Attempts have been made to extend these classical SISO theories to the multi-input multi-output (MIMO) case. Often, however, these multivariable generalizations do not accurately represent the stability margin and performance characterizations of the MIMO system. A prime example is the multivariable generalization of the Nyquist Theorem. Although the stability of a MIMO system can

be determined from a multivariable Nyquist diagram, the classical gain and phase margins are not meaningful.

It has, therefore, become necessary to redefine the measures of multivariable stability margin and system performance. In recent years a number of control theorists, including Doyle, Safonov, MacFarlane, and Lehtomaki among others, have conducted considerable research on the analysis of multivariable system robustness [Refs. 1, 2, 3, 4, 5]. As a result of renewed concern with such multivariable feedback issues as stability margin, disturbance attenuation, and sensitivity, singular value Bode plots of return difference and loop gain matrices have emerged as useful frequency domain indicators of multivariable robustness [Refs. 1, 3]. The term robust or good robustness is used to describe a multivariable feedback control system characterized by a large stability margin, good disturbance attenuation, and low sensitivity [Ref. 3].

The development of H_∞, frequency-weighted linear quadratic guassian (LQG) (or H_2), and LQG loop transfer recovery control theories, as well as the numerical optimization technique investigated by Gordon [Ref. 6], have made singular value loop shaping a reasonable if not routine procedure. By singular value loop shaping is meant the purposeful manipulation of a feedback control system's loop gains over a specified frequency bandwidth in order to improve performance and stability margins. H_∞ and H_2 theories provide direct, reliable

techniques for synthesizing a controller which satisfies singular value loop shaping specifications. The LQG loop transfer recovery theory provides a less direct yet effective means of achieving singular value loop shaping requirements. The numerical optimization procedure is a relatively direct design method which manipulates the system feedback gains as design variables [Ref. 6:p. 4]. This manipulation is conducted such that singular value loop shaping requirements are met. [Ref. 7]

Most published H_∞ design examples have been textbook studies [Ref. 8]. It is the purpose of this thesis to assess the effectiveness of H_∞ control theory in synthesizing a stabilizing controller for a reduced order, linearized model of the X-29 longitudinal dynamics. Chapter II discusses multivariable feedback properties, the role of the return difference matrix in evaluating these feedback properties, and singular value loop shaping. H_∞ control theory and design implementation are presented in Chapter III. The results of the H_∞ synthesis of a controller for the X-29 longitudinal dynamics are discussed in Chapter IV. Conclusions are presented in the Chapter V.

II. FEEDBACK PROPERTIES OF MULTIVARIABLE SYSTEMS

The feedback properties of a linear system include stability and stability margin, sensitivity to plant and controller variations, and disturbance attenuation. These are the same system properties used in the Introduction to define the robustness of a multivariable feedback system, and can be altered only through the use of feedback. The characterization of a system's response to commands is omitted from this list of feedback properties since command response can be altered by prefiltering of the command signal. That is, feedback is not required for improving command response. This is not to imply that command response can not be controlled through feedback. However, purposeful manipulation of command response is best performed in the feedforward path. [Ref. 3]

Throughout this thesis, vectors are denoted by bold lower case letters while matrices are indicated by bold upper case letters.

A. RETURN DIFFERENCE MATRIX

The return difference matrix is fundamental in the measure of a system's feedback properties and, therefore, to its robustness. Originally associated with SISO systems, the return difference concept has been extended to a MIMO generalization as discussed by Doyle and Safonov [Refs. 1, 3].

Consider the feedback configuration presented in Figure 2.1, and let $\mathbf{G}(s)$ and $\mathbf{F}(s)$ be matrices of time invariant transfer functions for the system plant and controller, respectively. With the loop broken at the plant output, the transfer matrix

$$\mathbf{I} + \mathbf{G}(s)\mathbf{F}(s) \tag{2.1}$$

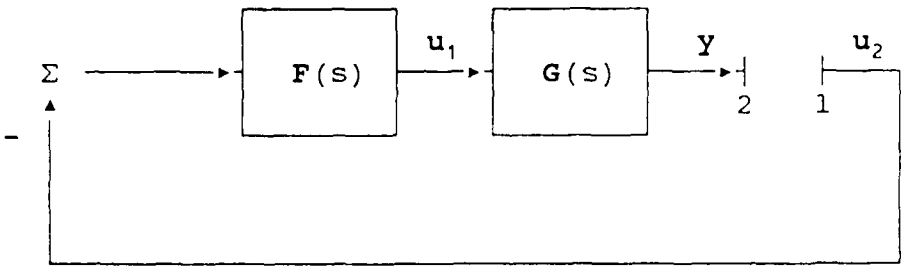

Figure 2.1 Return Difference Illustration

is referred to as the output return difference matrix. This definition is more apparent if an external input vector $\mathbf{u}_2$ is injected at point 1 of the loop. The transformed signal $\mathbf{y}$ returned at point 2 is

$$\mathbf{y}(s) = -\mathbf{G}(s)\mathbf{F}(s)\mathbf{u}_2(s), \tag{2.2}$$

and the difference between the injected input and the returned output vector is

$$\mathbf{u}_2(s) - \mathbf{y}(s) = [\mathbf{I} + \mathbf{G}(s)\mathbf{F}(s)]\mathbf{u}_2(s). \tag{2.3}$$

If this loop is broken at the plant input, the resulting input return difference matrix is

$$\mathbf{I} + \mathbf{F}(s)\mathbf{G}(s). \tag{2.4}$$

The inverse-return difference matrices are defined for the output and input nodes as

$$\mathbf{I} + (\mathbf{G}(s)\mathbf{F}(s))^{-1} \tag{2.5}$$

and

$$\mathbf{I} + (\mathbf{F}(s)\mathbf{G}(s))^{-1}, \tag{2.6}$$

respectively. Finally, the associated output and input loop gain matrices, also called return-ratio matrices, are

$$\mathbf{G}(s)\mathbf{F}(s) \tag{2.7}$$

and

$$\mathbf{F}(s)\mathbf{G}(s), \tag{2.8}$$

respectively. [Refs. 4, 9:p. 45]

B. MATRIX NORMS AND SINGULAR VALUES

The quantification of feedback qualities is necessary so that alternative feedback designs can be directly compared in the selection of an optimal design. To quantify the feedback

properties of a system, a frequency-dependent, scalar measure of the return difference matrix size is required. For SISO systems the appropriate measure of the return difference matrix is its magnitude, i.e., $|1 + g(j\omega)f(j\omega)|$. This is recognized as the distance to the critical point of the SISO Nyquist diagram for additive perturbation, and is a measure of the relative stability of the system.

The notion of matrix size is extended to multivariable systems through matrix norms. The spectral norm, routinely used in the analysis of MIMO systems, is defined as

$$\|\mathbf{A}\|_2 = \max_i \lambda_i^{1/2}(\mathbf{A}^H\mathbf{A}) = \sigma_{max}(\mathbf{A}) \tag{2.9}$$

where λ_i is the i^{th} eigenvalue of $\mathbf{A}^H\mathbf{A}$, and $\mathbf{A}^H$ refers to the complex conjugate transpose of matrix $\mathbf{A}$. The singular values of a complex nxn matrix $\mathbf{A}$, denoted $\sigma_i(\mathbf{A})$, are the non-negative square roots of the eigenvalues of $\mathbf{A}^H\mathbf{A}$, that is

$$\sigma_i(\mathbf{A}) = \lambda_i^{1/2}(\mathbf{A}^H\mathbf{A}) \tag{2.10}$$

where $\sigma_1 \geq \sigma_2 \geq \ldots \geq \sigma_n$. The maximum and minimum singular values of $\mathbf{A}$ are denoted by σ_{max} and σ_{min}, respectively.

Some useful properties of matrix singular values are [Ref. 5]:

1. $\sigma_{max}(\mathbf{A}) = \max_{\mathbf{x}} \dfrac{\|\mathbf{Ax}\|_2}{\|\mathbf{x}\|_2}$

2. $\sigma_{min}(\mathbf{A}) = \min_{\mathbf{x}} \dfrac{\|\mathbf{Ax}\|_2}{\|\mathbf{x}\|_2}$

3. $\sigma_{min}(\mathbf{A}) \leq |\lambda_i(\mathbf{A})| \leq \sigma_{max}(\mathbf{A})$

4. if $\mathbf{A}^{-1}$ exists, $\sigma_{min}(\mathbf{A}) = \dfrac{1}{\sigma_{max}(\mathbf{A}^{-1})}$ and $\sigma_{max}(\mathbf{A}) = \dfrac{1}{\sigma_{min}(\mathbf{A}^{-1})}$

5. $\sigma_{max}(\alpha\mathbf{A}) = |\alpha|\sigma_{max}(\mathbf{A})$

6. $\sigma_{max}(\mathbf{A} + \mathbf{B}) \leq \sigma_{max}(\mathbf{A}) + \sigma_{max}(\mathbf{B})$

7. $\sigma_{max}(\mathbf{AB}) \leq \sigma_{max}(\mathbf{A})\sigma_{max}(\mathbf{B})$

8. $\max\{\sigma_{max}(\mathbf{A}), \sigma_{max}(\mathbf{B})\} \leq \sigma_{max}([\mathbf{AB}])$
$\leq \sqrt{2}\ \max\{\sigma_{max}(\mathbf{A}), \sigma_{max}(\mathbf{B})\}.$

Properties 1 and 2 are significant as they establish the maximum and minimum gains of the matrix, respectively. The minimum singular value, property 2, is also used to measure a matrix's nearness to singularity. Finally, the multivariable generalization of return difference matrix size is

$$\sigma_i[\mathbf{I} + \mathbf{G}(j\omega)\mathbf{F}(j\omega)] \tag{2.11}$$

or

$$\sigma_i[\mathbf{I} + (\mathbf{G}(j\omega)\mathbf{F}(j\omega))^{-1}] \tag{2.12}$$

for additive and multiplicative perturbations, respectively. The significance of Equations (2.11) and (2.12) will be fully explored in the following section.

C. MULTIVARIABLE ROBUSTNESS AND SINGULAR VALUE LOOP SHAPING

Large loop gains, i.e., $\mathbf{G}(s)\mathbf{F}(s) >> 1$, are necessary to ensure good performance from a feedback control system.

However, the need for a system's tolerance to plant uncertainties restricts the frequency range over which the loop gains are permitted to be large. This tolerance to uncertainties, or modeling errors, is a measure of a system's relative stability. Therefore, the design of a feedback control system requires a trade-off between performance and stability robustness. These concepts are fully developed in this section.

Consider the multivariable feedback control system presented in Figure 2.2. Included are the transfer function matrices for the plant, $\mathbf{G}(s)$, and stabilizing controller, $\mathbf{F}(s)$, which are driven by the command, $\mathbf{r}$, disturbance, $\mathbf{d}$, and sensor noise, η, vectors. In this configuration, $\mathbf{d}$ is represented as the equivalent disturbance at the controlled or output variable vector, $\mathbf{y}$ [Ref. 9:pp. 168-174]. The feedback properties of this system, i.e., the multivariable stability margins and performance, can be measured using the closed loop transfer function matrices from the driving inputs, $\mathbf{r}$, $\mathbf{d}$, and η, to each of the outputs, $\mathbf{y}$ and the control vector, $\mathbf{u}$. Namely, these matrices are

$$\mathbf{S}(s) = [\mathbf{I} + \mathbf{G}(s)\mathbf{F}(s)]^{-1} \tag{2.13}$$

$$\mathbf{T}(s) = \mathbf{G}(s)\mathbf{F}(s)[\mathbf{I} + \mathbf{G}(s)\mathbf{F}(s)]^{-1} = \mathbf{I} - \mathbf{S}(s) \tag{2.14}$$

and

$$\mathbf{N}(s) = \mathbf{F}(s)[\mathbf{I} + \mathbf{G}(s)\mathbf{F}(s)]^{-1} \tag{2.15}$$

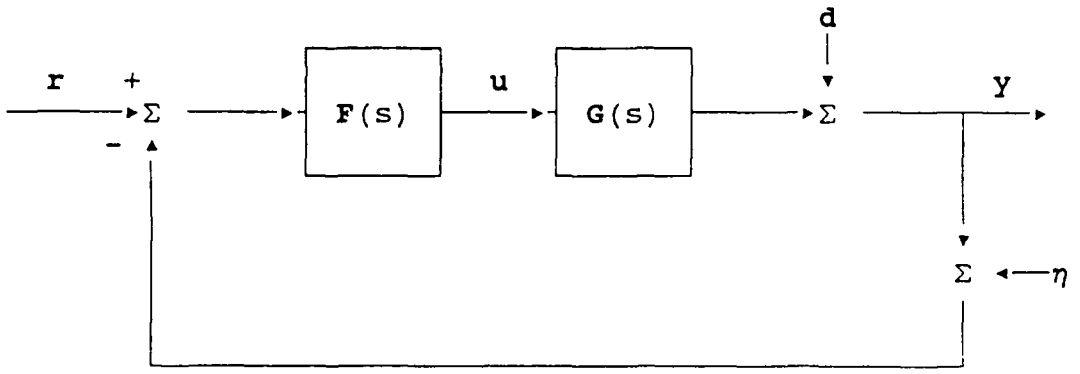

Figure 2.2 Feedback Control System

where **S**(s), the sensitivity function, represents the transfer function matrix from **d** to **y**, **T**(s), the complementary sensitivity function, represents the transfer function matrix from **r** or $-\eta$ to **y**, and **N**(S) represents the transfer function matrix from **r** to **u** [Ref. 7]. The fundamental relationships between system performance and the above matrices can be realized by the following representations:

1. input-output behavior [Ref. 1]:

$$\mathbf{Y}(s) = \mathbf{G}(s)\mathbf{F}(s)[\mathbf{I} + \mathbf{G}(s)\mathbf{F}(s)]^{-1}(\mathbf{r}-\eta) + [\mathbf{I} + \mathbf{G}(s)\mathbf{F}(s)]^{-1}\mathbf{d} \tag{2.16}$$

$$\begin{aligned}\mathbf{e} &= \mathbf{r}-\mathbf{y} \\ &= [\mathbf{I} + \mathbf{G}(s)\mathbf{F}(s)]^{-1}(\mathbf{r}-\mathbf{d}) + \mathbf{G}(s)\mathbf{F}(s)[\mathbf{I} + \mathbf{G}(s)\mathbf{F}(s)]^{-1}\eta \\ &= \mathbf{S}(s)(\mathbf{r}-\mathbf{d}) + \mathbf{T}(s)\eta\end{aligned} \tag{2.17}$$

2. system sensitivity to variations [Ref. 9:p. 180]:

$$\Delta \mathbf{T}(S) = [\mathbf{I} + \mathbf{G}(s)\mathbf{F}(s)]^{-1}\Delta \mathbf{G}(s)\mathbf{F}(s)[\mathbf{I} + \mathbf{G}(s)\mathbf{F}(s)]^{-1}$$

$$= \mathbf{S}(s)\Delta \mathbf{G}(s)\mathbf{N}(s). \tag{2.18}$$

In Equation (2.18), $\Delta \mathbf{T}(s)$ denotes the changes in the closed loop system as caused by plant variations or additive uncertainties, $\Delta \mathbf{G}(s)$, where

$$\hat{\mathbf{G}}(s) = \Delta \mathbf{G}(s) + \mathbf{G}(s). \tag{2.19}$$

Equation (2.17) shows that system errors resulting from commands and disturbances can be made small by making the sensitivity function small or the return difference matrix, $[\mathbf{I} + \mathbf{G}(s)\mathbf{F}(s)]$, large. Equation (2.18) shows that closed loop changes, or loop sensitivity, is improved under the same conditions provided $\hat{\mathbf{G}}(s) \approx \mathbf{G}(s)$ [Ref. 9:p. 180]. Thus, the disturbance and sensitivity performance objectives of a multivariable feedback system can be represented in the following manner using the matrix singular values previously discussed:

$$\sigma_{max}[\mathbf{I} + \mathbf{G}(j\omega)\mathbf{F}(j\omega)]^{-1} \leq |W_1^{-1}(j\omega)| \tag{2.20}$$

or equivalently, using singular value property 4,

$$\sigma_{min}[\mathbf{I} + \mathbf{G}(j\omega)\mathbf{F}(j\omega)] \geq |W_1(j\omega)| \tag{2.21}$$

where $|W_1(j\omega)|$ is a scalar function representing the desired disturbance attenuation and sensitivity factor. Equation (2.21) states that good feedback performance is achieved with

large loop gains. This follows from the fact that the size of the return difference matrix approximates the loop gains whenever the loop gains are large:

$$\sigma_{min}[\mathbf{I} + \mathbf{G}(s)\mathbf{F}(s)] \approx \sigma_{min}(\mathbf{G}(s)\mathbf{F}(s) \tag{2.22}$$

for

$$\sigma_{min}(\mathbf{G}(s)\mathbf{F}(s)) >> 1. \text{ [Refs. 1, 7]}$$

While large loop gains over a specified frequency range improve system performance with respect to disturbances and plant variations, they cause increased errors for large sensor noise inputs, η. As seen in Equation (2.16), large loop gains result in $\mathbf{G}(s)\mathbf{F}(s)[\mathbf{I} + \mathbf{G}(s)\mathbf{F}(s)]^{-1}$, i.e., $\mathbf{T}(s)$, near one. Therefore, sensor noise is passed through to the system outputs over the frequencies that the loop gains are large. It is obvious that a performance tradeoff must be made in the feedback design. [Refs. 1, 9:pp. 174-178]

A more crucial limitation to high loop gains results from the need for tolerance to uncertainties. These uncertainties are due to deviations of the physical plant from its linear, time invariant model, and restrict the frequency range over which the loop gains may be large. The magnitude of the tolerance to these uncertainties is a measure of the stability margin enjoyed by the system. Representation of unstructured uncertainty, that uncertainty which is characterized solely by its magnitude, depends on the errors the model is expected to make. However, a common method of representation is the

multiplicative form. In this form, the true plant matrix $\hat{\mathbf{G}}(j\omega)$ is given as

$$\hat{\mathbf{G}}(j\omega) = \mathbf{G}(j\omega)[\mathbf{I} + \mathbf{E}_m(j\omega)] \tag{2.23}$$

with

$$\mathbf{E}_m(j\omega) = \mathbf{G}^{-1}(j\omega)[\hat{\mathbf{G}}(j\omega) - \mathbf{G}(j\omega)]$$

and

$$\sigma_{max}(\mathbf{E}_m(j\omega)) < |W_3(j\omega)| \qquad \forall\ \omega \geq 0$$

where $\mathbf{E}_m(j\omega)$ is the relative (multiplicative) modeling error, $\mathbf{G}(j\omega)$ the nominal plant, and $|W_3(j\omega)|$ a scalar function which serves as an upper bound on the relative error. That is, $|W_3(j\omega)|$ represents the size of the largest multiplicative modeling error anticipated for the respective frequency ω. The use of multiplicative error is preferable over absolute (additive) modeling error, denoted by Equation (2.19), since relative uncertainty applies equally to the compensated system $\mathbf{G}(s)\mathbf{F}(s)$ and the raw plant $\mathbf{G}(s)$. This is not the case with absolute modeling error. [Refs. 1, 5:pp. 73-85 and Refs. 7, 10:pp. 19-22]

The properties of the bounding function $|W_3(j\omega)|$ are such that it is small ($<< 1$) at low frequencies and increases to one and above at higher frequencies (Figure 2.3). The maximum frequency ω at which the bounding function is less than or equal to unity (the crossover frequency) is referred to as the multiplicative robust frequency, and is denoted by ω_{rm}. As will be discussed later, this frequency provides an upper

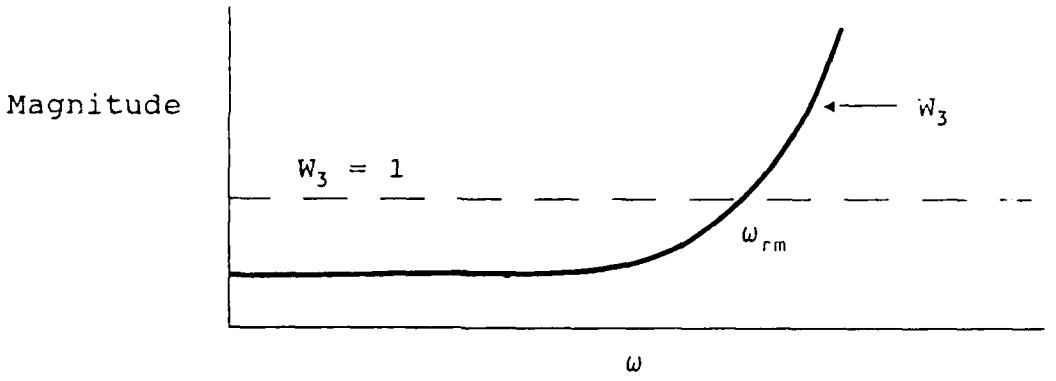

Figure 2.3 Properties of the Relative Error Bounding Function

constraint on the frequency band of the control system. A final comment concerning $|W_3(j\omega)|$ is that this bound assumes a worst case for the magnitude of the unstructured uncertainty that applies to all system loops. [Refs. 1, 7]

Given the nominal plant model $\mathbf{G}(s)$, the performance objectives, and knowledge of the unstructured uncertainties, the problem is to synthesize a controller such that [Ref. 1]

1. the feedback control system, $\mathbf{G}(s)\mathbf{F}(s)[\mathbf{I} + \mathbf{G}(s)\mathbf{F}(s)]^{-1}$, is stable,
2. the stability margin is sufficient to cause stability of the actual feedback control system, $\hat{\mathbf{G}}(s)\mathbf{F}(s)[\mathbf{I} + \hat{\mathbf{G}}(s)\mathbf{F}(s)]^{-1}$, for the largest anticipated relative error, $\mathbf{E}_m(s)$, and
3. the performance objectives are achieved considering the largest anticipated $\mathbf{E}_m(s)$.

These three conditions can be viewed as performance and stability margin specifications in terms of singular value loop shaping requirements [Ref. 7].

Condition 1 requires fulfillment of the multivariable generalization of the Nyquist Theorem [Ref. 5:p. 59 and Ref. 6:p. 27]. The satisfaction of condition 2 is assured if and only if

$$\sigma_{max}\{\mathbf{G}(j\omega)\mathbf{F}(j\omega)[\mathbf{I} + \mathbf{G}(j\omega)\mathbf{F}(j\omega)]^{-1}\} < |W_3^{-1}(j\omega)| \qquad (2.24)$$

or equivalently

$$\sigma_{min}[\mathbf{I} + (\mathbf{G}(j\omega)\mathbf{F}(j\omega))^{-1}] > |W_3(j\omega)|. \qquad (2.25)$$

Equation (2.24) states that in order for a feedback system to be stability robust, its loop gains must be small when the unstructured uncertainty magnitudes are large, i.e., $|W_3(j\omega)| >> 1$. This follows from the fact that the complementary sensitivity function $\mathbf{T}(s)$ approximates the loop gain as the loop gain becomes small:

$$\sigma_{max}\{\mathbf{G}(s)\mathbf{F}(s)[\mathbf{I} + \mathbf{G}(s)\mathbf{F}(s)]^{-1}\} \approx \sigma_{max}(\mathbf{G}(s)\mathbf{F}(s)) \qquad (2.26)$$

for

$$\sigma_{max}(\mathbf{G}(s)\mathbf{F}(s)) << 1.$$

[Refs. 1, 5:pp. 76-84 and Ref. 7]

Equations (2.20) and (2.21) have already established the requirements for meeting the performance objectives as stipulated in condition 3. However, to account for the relative modeling error encountered at low frequencies,

$|W_1(j\omega)|$ is now considered to include the unstructured uncertainty for $|W_3(j\omega)| < 1$. Therefore, restating the performance objective requirement:

$$\sigma_{min}[\mathbf{I} + \mathbf{G}(j\omega)\mathbf{F}(j\omega)] \geq |W_1(j\omega)| \tag{2.27}$$

for all ω such that

$$|W_3(j\omega)| < 1 \text{ and } \sigma_{min}(\mathbf{G}(j\omega)\mathbf{F}(j\omega)) >> 1$$

[Refs. 1, 7].

The singular value loop shaping requirements established by the performance and stability bounds are depicted in Figure 2.4. The design of a MIMO feedback control system can be summarized as the use of high loop gains at low frequencies

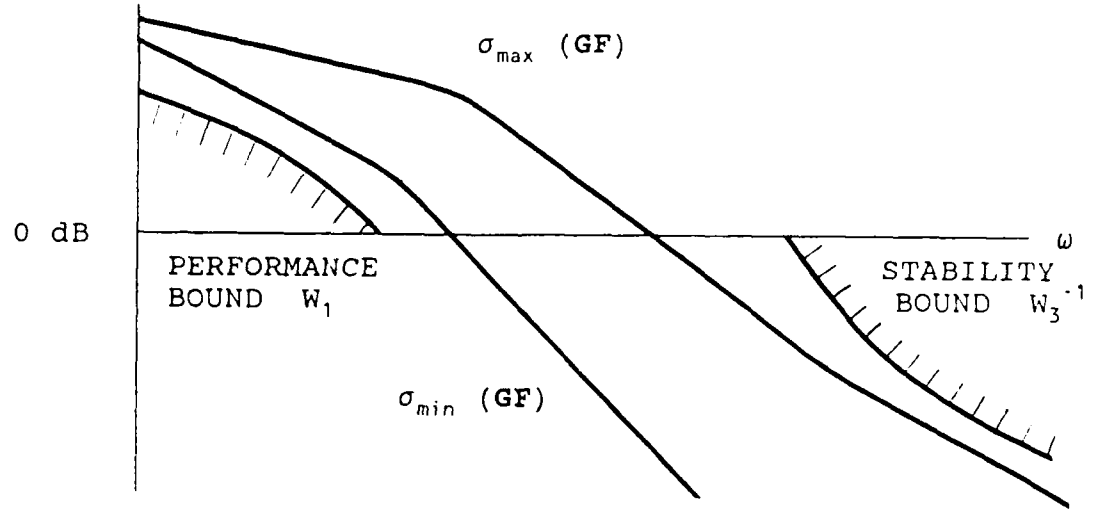

Figure 2.4 MIMO Singular Value Loop Shaping Requirements

where performance requirements are defined and the use of low loop gains at high frequencies where stability robustness constraints lie. While the low frequency bound on the loop gains is desirable to meet specified performance objectives, the upper frequency bound is a hard requirement. For if the uncertainties are unstructured and Equation (2.25) is violated, then there exists a modeling error $\mathbf{E}_m(s)$ permitted by Equation (2.23) for which the system is unstable [Ref. 1].

As alluded to earlier, the robust frequency ω_{rm} is an upper bound on the bandwidth ω_B of a multivariable control system where ω_B is the frequency range for $\sigma_{min}(\hat{\mathbf{G}}(s)\mathbf{F}(s)) >> 1$. Thus permitting the loop gain to be greater than unity above ω_{rm} violates the required condition for stability of the actual feedback system. The roll-off (attenuation) rate of the loop gains, $\sigma_{min}(\mathbf{G}(s)\mathbf{F}(s))$ and $\sigma_{max}(\mathbf{G}(s)\mathbf{F}(s))$, determine the severity of the ω_B constraint. Large roll-off rates permit a wider ω_B. However, steep loop gain roll-offs are achieved at the expense of small $\sigma_{min}[\mathbf{I} + \mathbf{G}(s)\mathbf{F}(s)]$ and $\sigma_{min}[\mathbf{I} + (\mathbf{G}(s)\mathbf{F}(s))^{-1}]$ values when the loop gains are approximately unity. This means both performance and stability margins are poor at the loop gain cross over frequency. This correlates with classical SISO analysis that suggests the slope of Bode magnitude plots be more gradual than -40 dB/decade to ensure an adequate stability margin [Ref. 11:p. 433]. [Refs. 1, 7]

To better appreciate the design tradeoff required to achieve both performance objectives and stability robustness

requirements, it is helpful to observe the algebraic relationship between $\sigma_{min}[\mathbf{I} + \mathbf{G}(s)\mathbf{F}(s)]$ and $\sigma_{min}[\mathbf{I} + (\mathbf{G}(s)\mathbf{F}(s))^{-1}]$. From Equations (2.25) and (2.27) it is seen that the bounds on low and high frequency unstructured uncertainty, as well as that on performance, become less restrictive if both of the above singular values can be made as large as possible. Unfortunately, these return difference quantities are related so both cannot be made large simultaneously:

$$[\mathbf{I} + \mathbf{G}(s)\mathbf{F}(s)]^{-1} + [\mathbf{I} + (\mathbf{G}(s)\mathbf{F}(s))^{-1}]^{-1} \equiv \mathbf{I} \qquad (2.28)$$

equivalently

$$\mathbf{S}(s) + \mathbf{T}(s) \equiv \mathbf{I}.$$

The bounded region of Figure 2.5 shows the allowable values of the minimum singular values of the return difference and the inverse return difference matrices. When the loop gains are large, i.e., $\sigma_{min}(\mathbf{G}(s)\mathbf{F}(s)) >> 1$ at low ω,

$$\sigma_{min}[\mathbf{I} + \mathbf{G}(s)\mathbf{F}(s)] >> 1 \quad \text{or} \quad \mathbf{S}(s) \longrightarrow \mathbf{0}$$

while

$$\sigma_{min}[\mathbf{I} + (\mathbf{G}(s)\mathbf{F}(s))^{-1}] \longrightarrow 1 \quad \text{or} \quad \mathbf{T}(s) \longrightarrow \mathbf{I}$$

Conversely, when the loop gains are small, i.e., $\sigma_{max}(\mathbf{G}(s)\mathbf{F}(s)) < 1$ at high ω,

$$\sigma_{min}[\mathbf{I} + (\mathbf{G}(s)\mathbf{F}(s))^{-1}] >> 1 \quad \text{or} \quad \mathbf{T}(s) \longrightarrow \mathbf{0}$$

while

$$\sigma_{min}[\mathbf{I} + \mathbf{G}(s)\mathbf{F}(s)] \longrightarrow 1 \quad \text{or} \quad \mathbf{S}(s) \longrightarrow \mathbf{I}.$$

[Refs. 3, 5:pp. 89-91]

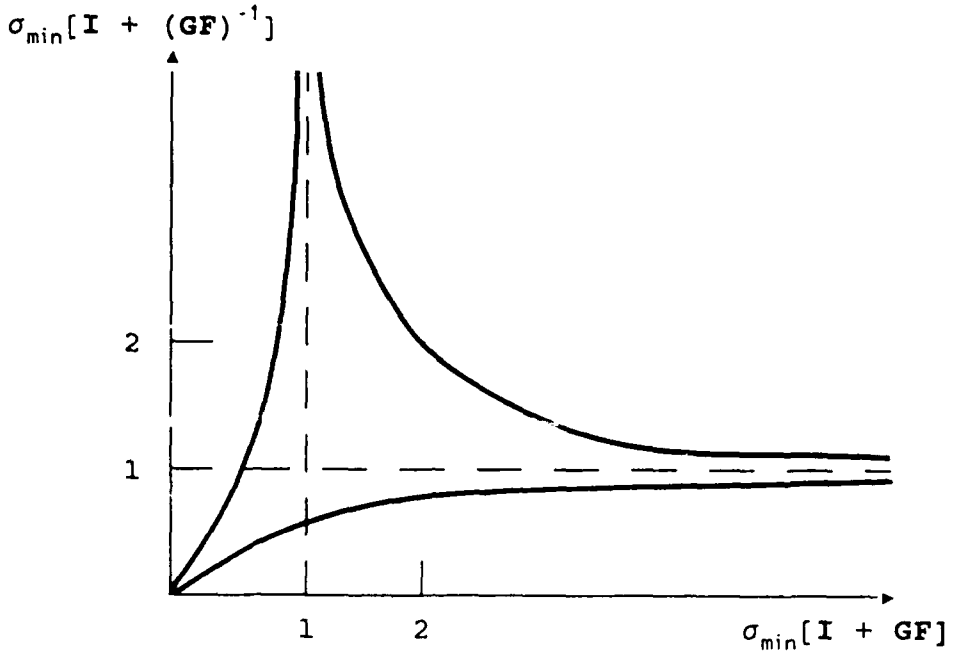

Figure 2.5 Relationship Between $\sigma_{min}[\mathbf{I} + \mathbf{G}(s)\mathbf{F}(s)]$ and $\sigma_{min}[\mathbf{I} + (\mathbf{G}(s)\mathbf{F}(s))^{-1}]$

Finally, while $\sigma_{min}[\mathbf{I} + \mathbf{G}(s)\mathbf{F}(s)]$ and $\sigma_{min}[\mathbf{I} + (\mathbf{G}(s)\mathbf{F}(s))^{-1}]$ are multivarible generalizations of SISO performance and stability margin concepts, it is important to note that these multivariable return difference singular values measure the uncertainty tolerances at the plant outputs only (see the development of Equations (2.1) and (2.4)). In order to measure the performance and relative stability at the plant inputs, it is necessary to evaluate $\sigma_{min}[\mathbf{I} + \mathbf{F}(s)\mathbf{G}(s)]$ and $\sigma_{min}[\mathbf{I} + (\mathbf{F}(s)\mathbf{G}(s)^{-1}]$.

III. H_∞ CONTROL DESIGN

H_∞ control theory provides a very powerful and direct, iterative procedure for the synthesis of a feedback controller designed to meet singular value loop shaping requirements. Its capabilities extend across the full range of performance and stability loop shaping objectives that can be formulated within the singular value Bode plot framework. The standard configuration of an H_∞ problem is presented in Figure 3.1. The objective is to design a controller **F**(s) in state space form that stabilizes the augmented plant **P**(s) while satisfying specified performance and stability margin requirements as discussed in Chapter II. [Refs. 8, 12]

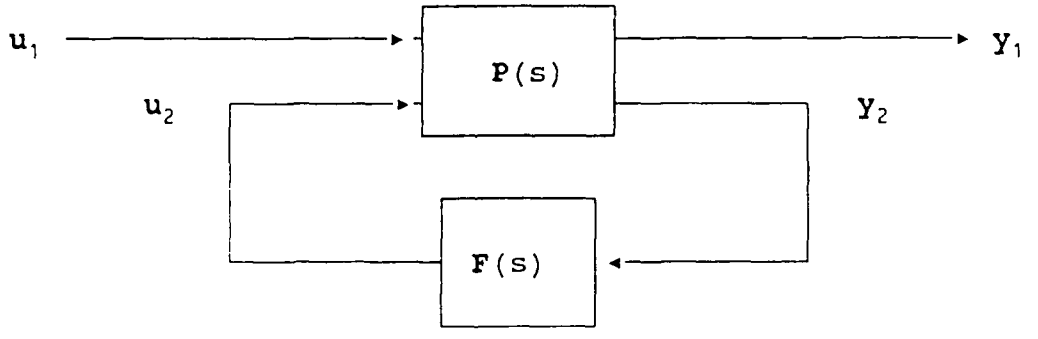

Figure 3.1 Standard H_∞ Small Gain Problem

This chapter briefly discusses the three major steps in the H_∞ design procedure; the formulation of an H_∞ control system problem, the selection of weightings to achieve design objectives, and the synthesis of an H_∞ controller [Ref. 8]. In addition, a comparison is made among LQG, H_2, and H_∞ control syntheses.

A. PROBLEM FORMULATION

Consider the problem of designing a feedback controller $\mathbf{F}(s)$ for a multivariable plant with a transfer function matrix $\mathbf{G}(s)$ where $\mathbf{G}(s) = \mathbf{C}(s\mathbf{I}-\mathbf{A})^{-1}\mathbf{B}+\mathbf{D}$. The requirements for performance and stability robustness are defined by Equations (2.27) and (2.25), respectively, in terms of the system's return difference matrices. These requirements are redefined here in terms of the sensitivity $\mathbf{S}(s)$ and complementary sensitivity $\mathbf{T}(s)$ functions as

$$\frac{1}{\sigma_{max}(\mathbf{S}(j\omega))} \geq |\gamma W_1(j\omega)| \qquad \omega < \underline{\omega}_c \tag{3.1}$$

and

$$\sigma_{max}(\mathbf{T}(j\omega)) \leq |W_3^{-1}(j\omega)| \qquad \omega > \overline{\omega}_c \tag{3.2}$$

where $\underline{\omega}_c$ and $\overline{\omega}_c$ are the respective 0 dB crossover frequencies of γW_1 and W_3^{-1} and γ is a positive scalar constant. Gamma (γ) is added to facilitate iterative attenuation of the sensitivity function during design implementation. [Ref. 12]

Within the framework of H_∞ control theory, the requirements of Equations (3.1) and (3.2) can be combined into a single infinity norm specification as

$$\|\mathbf{T}_{y1u1}\|_\infty \leq 1 \tag{3.3}$$

where

$$\mathbf{T}_{y1u1} = \begin{bmatrix} \gamma \mathbf{W}_1 \mathbf{S} \\ \mathbf{W}_3 \mathbf{T} \end{bmatrix}. \tag{3.4}$$

$\mathbf{T}_{y1u1}(s)$ is the closed loop transfer function of the augmented feedback control system shown in Figure 3.1 from input $\mathbf{u}_1$ to output $\mathbf{y}_1$. The H_∞ norm of a transfer function matrix $\mathbf{K}(s)$ is denoted in terms of its frequency-dependent singular values $\sigma_i(j\omega)$ as

$$\|\mathbf{K}\|_\infty = \sup_\omega \sigma_{max}(\mathbf{K}(j\omega)) \tag{3.5}$$

where "sup" or "supreme" refers to the least upper bound [Ref. 7]. Therefore, the H_∞ small gain problem $\|\mathbf{T}_{y1u1}\|_\infty \leq 1$ states that the maximum singular value of $\mathbf{T}_{y1u1}(s)$, as defined in Equation (2.9), is to be less than or equal to one for all frequencies ω. As a consequence of singular value property 8, i.e.,

$$\frac{1}{\sqrt{2}} \sigma_{max}\begin{bmatrix} \mathbf{A} \\ \mathbf{B} \end{bmatrix} \leq \max\{\sigma_{max}(\mathbf{A}), \sigma_{max}(\mathbf{B})\} \leq \sigma_{max}\begin{bmatrix} \mathbf{A} \\ \mathbf{B} \end{bmatrix},$$

Equation (3.4) approximates the requirements of Equations (3.1) and (3.2) to within a factor of $\sqrt{2}$, or 3 dB [Refs. 7, 12].

The development of $\mathbf{T}_{y1u1}$ can be shown with the plant $\mathbf{G}(s)$ augmented by the weighting functions γW_1, W_2, and W_3 as presented in Figure 3.2. As evident from the figure, γW_1 weights the error signal $\mathbf{e}$, W_2 weights the control inputs $\mathbf{u}$, and W_3 weights the plant outputs $\mathbf{y}_{1c}$. The area enclosed by asterisks is $\mathbf{P}(s)$, the augmented plant, previously shown in Figure 3.1 where

$$\mathbf{P}(s) = \left[\begin{array}{c|c} \mathbf{P}_{11} & \mathbf{P}_{12} \\ \hline \mathbf{P}_{21} & \mathbf{P}_{22} \end{array}\right] \tag{3.6}$$

or

$$\mathbf{P}(s) = \left[\begin{array}{c|c} \gamma\mathbf{W}_1 & -\gamma\mathbf{W}_1\mathbf{G} \\ 0 & \mathbf{W}_2 \\ 0 & \mathbf{W}_3\mathbf{G} \\ \hline \mathbf{I} & -\mathbf{G} \end{array}\right]. \tag{3.7}$$

Given an input/output relationship of the augmented plant $\mathbf{P}(s)$ as

$$\left[\begin{array}{c} \mathbf{y}_1 \\ \mathbf{y}_2 \end{array}\right] = \left[\begin{array}{c|c} \mathbf{P}_{11} & \mathbf{P}_{12} \\ \hline \mathbf{P}_{21} & \mathbf{P}_{22} \end{array}\right] \left[\begin{array}{c} \mathbf{u}_1 \\ \mathbf{u}_2 \end{array}\right], \tag{3.8}$$

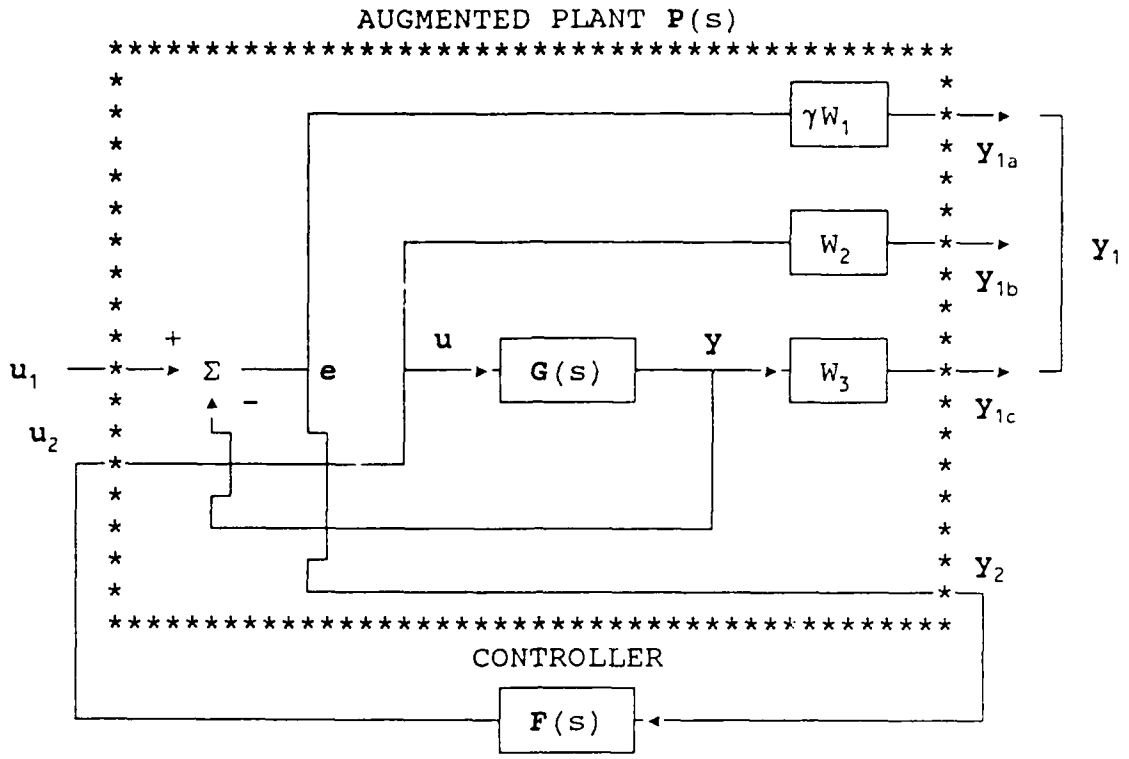

Figure 3.2 Augmented Plant

it is seen that

$$\mathbf{y}_1 = \mathbf{P}_{11}\mathbf{u}_1 + \mathbf{P}_{12}\mathbf{u}_2$$

and

$$\mathbf{y}_2 = \mathbf{P}_{21}\mathbf{u}_1 + \mathbf{P}_{22}\mathbf{u}_2. \tag{3.9}$$

From Figure 3.2, $\mathbf{u}_2$ may be expressed as

$$\mathbf{u}_2 = \mathbf{F}\mathbf{y}_2 \tag{3.10}$$

permitting $\mathbf{y}_1$ to be written as

$$\mathbf{y}_1 = \mathbf{P}_{11}\mathbf{u}_1 + \mathbf{P}_{12}\mathbf{F}\mathbf{y}_2. \tag{3.11}$$

Putting $\mathbf{y}_2$ in terms of $\mathbf{u}_1$, $\mathbf{F}$, and $\mathbf{P}_{ij}$ and substituting into Equation (3.11) gives

$$\mathbf{T}_{y1u1} = \frac{\mathbf{y}_1}{\mathbf{u}_1} = \mathbf{P}_{11} + \mathbf{P}_{12}\mathbf{F}(\mathbf{I} - \mathbf{P}_{22}\mathbf{F})^{-1}\mathbf{P}_{21}. \tag{3.12}$$

Substitution of the appropriate $\mathbf{P}_{ij}$ elements from Equation (3.7) into Equation (3.12) results in

$$\mathbf{T}_{y1u1} = \begin{bmatrix} \gamma \mathbf{W}_1 \mathbf{S} \\ \mathbf{W}_2 \mathbf{N} \\ \mathbf{W}_3 \mathbf{T} \end{bmatrix}. \tag{3.13}$$

Ignoring the W_2 weighting function gives Equation (3.4). The W_2 function can be used to weight or penalize the control input $\mathbf{u}$ to the plant $\mathbf{G}(s)$.

The augmented plant $\mathbf{P}(s)$ has a state space realization of [Ref. 7]

$$\mathbf{P}(s) = \left[\begin{array}{c|cc} \mathbf{A} & \mathbf{B}_1 & \mathbf{B}_2 \\ \hline \mathbf{C}_1 & \mathbf{D}_{11} & \mathbf{D}_{12} \\ \mathbf{C}_2 & \mathbf{D}_{21} & \mathbf{D}_{22} \end{array}\right]. \tag{3.14}$$

By putting each weighting function and the plant $\mathbf{G}(s)$ from Figure 3.2 into standard state space form, i.e.,

$$\dot{\mathbf{x}} = \mathbf{Ax} + \mathbf{Bu}$$

$$\mathbf{y} = \mathbf{Cx} + \mathbf{Du},$$

Equation (3.14) may be represented as

$$\mathbf{P}(s) = \left[\begin{array}{cccc|c|c} \mathbf{A}_G & \mathbf{0} & \mathbf{0} & \mathbf{0} & \mathbf{0} & \mathbf{B}_G \\ -\mathbf{B}_{W1}\mathbf{C}_G & \mathbf{A}_{W1} & \mathbf{0} & \mathbf{0} & \mathbf{B}_{W1} & -\mathbf{B}_{W1}\mathbf{D}_G \\ \mathbf{0} & \mathbf{0} & \mathbf{A}_{W2} & \mathbf{0} & \mathbf{0} & \mathbf{B}_{W2} \\ \mathbf{B}_{W3}\mathbf{C}_G & \mathbf{0} & \mathbf{0} & \mathbf{A}_{W3} & \mathbf{0} & \mathbf{B}_{W3}\mathbf{D}_G \\ \hline -\mathbf{D}_{W1}\mathbf{C}_G & \mathbf{C}_{W} & \mathbf{0} & \mathbf{0} & \mathbf{D}_{W1} & -\mathbf{D}_{W1}\mathbf{D}_G \\ \mathbf{0} & \mathbf{0} & \mathbf{C}_{W2} & \mathbf{0} & \mathbf{0} & \mathbf{D}_{W2} \\ \mathbf{D}_{W3}\mathbf{C}_G & \mathbf{0} & \mathbf{0} & \mathbf{C}_{W3} & \mathbf{0} & \mathbf{D}_{W3}\mathbf{D}_G \\ \hline -\mathbf{C}_G & \mathbf{0} & \mathbf{0} & \mathbf{0} & \mathbf{I} & -\mathbf{D}_G \end{array}\right] . \tag{3.15}$$

As is apparent from Equation (3.4), the closed loop transfer function $\mathbf{T}_{y1u1}(s)$ is partitioned into submatrices representing the performance and stability robustness requirements. The weighting functions γW_1 and W_3 serve as low-pass or high-pass filters in order to emphasize or de-emphasize, as appropriate, the maximum singular values of $\mathbf{T}_{y1u1}(s)$. These weighting functions are applied over the range of frequencies necessary to achieve the desired performance objectives while meeting design constraints [Ref. 8].

Therefore, the control problem defined by the singular value loop shaping requirements of Equations (3.1) and (3.2)

is realized with the solution of the H_∞ small gain problem (Figure 3.1) [Ref. 7]:

> Given a transfer function matrix $\mathbf{P}(s)$, find a stabilizing controller $\mathbf{F}(s)$ such that the closed loop transfer function $\mathbf{T}_{y1u1}(s)$ is internally stable and its infinity norm is less than or equal to one:
>
> $$\|\mathbf{T}_{y1u1}(j\omega)\|_\infty \leq 1. \tag{3.3}$$

The compensated system shown in Figure 3.1 is said to be internally stable if the $\mathbf{A}$ matrix of the augmented plant $\mathbf{P}(s)$ is stable. In other words, with the external input $\mathbf{u}_1$ equal to zero, all states of the $\mathbf{P}(s)$ and $\mathbf{F}(s)$ transfer function matrices will asymptotically go to zero for any initial condition [Ref. 8]. As indicated by Francis [Ref. 13:pp.34-35], a sufficient condition to stabilize $\mathbf{P}(s)$ is for $\mathbf{F}(s)$ to stabilize $\mathbf{P}_{22}(s)$.

In general, the solution to the H_∞ small gain problem is not unique since a number of stabilizing controllers will satisfy Equation (3.3). Conversely, a solution to the small gain problem does not exist for every $\mathbf{P}(s)$ due to violation of well-posedness conditions or infeasible singular value Bode plot specifications. In order for an H_∞ stabilizing compensator to exist, it is necessary for $(\mathbf{A},\mathbf{B}_1)$ and $(\mathbf{A},\mathbf{B}_2)$ to be stabilizable and $(\mathbf{C}_1,\mathbf{A})$ and $(\mathbf{C}_2,\mathbf{A})$ to be detectable. Additionally, for the infinity norm specification of Equation (3.3) to be realized, $\mathbf{T}_{y1u1}(s)$ must have no eigenvalues on the imaginary $j\omega$ axis. If such poles exist then $\|\mathbf{T}_{y1u1}\|_\infty > 1$. Finally, it is necessary for the $\mathbf{D}_{12}$ and $\mathbf{D}_{21}^T$ submatrices of

Equation (3.14) to have full column rank. The $\mathbf{D}_{12}$ submatrix physically weights the plant's control inputs. That is, the matrix $[\mathbf{D}_{12}^T\mathbf{D}_{12}]$ is comparable to the LQG control weighting matrix **R** of the full state cost function. A full column rank $\mathbf{D}_{12}$ matrix ensures all control inputs are weighted, thereby eliminating infinite impulses. The W_2 weighting function can be used to ensure $\mathbf{D}_{12}$ is full column rank as is evident in the augmented plant **P**(s) state space realization, i.e., Equation (3.15). [Refs. 7, 14]

The software program used to solve the H_∞ control problem outlined in the following chapter is hinf which is included in the Matlab Robust-Control Toolbox package. Hinf employs a variant of a two Riccati formula of Doyle et al. The advantage of using hinf to solve the small gain problem is that the two Riccati formula eliminates the lengthy and numerically sensitive model reduction work characteristic of earlier algorithms. The H_∞ controller produced by hinf has the same number of states as the augmented plant **P**(s). [Ref. 7]

B. SELECTION OF WEIGHTS

The weighting functions γW_1 and W_3 are transfer function matrices whose diagonal elements are frequency-dependent constants. The size of these weighting matrices is consistent with the number of plant output states. As the weighting functions act as filters, their design parameters include

gain, corner frequency, attenuation, and order. The goal in the selection of these design parameters is to achieve small singular values of the sensitivity function $\mathbf{S}(s)$, i.e., large loop gains, over the broadest possible bandwidth subject to the constraints imposed by stability robustness, i.e., the W_3 design constraint. [Refs. 8, 12]

The weighting functions are directly associated with the physical characteristics of the feedback control system being designed. These characteristics include time domain specifications (rise time, settling time, and overshoot), performance bounds, and command response in the case of γW_1, magnitude of the control inputs in the case of W_2, and largest anticipated relative modeling error $\mathbf{E}_m(s)$ in the case of W_3. It should be understood that the resultant H_∞ controller is only optimal with respect to the γW_1, W_2, and W_3 weights selected. It is necessary, therefore, that the designer have a good insight into the physical capabilities of the system, including stability robustness constraints, to ensure that a reasonable H_∞ problem is posed. Postlethwaite [Ref. 8] suggests selecting a fixed weighting W_3 representing the stability robustness constraints, and as large a weighting γW_1 as possible representing system performance. The objective is to make the largest singular value of $\mathbf{S}(s)$ as small as possible over some operating frequency band by making γW_1 as large as possible over the same frequency band. This is done while satisfying Equation (3.3). The following

algorithm is recommended in choosing appropriate weights for the H_∞ control problem [Refs. 7, 8]:

1. Select the weight W_3 to represent the stability robustness (design) constraints.

2. Select the weight W_1 and set $\gamma=1$ to represent an initial guess of the performance objectives over the desired operating bandwidth. The γW_1 0 dB crossover frequency $\underline{\omega}_c$ must be less than the W_3 crossover frequency ω_c in order that the stability robustness constraint, Equation (3.2), is not violated.

3. Solve the small gain problem in search of a stabilizing controller that satisfies Equation (3.3), i.e., $\|\mathbf{T}_{y1u1}\|_\infty \leq 1$.

4. If $\|\mathbf{T}_{y1u1}\|_\infty < 1$, select a larger γ and repeat step 3.

5. Continue increasing γ until a stabilizing controller no longer exists that satisfies Equation (3.3), i.e., $\|\mathbf{T}_{y1u1}\|_\infty > 1$ or the stability robustness constraint, Equation (3.2), is violated.

6. If it is necessary to make the $\mathbf{D}_{12}$ submatrix full column rank, choose a W_2 weighting with an invertible **D** matrix, i.e., $W_2(s)=\epsilon\mathbf{I}$ where ϵ is any non-zero number. A W_2 weighting can also be used to regulate the magnitude of the control energy input to the system plant **G**(s). As the magnitude of ϵ is increased relative to γ, a larger weighting is placed upon the control inputs **u**. This results in a smaller control energy input to the plant **G**(s). Decreasing the magnitude of ϵ relative to γ has the opposite effect.

C. CONTROL SYNTHESIS

Once the design requirements are specified in terms of the weighting functions γW_1, W_2, and W_3, the H_∞ controller is calculated within a computer aided design environment. The procedure involves an iterative process accomplished by increasing the coefficient γ. Increasing γ, or decreasing

γ^{-1}, results in a smaller DC gain and higher $\underline{\omega}_c$ for $(\gamma W_1)^{-1}$. Therefore, the iterative increase of γ results in a continual suppression of the sensitivity function **S**(s) and a widening of the control bandwidth ω_B. This iteration is continued until the sensitivity function **S**(s) is forced against its upper constraint of $(\gamma W_1)^{-1}$ for $\omega<\underline{\omega}_c$ (Figure 3.3). Due to the

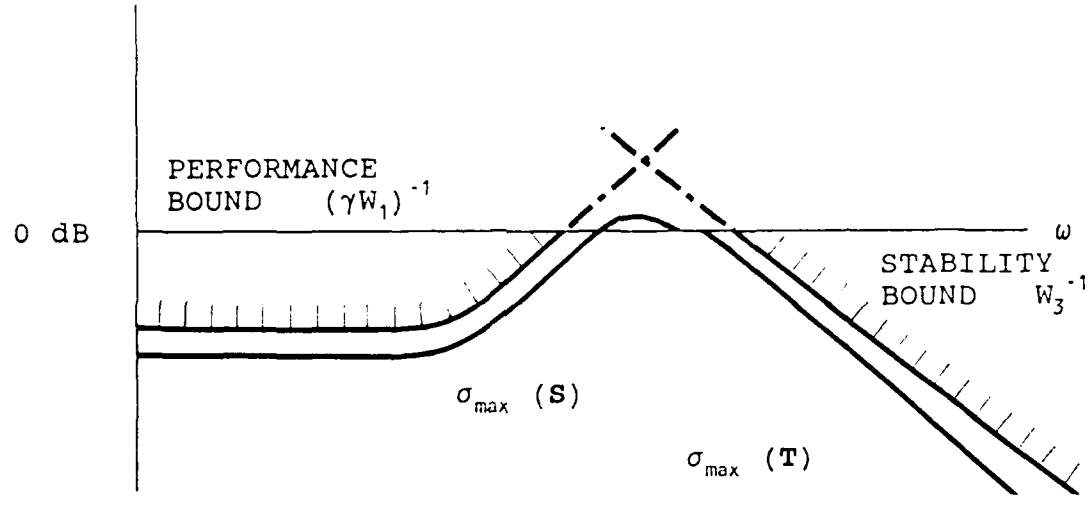

Figure 3.3 Singular Value Bode Plot of **S**, **T**, W_1^{-1}, and W_3^{-1}

relationship between the sensitivity function **S**(s) and complementary sensitivity function **T**(s), i.e., Equation (2.28), **T**(s) goes to **I** as **S**(s) goes to **0**. Therefore, increasing γ forces the complementary sensitivity function **T**(s) against its upper constraint of W_3^{-1} for $\omega>\overline{\omega}_c$ (Figure 3.3)

[Ref. 12]. Figure 3.4 presents a flow chart of the H_∞ iterative procedure [Ref. 7]. Augmentation of the plant G(s) with the weighting functions and presentation of the necessary singular value Bode plots are performed by separate M-files within the Matlab Robust-Control Toolbox package.

D. COMPARISON OF LQG, H_2, AND H_∞ CONTROL SYNTHESES

The intent of the following discussion is to provide an appreciation for the advantages of using H_∞ control synthesis over the use of other modern methodologies such as LQG and H_2 norm (also known as frequency-weighted LQG). This end will be accomplished by revealing the disadvantages and shortcomings of these latter two synthesis methods. Only a cursory discussion of the LQG and H_2 methods will be presented. Those unfamiliar with these methods are referred to the listed references for a more thorough explanation.

In the following discussion, reference to linear quadratic (LQ) regulators refers to those regulators with full state feedback. LQG refers to regulators that have output feedback and use a Kalman filter to provide state estimates for feedback. LQG problems involve the solution of two Riccati equations, one to solve for the optimal state feedback gain and a second to solve for the optimal filter gain.

It is well documented [Ref. 5:pp. 191-211] that linear quadratic (LQ) regulators possess guaranteed minimum gain and phase margins of -6 dB to ∞ and $\pm$60 degrees, respectively.

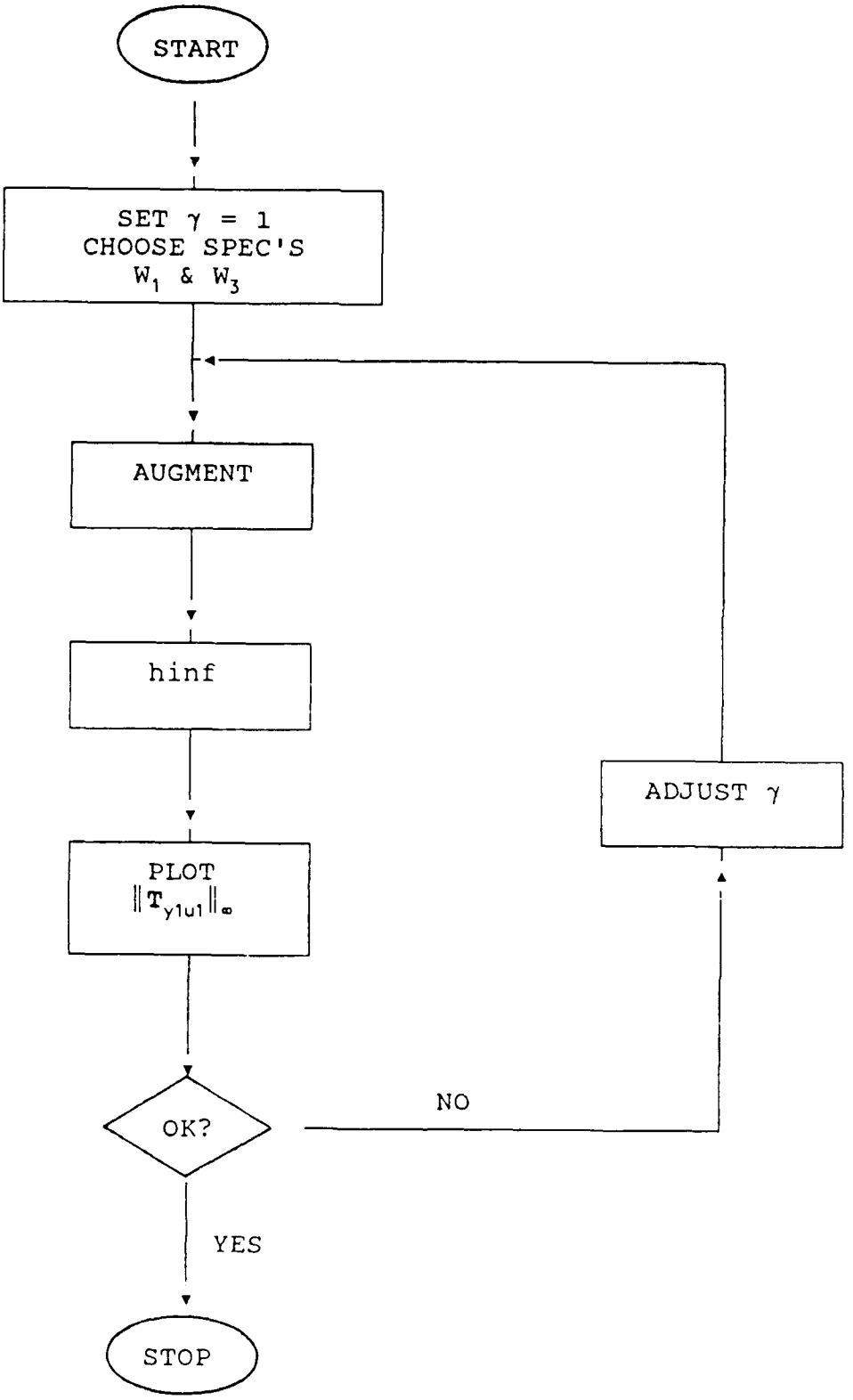

Figure 3.4 H_∞ Iterative Process

This is true for a diagonal control weighting matrix **R**. These guaranteed stability margins imply "desirable" loop gain properties which, as discussed in Chapter II, define system performance and stability robustness. Unfortunately, these LQ stability margins and associated loop gain properties do not necessarily apply at the plant inputs and outputs of LQG regulators. As discussed by Lehtomaki [Ref. 5:pp. 217-226], the Kalman filter is the dual of the LQ regulator and does possess the above guaranteed stability margins. The Kalman filter, therefore, possesses the desirable loop gain properties.

The standard LQG control system block diagram is presented in Figure 3.5. The points marked 2 and 3 represent the feedback control system input $\mathbf{F}(S)\mathbf{G}(s)$ and output $\mathbf{G}(s)\mathbf{F}(s)$ loop gain matrices, respectively. It is at these locations that the guaranteed stability margins of the LQ problem are desired. However, it is at the loop gain matrices of points 1 and 4, inside the Kalman filter loop, that the guaranteed stability robustness properties apply. This limitation to LQG robustness is caused by the Kalman filter's inability to account for modeling errors. That is, the Kalman filter models the nominal plant and not the actual plant as given in Equation (2.23). [Refs. 1, 5:pp. 217-226]

There are, however, two dual procedures that will adequately recover the loop gain properties at the plant input (point 2) or output (point 3) to approximate the loop gain

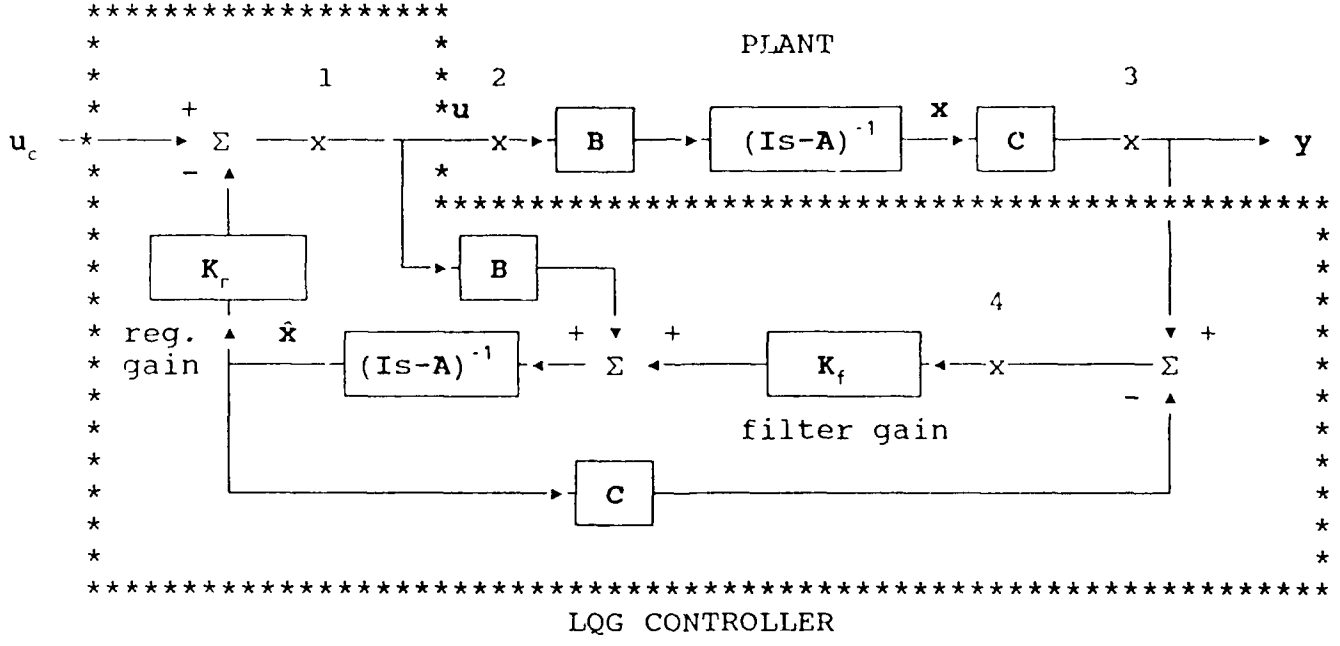

Figure 3.5 LQG Control System

functions at points 1 and 4, respectively. Each of these two procedures, referred to as "full-state loop transfer recovery," permits the recovery of desirable performance and stability robustness properties at the plant input or output as appropriate. A limitation to these recovery procedures is that they work only for a minimum phase plant **G**(s). An additional limitation is the loop gain recovery applies only at the input or output of the physical plant but not necessarily at both. As performance and stability robustness qualities are important at both the plant input and output, some design tradeoffs must be made. Finally, the regulator or Kalman filter gains necessary to effect the loop gain recovery at the plant input and output, respectively, are often very large and physically impractical. [Refs. 1, 5:pp. 226-229 and Ref. 7:pp. RR42-RR44]

A primary difference between LQG and H_∞ control syntheses is the absence of frequency-dependent shaping of the loop gains with the LQG methodology. Thus, H_∞ control synthesis provides the designer more control over the shaping of performance and stability robustness attributes due to the inclusion of the weighting functions γW_1 and W_3. H_2 control synthesis is a frequency-weighted LQG process that, like H_∞, uses the frequency-dependent γW_1, W_2, and W_3 weighting functions and augmented plant **P**(s). In the case of the H_2 control problem, however, the objective is to calculate a

stabilizing controller $\mathbf{F}(s)$ that minimizes the H_2 norm of the closed loop transfer function $\mathbf{T}_{y1u1}(s)$, that is [Ref. 7]

$$\min \|\mathbf{T}_{y1u1}\|_2$$

where

$$\|\mathbf{T}_{y1u1}\|_2 = \left[\int_{-\infty}^{\infty} \sum_{i=1}^{n} (\sigma_i(\mathbf{T}_{y1u1}(j\omega)))^2 \, d\omega \right]^{\frac{1}{2}}. \qquad (3.16)$$

Using the Matlab h2lqg M-file, the H_2 norm control problem is solved as a conventional LQG problem involving two Riccati equation solutions, one each for the full state regulator and Kalman filter optimal gains. The H_2 control problem formulation, weight selection, and synthesis format is identical to the H_∞ control problem. H_2 synthesis is often used with H_∞ synthesis as a first cut to determine the levels of performance achievable. Figure 3.6 presents a flow chart of the combined H_2/H_∞ synthesis process.

An interesting feature of the H_∞ two Riccati equation solution is that the resultant controller displays a separation structure similar to that observed in LQG or H_2 problems. That is, the algebraic Riccati equations provide solutions to what can be considered a suboptimal state feedback gain and a suboptimal filter gain. [Ref. 7]

Although H_2 synthesis shares the singular value loop shaping capabilities of the H_∞ procedure, the H_2 designed controller usually does not match the robustness levels attained by the H_∞ design. That is, an H_∞ designed controller

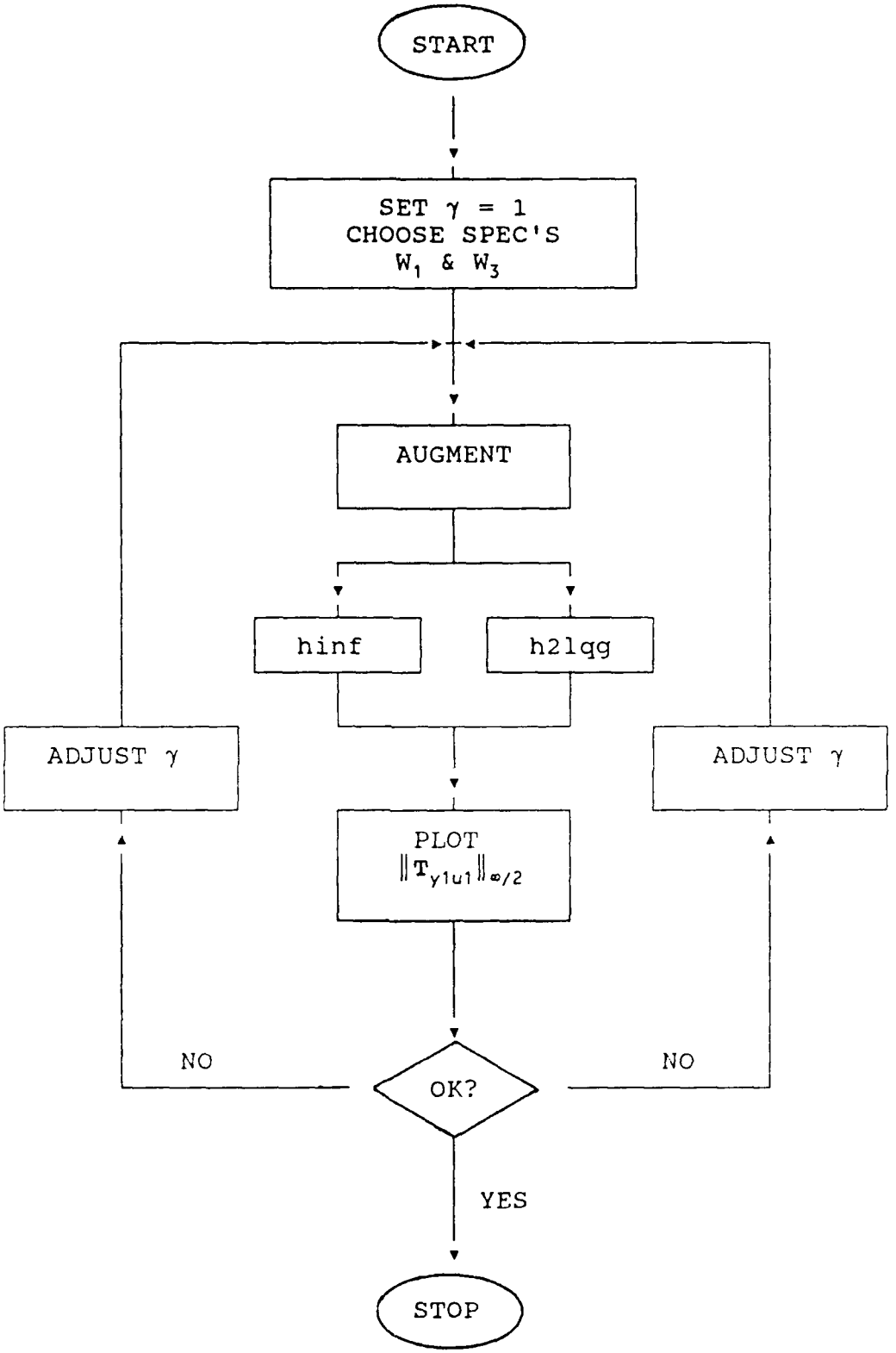

Figure 3.6 H_2/H_∞ Iterative Process

will, in general, provide a larger bandwidth of operation and greater disturbance and uncertainty attenuation within the stipulated stability constraints.

IV. X-29 H_∞ CONTROLLER SYNTHESIS

A challenging application of H_∞ control theory is the synthesis of a stabilizing controller for the longitudinal dynamics of the X-29. The X-29 is a technology demonstrator with a unique forward swept wing design that offers the advantages of improved maneuverability, better low speed handling, and reduced stall speeds. The X-29's longitudinal dynamics are designed with 35 per cent negative static stability margin [Ref. 15]. Unlike the advanced fighter model with an unstable phugoid mode used by Safonov [Ref. 7] to demonstrate H_2 and H_∞ methodology, the X-29 has an unstable short period mode, i.e., a real pole on the positive axis.

The X-29 controller synthesis was performed using Pro-Matlab and the Matlab Robust-Control Tool Box software. These application packages were run on a Sun 386i work station. The script files specifically written or modified for this problem are listed in Appendix A.

This chapter discusses the X-29 state space model, the H_∞ design objectives and specifications, the controller synthesis, and the design results including the aircraft's longitudinal responses to test inputs.

A. X-29 MODEL DESCRIPTION

The X-29 longitudinal dynamics model is that of the aircraft's analog reversion mode with the aircraft trimmed at .5 mach, 30,000 feet. An 83rd order model was reduced to a 14 state model that includes a short period approximation of the aircraft longitudinal dynamics, vertical velocity w and pitch rate q, and fourth order actuator dynamics for each of the three longitudinal control surfaces, i.e., the canards, flaps, and strakes. Eliminated from the 83rd order model were the flexible mode dynamics, aerodynamic lag terms, sensor dynamics, and notch filter.

Figure 4.1 presents the physical configuration of the open loop actuator/aircraft dynamics model. Some of the actuator gains shown in Figure 4.1 may have changed in the current aircraft configuration. For the purposes of this study, two separate commands, r_1 and r_2, are input to the three control surface actuators with r_1 controlling the canards and r_2 controlling the flaps and strakes. Although not truly representative of the X-29, this configuration provides multiple, independently controlled surfaces representative of a super-maneuverable aircraft. As will be seen, this configuration results in the synthesis of advanced control modes which are characteristic of super-maneuverable aircraft designs. The control inputs to the aircraft dynamics are the canards δ_c, the flaps δ_f, the strakes δ_s and their respective first and second derivatives. The measured outputs are the

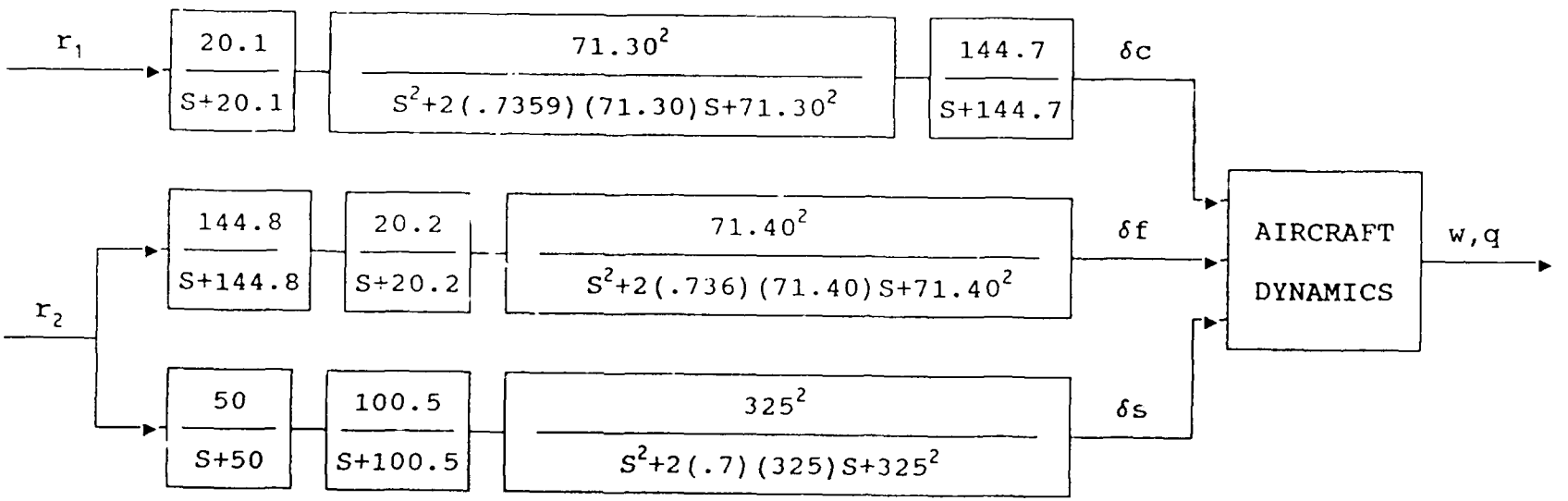

Figure 4.1 Uncompensated X-29 Open Loop Configuration

two aircraft states, w and q. Thus, the model has two inputs, two outputs, and 14 states.

The 14th order model was scaled in order to improve the numerical conditioning of its state space representation. In the scaling process the w state was transformed to angle-of-attack α, i.e., $\alpha = w/u_o$ where u_o is the initial forward velocity, and the units of the actuator third derivative states were transformed from rad/sec^3 to 1e+04 rad/sec^3. This scaling was effective in reducing the condition number of the system's A matrix from an order of magnitude of 10^{10} to 10^4.

The state space realization of the resultant 14 state linear model $\mathbf{G}(s) = \mathbf{C}(s\mathbf{I} - \mathbf{A})^{-1}\mathbf{B}+\mathbf{D}$ is presented in Appendix B. The order of the state variables, their description, and respective units are listed in Table 4.1. Finally, the open loop poles of the X-29 model are listed in Table 4.2. Note that the unstable short period mode has a real pole at 1.9550.

B. DESIGN OBJECTIVES

The singular value plot of the X-29 plant $\mathbf{G}(s)$ is presented in Figure 4.2 where the solid curve is $\sigma_{max}(\mathbf{G}(j\omega))$ and the dashed curve is $\sigma_{min}(\mathbf{G}(j\omega))$. The uncompensated X-29 model possesses poor disturbance attenuation, high sensitivity to variations and modeling errors, and a small control bandwidth ω_B as evidenced in Figure 4.2 by the small loop gains at the lower frequencies. These performance characterizations are to be improved by suppressing the

TABLE 4.1

ORDERED LIST OF THE UNCOMPENSATED X-29 MODEL STATES

State	Description	Units
α	angle-of-attack	rad
q	pitch rate	rad/sec
δ_c	canard control input	rad
δ_f	flap control input	rad
δ_s	strake control input	rad
$\dot{\delta}_c$	canard control rate	rad/sec
$\dot{\delta}_f$	flap control rate	rad/sec
$\dot{\delta}_s$	strake control rate	rad/sec
$\ddot{\delta}_c$	canard control accel.	rad/sec^2
$\ddot{\delta}_f$	flap control accel.	rad/sec^2
$\ddot{\delta}_s$	strake control accel.	rad/sec^2
$\dddot{\delta}_c$	canard control jerk	$1e+04\ rad/sec^3$
$\dddot{\delta}_f$	flap control jerk	$1e+04\ rad/sec^3$
$\dddot{\delta}_s$	strake control jerk	$1e+04\ rad/sec^3$

TABLE 4.2

UNCOMPENSATED X-29 OPEN LOOP POLES

-2.2746e+02 ± 2.3201e+02i
-1.4491e+02
-1.4455e+02
1.9550e+00
-1.0031e+02
-2.7155e+00
-5.2506e+01 ± 4.8410e+01i
-5.2518e+01 ± 4.8255e+01i
-5.0067e+01
-2.0172e+01
-2.0115e+01

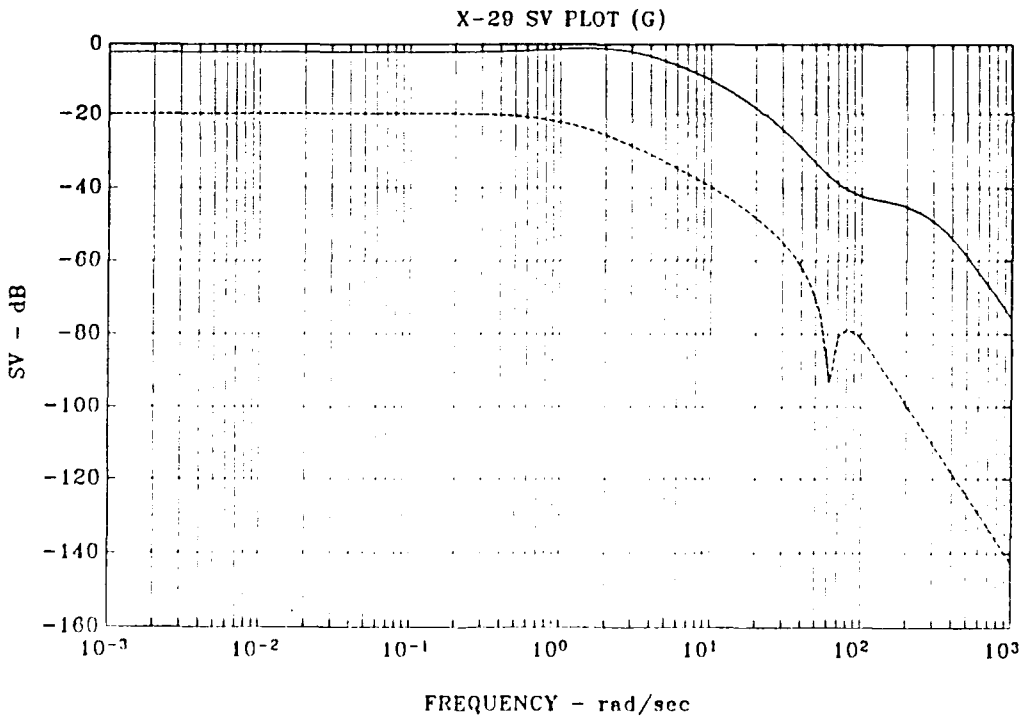

Figure 4.2 Singular Value Plot of the X-29 Plant G(s)

sensitivity function singular values $\sigma_i(\mathbf{S}(j\omega))$ as much as possible, i.e., making the loop gains as large as possible, over as wide a bandwidth as possible. These performance objectives must be performed within the bounds of the system's stability constraints. In this problem, it is necessary to attenuate the closed loop singular values of the complementary sensitivity function $\sigma_i(\mathbf{T}(j\omega))$ by 20 dB at frequencies beyond 100 rad/sec, and to exhibit a second order roll-off beyond 100 rad/sec. These stability requirements ensure that the X-29 system has sufficient stability margin to tolerate modeling errors or loop transfer function variations which could arise from the unmodeled flexible modes. These flexible modes are observed in the Bode plot of the 83rd order X-29 model (Figure 4.3) at the frequencies 100 rad/sec to 250 rad/sec. The second order roll-off also closely matches that of the open loop plant (Figure 4.2).

The following $(\gamma W_1)^{-1}(s)$, $W_2(s)$, and $W_3^{-1}(s)$ weighting functions were selected to meet the above performance objectives and stability constraints:

$$(\gamma W_1)^{-1}(s) = \gamma^{-1} * \frac{.01(100s + 1)}{.01s + 1} * \mathbf{I}_{(2 \times 2)}$$

$$W_2(s) = \left[\begin{array}{c|c} \mathbf{A} & \mathbf{B} \\ \hline \mathbf{C} & \mathbf{D} \end{array}\right] = -.001 * \mathbf{I}_{(4 \times 4)}$$

$$W_3^{-1}(s) = \frac{1000}{s^2} * \mathbf{I}_{(2 \times 2)} . \qquad (4.1)$$

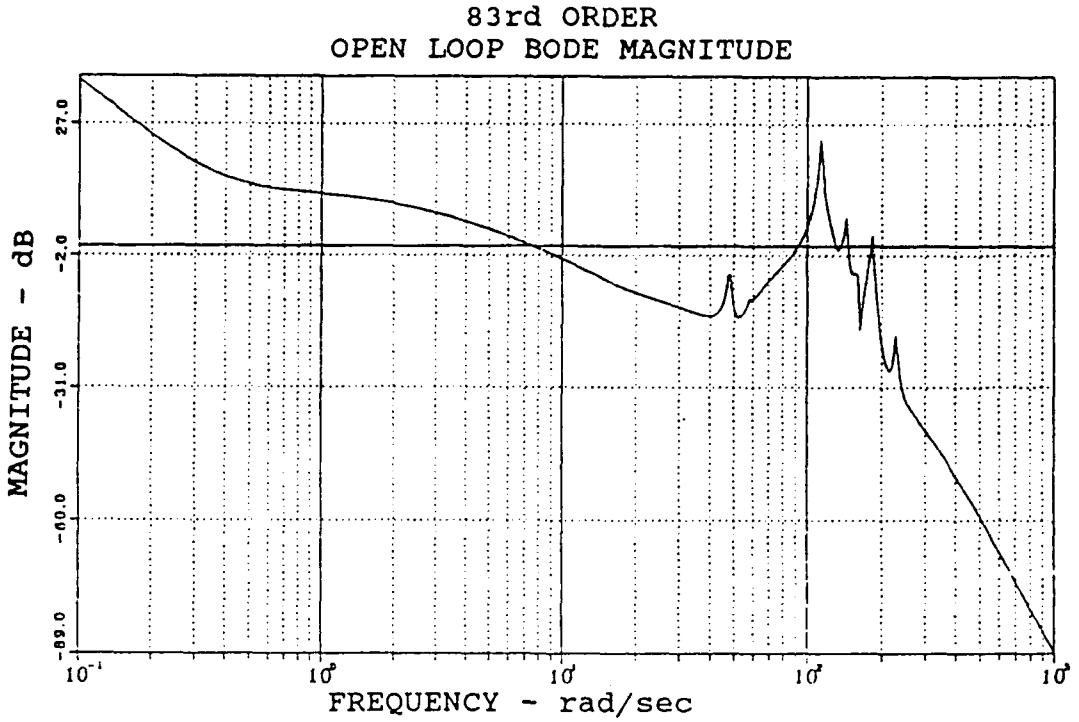

Figure 4.3 Open Loop Bode Plot of X-29 83rd Order Model

A plot of the H_∞ $W_1^{-1}(s)$ and $W_3^{-1}(s)$ weighting functions is shown in Figure 4.4. The $W_2(s)$ weighting is included to ensure the D_{12} submatrix of the augmented plant **P**(s) has full column rank (Equation (3.15)). This weighting function penalizes the control **u** input to the X-29 plant **G**(s) as shown in Figure 3.2. As the $W_3(s)$ weighting function is not proper, it has no state space realization. However, the term $W_3(s)$**G**(s) seen in the matrix representation of the augmented plant **P**(s) (Equation (3.7)) is proper and can be realized in the required state space form. The augx29.m script file listed in Appendix A performs the matrix calculations necessary for this realization. The results of this matrix manipulation are

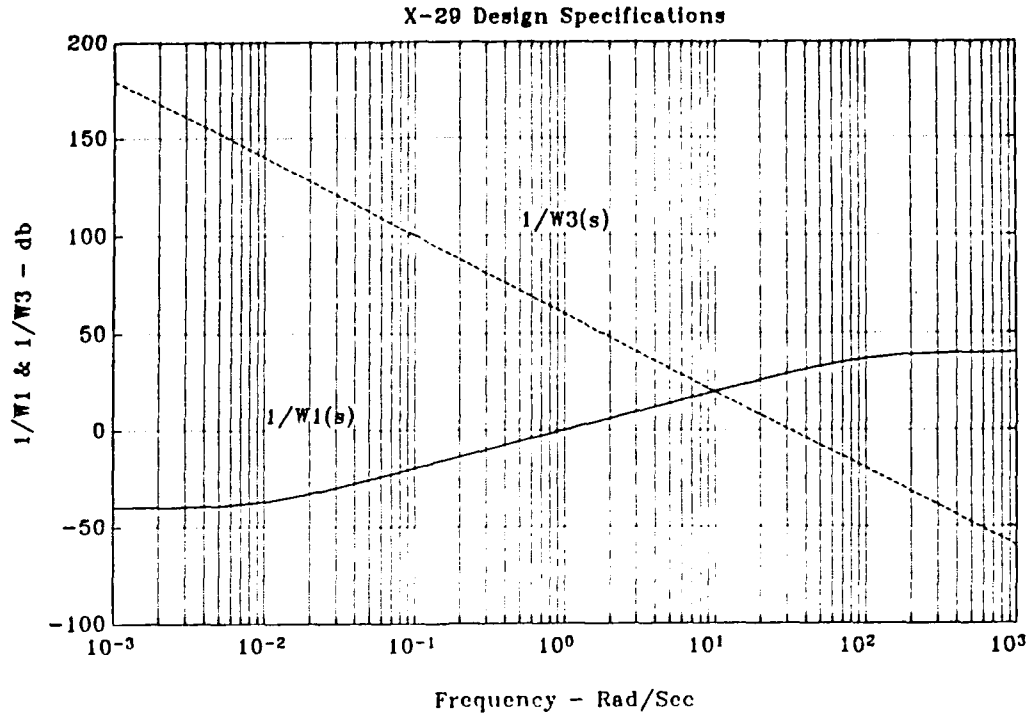

Figure 4.4 X-29 H_∞ Design Specifications

placed into the $D_{W3}C_G$ and $D_{W3}D_G$ terms of the augmented plant's C_1 and D_{12} submatrices, respectively, by the augx29pl.m script file (Appendix A).

The resultant X-29 augmented plant **P**(s) is an 18th order system with $W_1(s)$ and $W_2(s)$ each adding two states to the X-29 plant **G**(s). The $W_3(s)$ function does not add states to **G**(s) as a state space realization of this function does not exist. Using the two Riccati solution, H_2 and H_∞ synthesized controllers are the same size as the augmented plant **P**(s). As such, an 18th order X-29 controller is expected.

C. CONTROLLER SYNTHESIS

The H_2/H_∞ synthesis process outlined by Figure 3.6 was followed with the H_2 solution used as an initial indication of achievable performance levels. To ensure a well-posed H_2 problem, the upper corner frequency of the $W_1^{-1}(s)$ weighting function was removed by making the $W_1^{-1}(s)$ denominator a constant value. This ensured that the D_{11} submatrix of the augmented plant **P**(s) is **0** as required by H_2 control theory. A plot of the H_2 design specifications is presented in Figure 4.5.

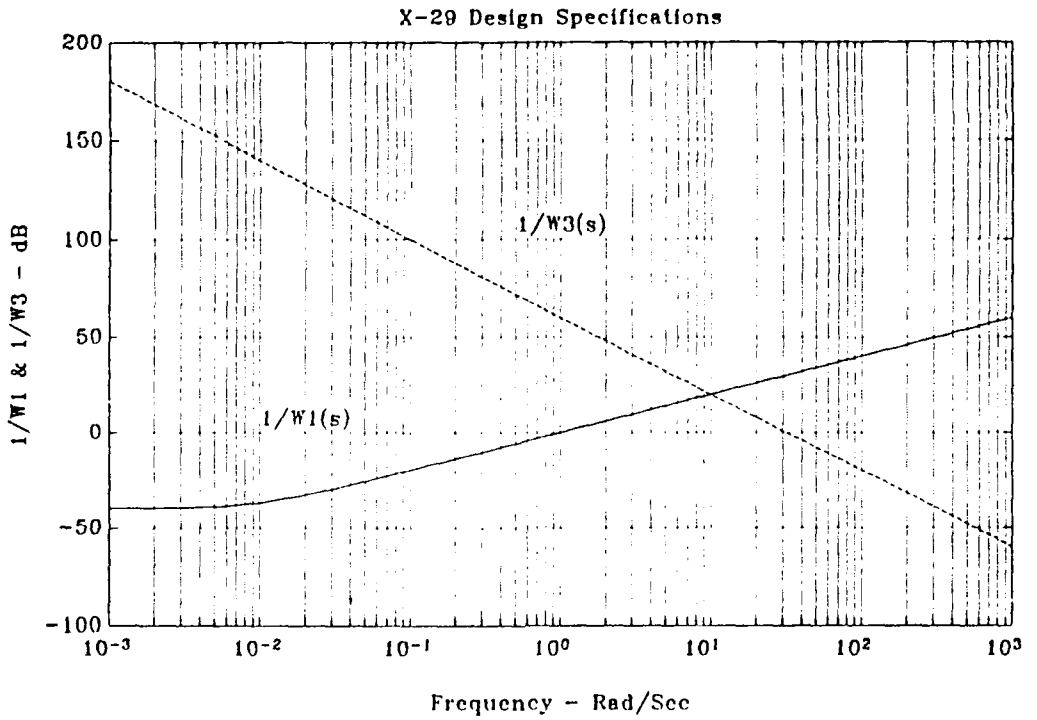

Figure 4.5 X-29 H_2 Design Specifications

Using the x29h2.m and x29hinf.m script files listed in Appendix A, solutions to the H_2 and the H_∞ small gain problems were obtained for increasing values of γ until:

1. For the H_2 solution, the cost function $\|\mathbf{T}_{y1u1}\|_2$ reached the "all pass limit", i.e., 0 dB.
2. For the H_∞ solution, no stabilizing controller satisfied the H_∞ small gain problem for a larger value of γ, i.e., no solution existed for a larger γ.

Figures 4.6 and 4.7 are singular value plots of the maximum (solid curve) and minimum (dashed curve) singular values of the H_2 cost function $\|\mathbf{T}_{y1u1}\|_2$ for γ values of one and 6.7, respectively. Figure 4.8 is an identical plot for the H_∞ cost function $\|\mathbf{T}_{y1u1}\|_\infty$ for a γ of 12.5. Figures 4.6 and 4.7 show that as γ increases from one to a maximum of 6.7 in the H_2 solution, the maximum singular value of $\|\mathbf{T}_{y1u1}\|_2$ increases to 0 dB. The H_2 solution pushes both $\|\mathbf{T}_{y1u1}\|_2$ singular values to within 2 dB of the "all pass limit" (Figure 4.7). However, with a maximum γ of 12.5, the H_∞ solution pushes the $\|\mathbf{T}_{y1u1}\|_\infty$ singular values to within .5 dB of the "all pass limit" (Figure 4.8). The significantly larger value of γ in the H_∞ solution indicates that a higher level of performance is achieved with the H_∞ solution compared to that reached by the H_2 solution.

Figures 4.9 through 4.11 are singular value plots of the sensitivity function $\mathbf{S}(s)$ and $(\gamma W_1)^{-1}(s)$ weighting function for the H_2 solution with γ values of one and 6.7, and the H_∞ solution with a γ of 12.5, respectively. The dotted curves

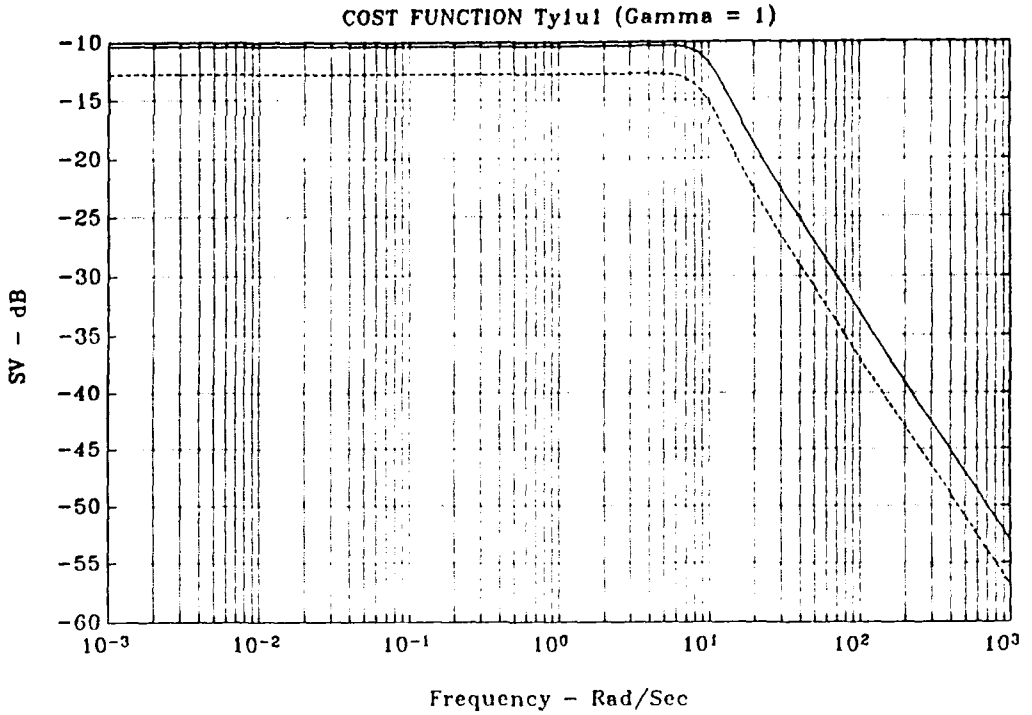

Figure 4.6 H_2 Cost Function $\|T_{y1u1}\|_2$ for γ=1

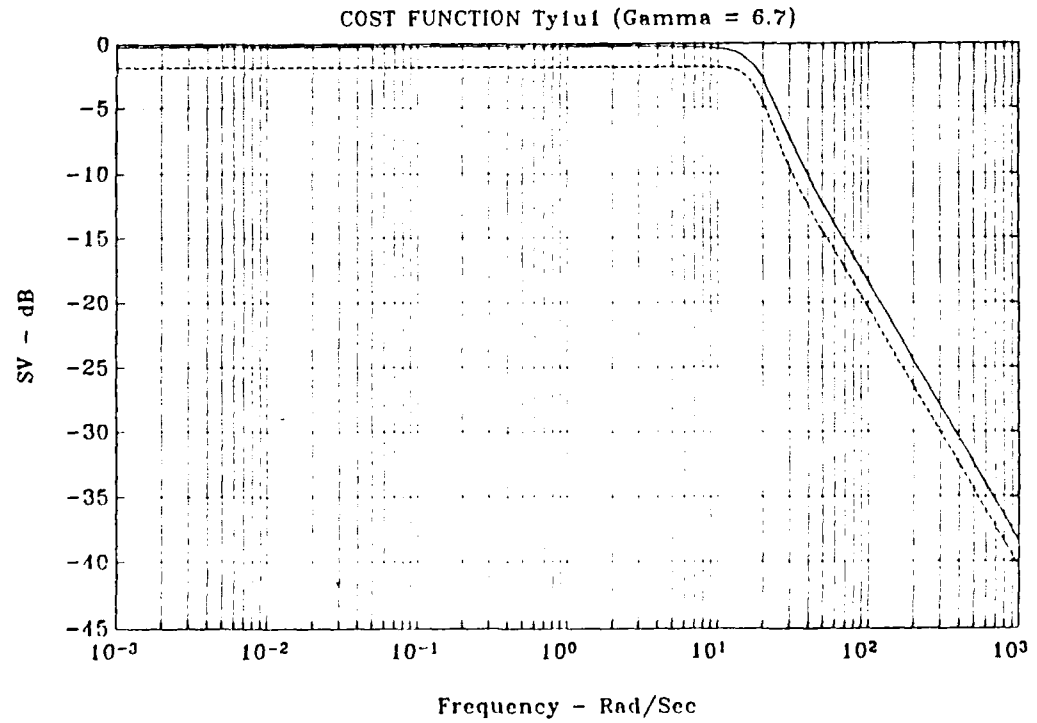

Figure 4.7 H_2 Cost Function $\|T_{y1u1}\|_2$ for γ=6.7

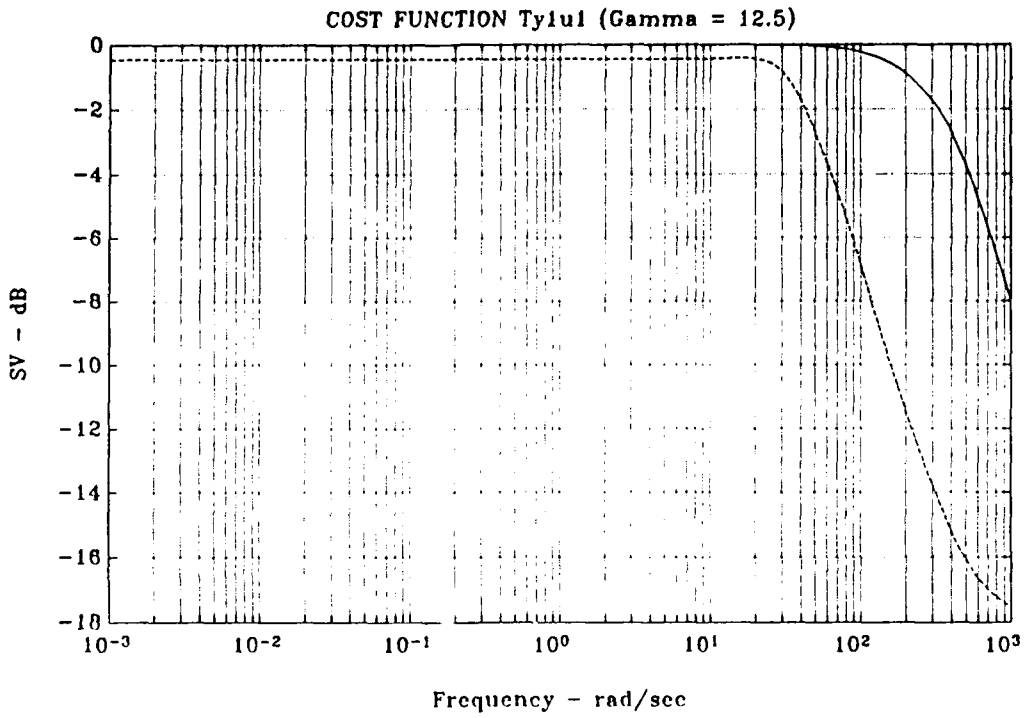

Figure 4.8 H_∞ Cost Function $\|T_{y1u1}\|_\infty$ for γ=12.5

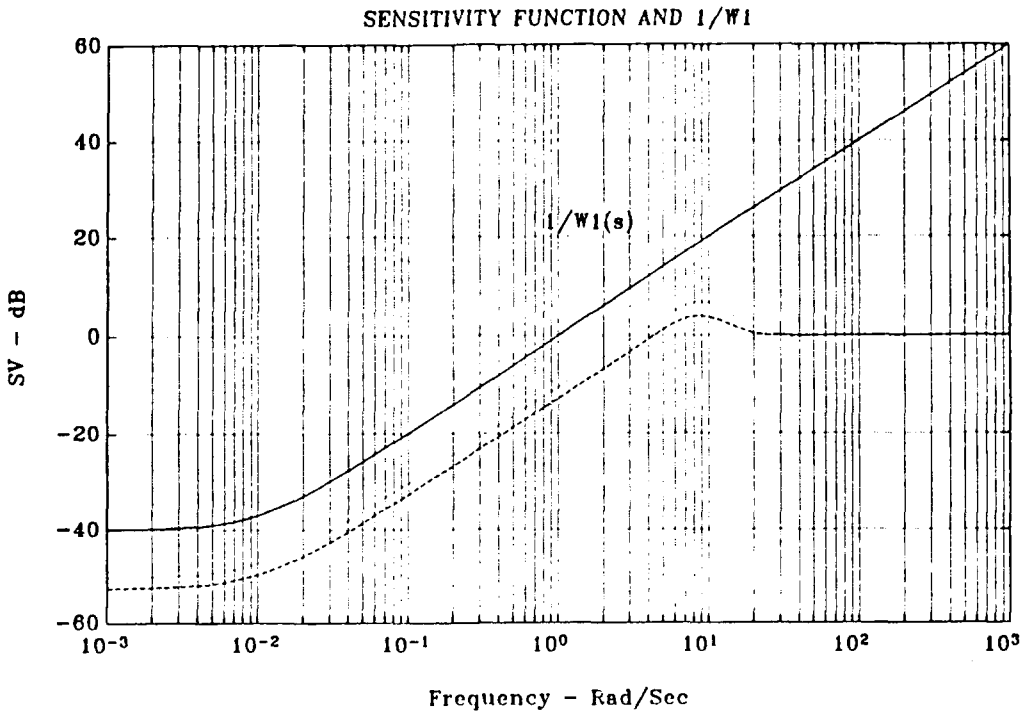

Figure 4.9 Sensitivity Function **S**(s) for H_2 Solution, γ=1

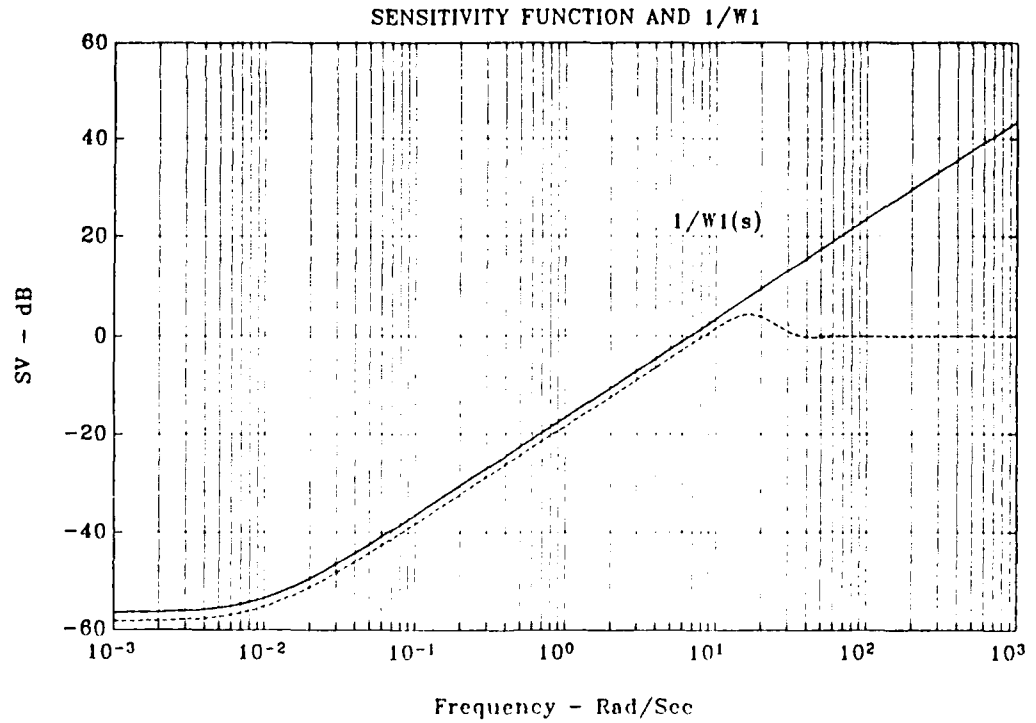

Figure 4.10 Sensitivity Function **S**(s) for H_2 Solution, γ=6.7

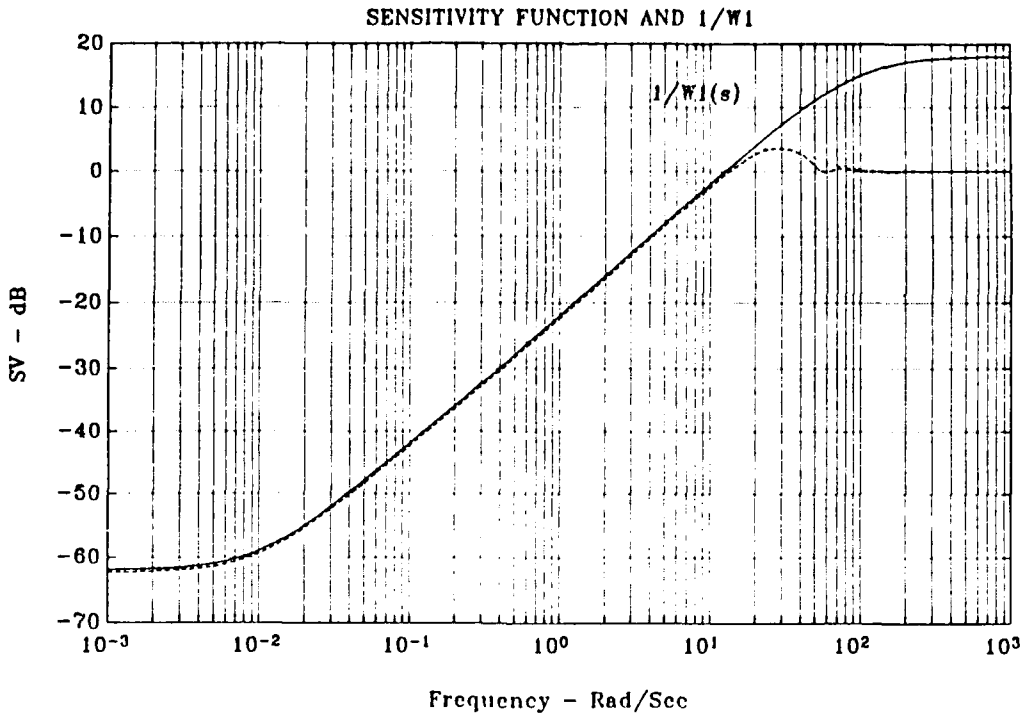

Figure 4.11 Sensitivity Function **S**(s) for H_∞ Solution, γ=12.5

are $\sigma_{max}(\mathbf{S}(j\omega))$ while the dashed curves are $\sigma_{min}(\mathbf{S}(j\omega))$. Figures 4.12 through 4.14 are singular value plots of the complementary sensitivity function **T**(s) and $W_3^{-1}(s)$ weighting function for the H_2 solution with γ values of one and 6.7, and H_∞ solution with a γ of 12.5, respectively. Here, the dashed curves are $\sigma_{max}(\mathbf{T}(j\omega))$ while the dotted curves are $\sigma_{min}(\mathbf{T}(j\omega))$. As γ is increased from one to 12.5, the sensitivity function **S**(s) is incrementally suppressed by the $(\gamma W_1)^{-1}(s)$ weighting function, and the complementary sensitivity function **T**(s) is pushed toward the stability constraint, i.e., the **S**(s) and **T**(s) singular values are forced against their respective upper limits $(\gamma W_1)^{-1}(s)$ and $W_3^{-1}(s)$. Comparing Figures 4.10 and 4.11,

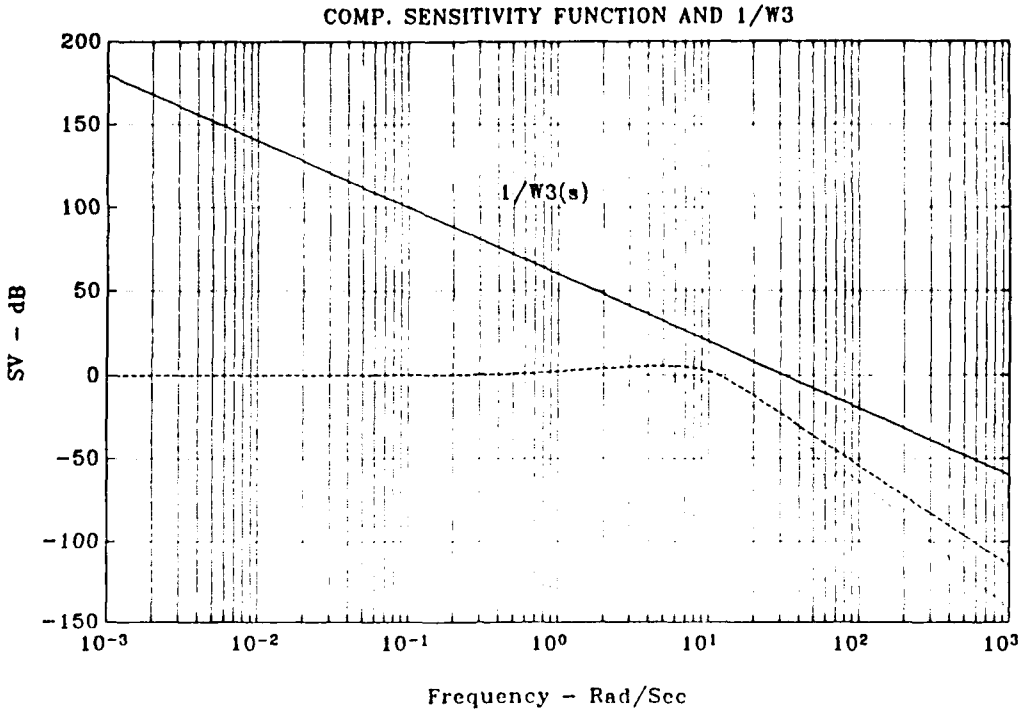

Figure 4.12 Complementary Sensitivity Function T(s) for H_2 Solution, γ=1

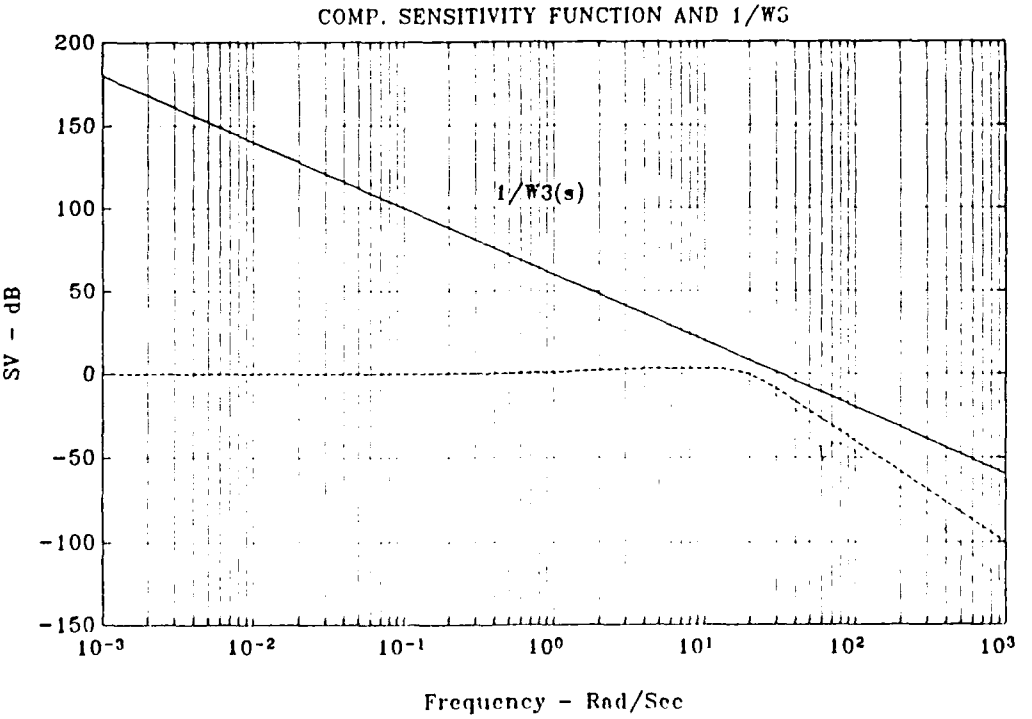

Figure 4.13 Complementary Sensitivity Function T(s) for H_∞ Solution, γ=6.7

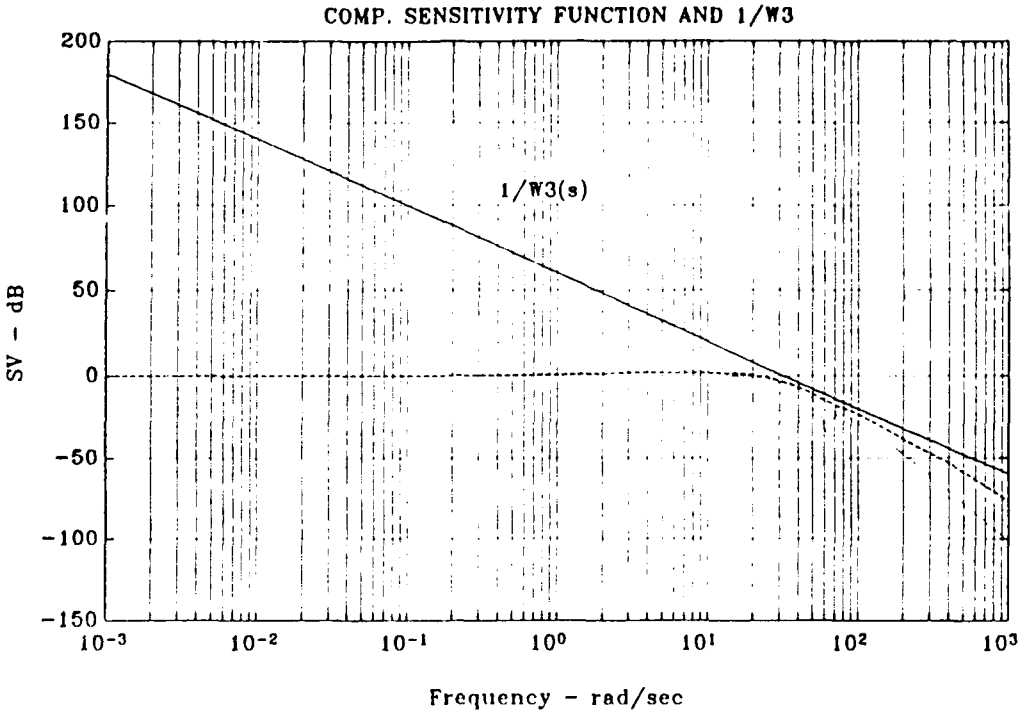

Figure 4.14 Complementary Sensitivity Function **T**(s) for H_∞ Solution, γ=12.5

it is seen that $\sigma_i(\mathbf{S}(j\omega))$ is suppressed more by the H_∞ solution meaning the H_∞ compensated X-29 is characterized by larger disturbance attenuation, lower sensitivity to plant variations and modeling errors, and a wider control bandwidth ω_B. Inspection of Figures 4.13 and 4.14 shows that the closed loop bandwidth of the H_∞ solution is larger, reaching nearly 30 rad/sec. This indicates the H_∞ compensated X-29 is a more responsive aircraft than the H_2 compensated aircraft.

As anticipated, the H_∞ solution to the small gain problem results in an 18th order controller. To "clean up" the solution, a minimal realization was performed using the Matlab minreal M-file to eliminate two uncontrollable and unobservable states. The minreal M-file finds the similarity

transformations of a system's state space realization such that the **A**, **B**, and **C** matrices are put into staircase controllability and observability forms. Minreal then removes the isolated uncontrollable or unobservable states from the system model. Next, the minimal 16th order controller was balanced using the Matlab obalreal M-file to improve the numerical conditioning of the controller model. The obalreal M-file finds a similarity transformation such that the mappings from inputs to states and states to outputs are balanced while preserving the input-output relationships. Finally, a fast transient pole at -1.6262e+05 was removed using the Matlab modred M-file. Modred eliminates specified states from a state space model while preserving the system's input-output relationships. Each of the 16 minimal states was individually eliminated until the state that removed the fast transient pole was identified. The resultant 15th order minimal controller was used in plotting the H_∞ cost function $\|\mathbf{T}_{y1u1}\|_\infty$, sensitivity function **S**(s), and complementary sensitivity function **T**(s) results presented in Figures 4.8, 4.11, and 4.14, respectively.

However, further reduction of the H_∞ controller size is desirable. Therefore, attempts were made to reduce the 15th order controller using the Schur additive error model reduction method [Ref. 7]. This model reduction method allows the size of the reduced order model to be selected. Additive modeling error $\mathbf{E}_A$ (s) is defined as

$$\mathbf{E}_A(s) = \mathbf{F}(s) - \acute{\mathbf{F}}(s) \tag{4.2}$$

where $\mathbf{F}(s)$ and $\acute{\mathbf{F}}(s)$ are the true transfer function matrix and its reduced model, respectively. To ensure the additive modeling error $\mathbf{E}_A$ will not destabilize the closed loop system, the control bandwidth ω_B of the reduced model must be less than the additive robust frequency ω_{ra}, i.e.,

$$\omega_B < \omega_{ra},$$

where

$$\omega_{ra} = \max\{\omega \mid \sigma_{min}(\acute{\mathbf{F}}(j\omega)) \geq \sigma_{max}(\mathbf{E}_A(j\omega))\}. \tag{4.3}$$

This condition for system stability assumes

$$\sigma_{max}(\mathbf{E}_A(j\omega)) \leq \sigma_{min}(\acute{\mathbf{F}}(j\omega)) \qquad \text{for } \omega \leq \omega_{ra}. \tag{4.4}$$

That is, given $\mathbf{E}_A$ is the only information available about the modeling error, the additive robust frequency ω_{ra} is an upper bound on the bandwidth of a multivariable control system without violating the required condition for stability, i.e., Equation (2.25). [Ref. 7]

Figure 4.15 compares the singular value plot of the 15th order controller with that of a selected eighth order controller. The upper (solid) curve is a plot of $\sigma_{max}(\mathbf{F}(j\omega))$ and $\sigma_{max}(\acute{\mathbf{F}}(j\omega))$ for the 15th order and 8th order controllers, respectively, while the lower (dashed) curves are plots of $\sigma_{min}(\mathbf{F}(j\omega))$ and $\sigma_{min}(\acute{\mathbf{F}}(j\omega)$ as indicated. Figure 4.16 displays

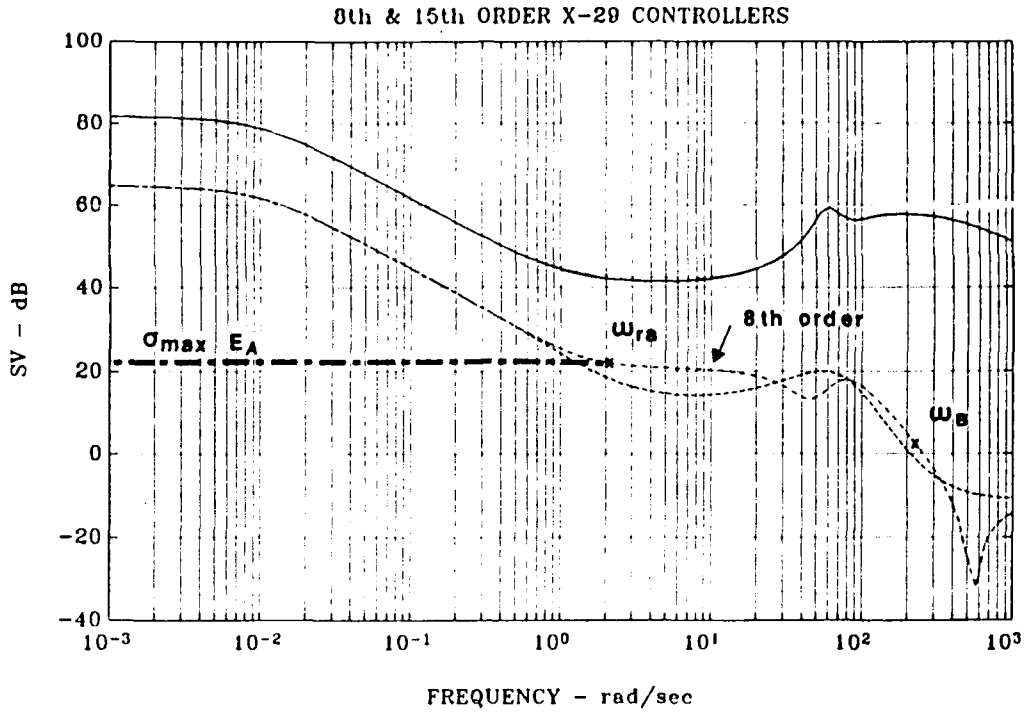

Figure 4.15 Comparison of 8th Order and 10th Order X-29 Controllers

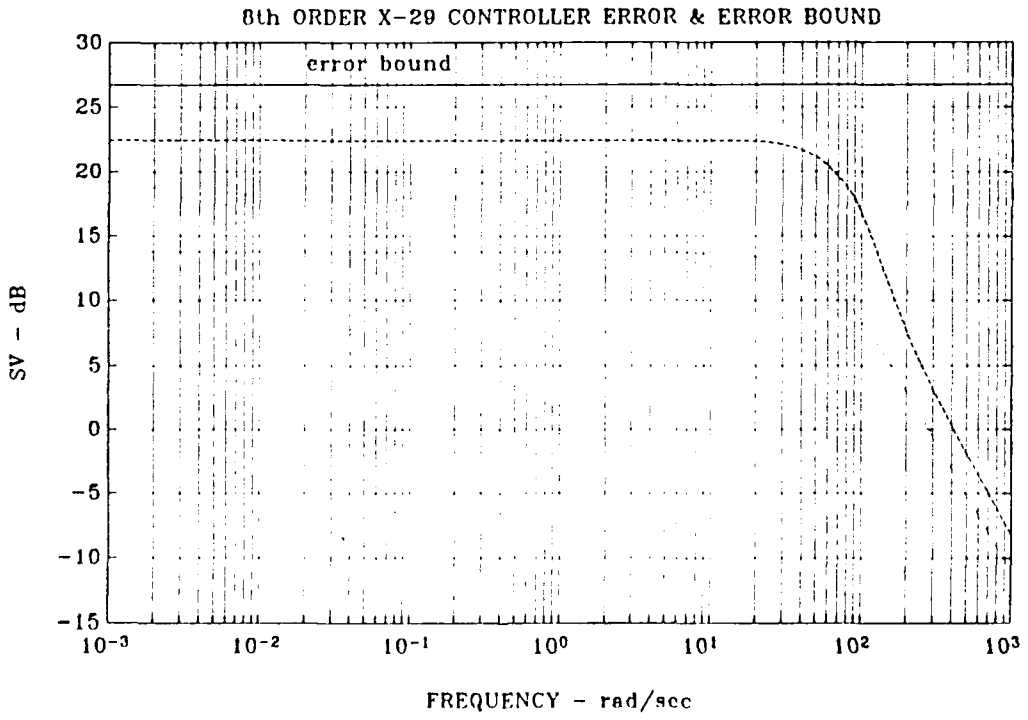

Figure 4.16 8th Order Controller Additive Error E_A

the singular values of the eighth order controller's additive error where the dashed and dotted curves are $\sigma_{max}(\mathbf{E}_A(j\omega))$ and $\sigma_{min}(\mathbf{E}_A(j\omega))$, respectively. The solid curve is an upper bound on $\sigma_{max}(\mathbf{E}_A(j\omega))$. As shown in Figure 4.15, the additive robust frequency ω_{ra}, i.e., where

$$\sigma_{max}(\mathbf{E}(j\omega)) = \sigma_{min}(\dot{\mathbf{F}}(j\omega)),$$

is approximately 2 rad/sec. The control bandwidth ω_B of over 200 rad/sec, defined at the 3 dB point, is clearly greater than the additive robust frequency ω_{ra}. As the closed loop feedback control system can be destabilized by the additive modeling error $\mathbf{E}_A$, the eighth order controller is not a suitable alternative for the 15th order controller.

However, examination of Figure 4.17, which compares the singular value plots of the 15th order and a selected 10th order controller, shows the two controllers to be well matched. Figure 4.18 shows the $\sigma_{max}(\mathbf{E}_A(j\omega))$ and $\sigma_{min}(\mathbf{E}_A(j\omega))$ plots of the 10th order controller's additive error, i.e., the dashed and dotted curves, respectively. Again, the solid curve is an upper bound on $\sigma_{max}(\mathbf{E}_A(j\omega))$. As can be seen from Figures 4.17 and 4.18, $\sigma_{max}(\mathbf{E}_A(j\omega))$ does not intersect $\sigma_{min}(\dot{\mathbf{F}}(j\omega))$ within the frequency range of the graph, i.e., $\omega_{ra} > 10^3$ rad/sec. Clearly, the control bandwidth ω_B of the 10th order controller, shown just below 200 rad/sec, is less than

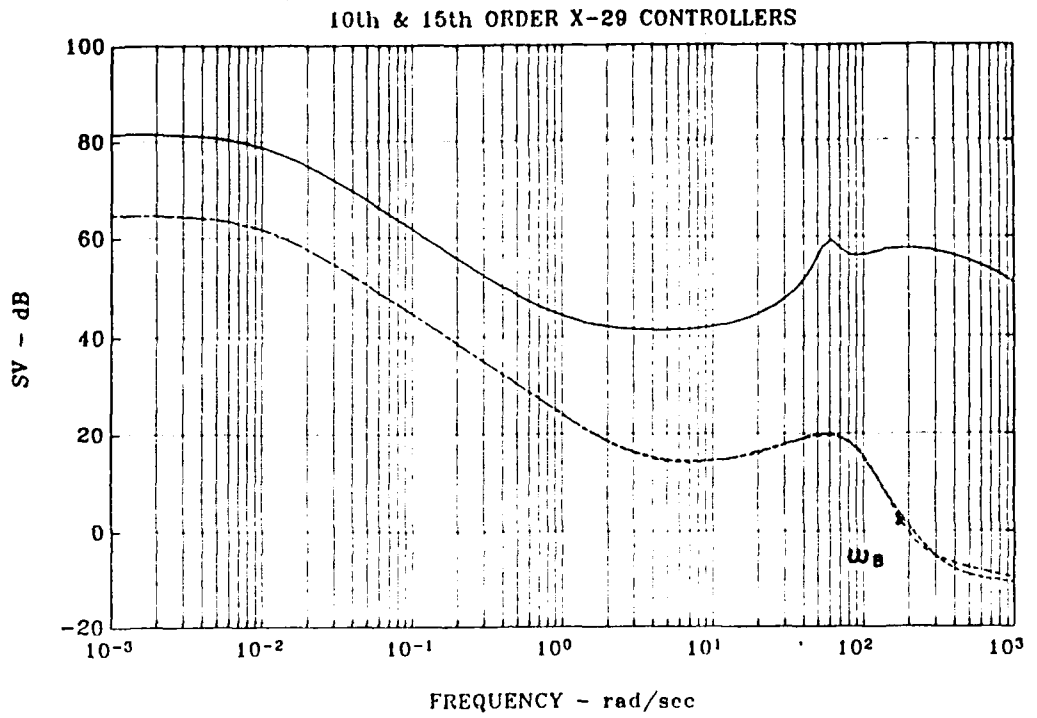

Figure 4.17 Comparison of 10th Order and 15th Order X-29 Controllers

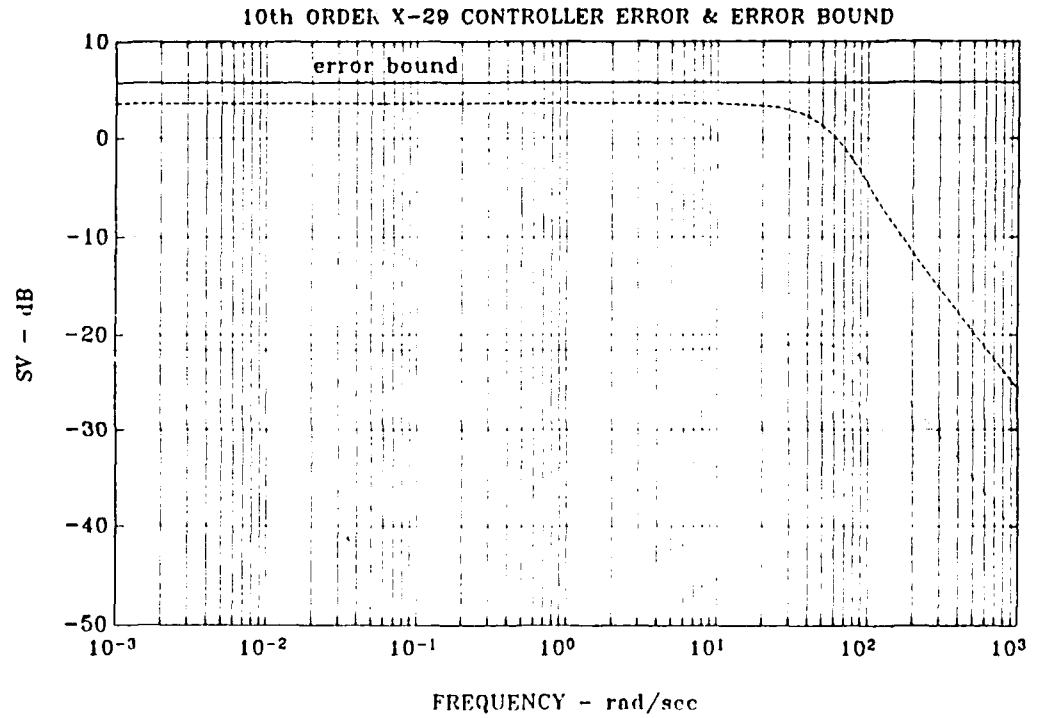

Figure 4.18 10th Order Controller Additive Error E_A

the additive robust frequency ω_{ra}, and the 10th order controller is a suitable alternative to the 15th order controller.

D. DESIGN RESULTS OF THE H_∞ CONTROLLER

The closed loop configuration of the H_∞ compensated X-29 is presented in Figure 4.19 where **F**(s) and **G**(s) are the 15th order controller and 14th order X-29 plant transfer function matrices, respectively. The output vector **y** is made up of the aircraft states α and q, and the command vector **r** is composed of separate command elements r_1 and r_2. Unlike the open loop actuator/aircraft dynamics model presented in Figure 4.1, r_1 and r_2 are reference commands to the controlled outputs, α and q. This is a result of the controller being placed in series with the X-29 plant in the feedforward loop and the

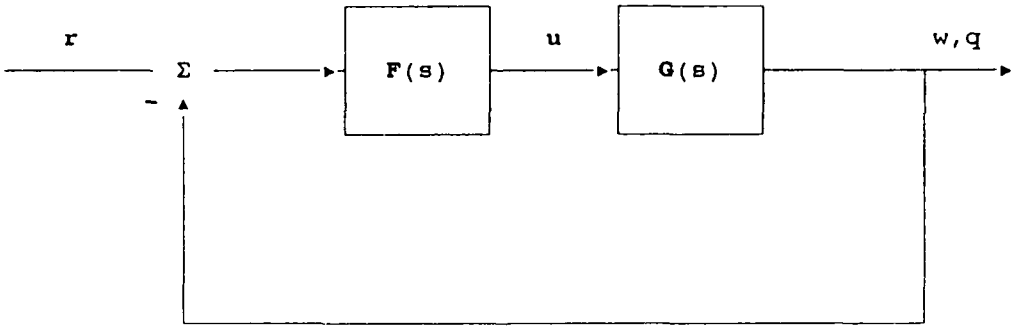

Figure 4.19 Feedback Configuration for H_∞ Compensated X-29

negative unity feedback. Thus, the closed loop, compensated X-29 model has two inputs, two outputs, and 29 states. As will be seen, this closed loop configuration still provides the multiple, independently controlled surfaces observed with the open loop, uncompensated X-29 plant **G**(s).

The state space realization of the 29th order, closed loop model is presented in Appendix B. A balanced realization was performed separately on the controller **F**(s) and the X-29 plant **G**(s) to improve their numerical conditioning. As a result of this balancing, the internal structures of **F**(s) and **G**(s) were altered making identification of the individual states difficult. The poles of the closed loop model are listed in Table 4.3. It is interesting to note that the unstable short period pole of the open loop system is mirrored into the left-half plane of the closed loop system, i.e., -1.9550. This is not a coincidence as an identical occurrence is observed in Safonov's advanced fighter example presented in Ref. 7. In Safonov's example, the unstable phugoid poles of the advanced fighter's open loop model are mirrored into the left-half plane of the compensated, closed loop model. This mirror imaging can represent a basic limitation to the system's performance if, as in the case of the compensated X-29, this is the dominate pole.

As discussed in Chapter II, the singular values of the return difference and inverse-return difference matrices quantify a system's feedback properties. In the following

TABLE 4.3

H_∞ COMPENSATED X-29 CLOSED LOOP POLES

-4.1327e+02
-2.2745e+02 ± 2.3201e+02i
-1.3068e+02 ± 4.6111e+01i
-5.3305e+01 ± 8.9700e+01i
-1.4491e+02
-1.4452e+02
-1.3014e+02
-1.3877e+01 ± 5.9243e+01i
-9.9794e+01
-5.2545e+01 ± 4.8359e+01i
-5.2503e+01 ± 4.8301e+01i
-7.4132e+01
-1.9550e+00
-2.7155e+00
-2.0379e+01 ± 2.1564e+01i
-2.0578e+01 ± 1.8907e+01i
-4.9199e+01 ± 6.5316e+00i
-4.2465e+01
-2.0184e+01
-2.0110e+01

paragraphs the feedback properties of the H_∞ compensated X-29 will be measured using singular value plots of its return difference matrices.

The singular value plots of the uncompensated and compensated X-29 output, return difference matrices are presented in Figures 4.20 and 4.21, respectively. In these figures, as with all the return difference matrix plots, the upper curves are σ_{max} while the lower curves are σ_{min}. Recall from Chapter II that the output return difference matrix $\mathbf{I} + \mathbf{G}(s)\mathbf{F}(s)$ (also referred to as the output, additive return difference matrix) is the inverse of the sensitivity function

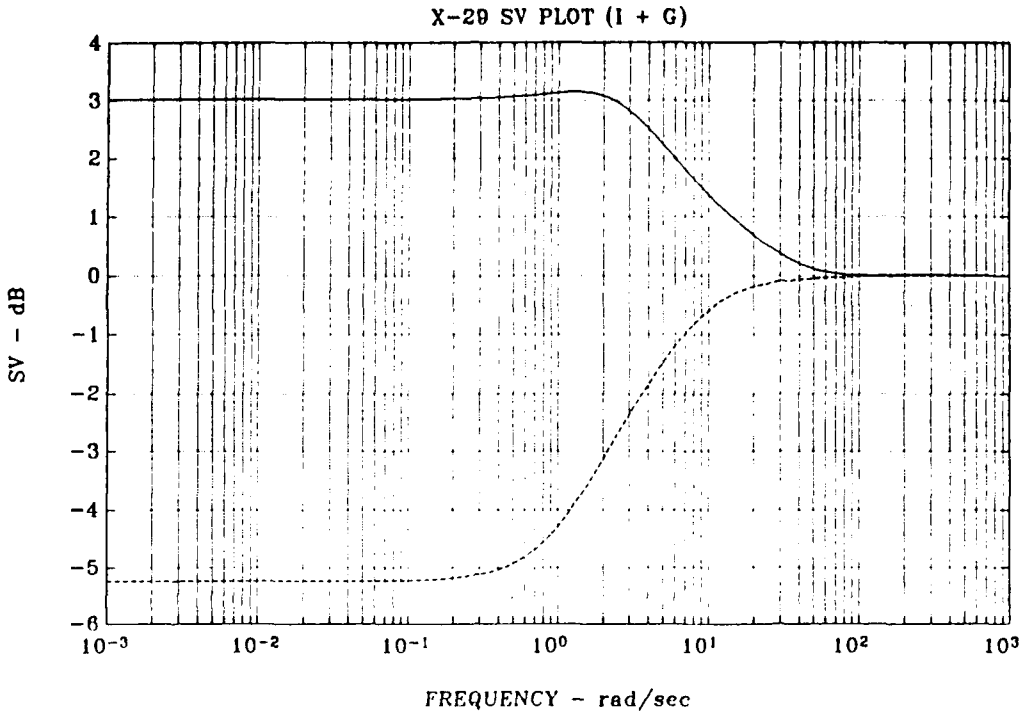

Figure 4.20 Singular Value Plot **I+G**(s), Uncompensated X-29

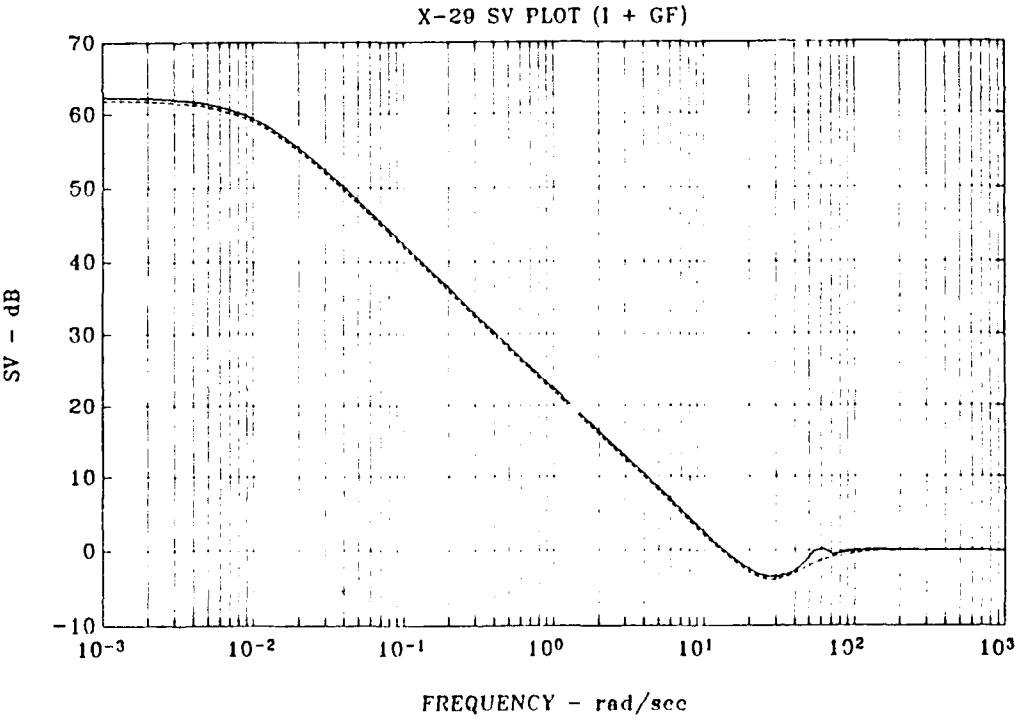

Figure 4.21 Singular Value Plot **I+G**(s)**F**(s), H_∞ Compensated X-29

$\mathbf{S}(s)$, and that the minimum singular value of this return difference matrix approximates the loop gains whenever the loop gains are large, i.e., Equation (2.22). Given this, Figure 4.20 indicates the uncompensated X-29 possesses small loop gains along with the corresponding traits of poor disturbance attenuation and high sensitivity to plant variations and modeling errors. Figure 4.21 shows how the H_∞ synthesized controller has markedly improved the X-29 performance properties. The large loop gains indicate good disturbance attenuation and low sensitivity to uncertainties over a control bandwidth ω_B of approximately 9 rad/sec. However, the dip of the singular values below the 0 dB line indicates that performance is lacking near the 0 dB crossover frequency. This is probably caused by the steep roll-off (-40 dB/decade) designed into the complementary sensitivity function. Finally, the 9 rad/sec control bandwidth ω_B of the compensated X-29 is less than the multiplicative robust frequency ω_{rm} of 30 rad/sec ensuring that the required condition for stability (Equation (2.25)) is not violated at the X-29 plant output.

The singular value plot of the output, inverse-return difference matrix $\mathbf{I} + (\mathbf{G}(s)\mathbf{F}(s))^{-1}$ (also referred to as the output, multiplicative return difference matrix) for the compensated X-29 is shown in Figure 4.22. The minimum singular value of this matrix, i.e., $\sigma_{min}[\mathbf{I} + (\mathbf{G}(j\omega)(\mathbf{F}(j\omega))^{-1}]$,

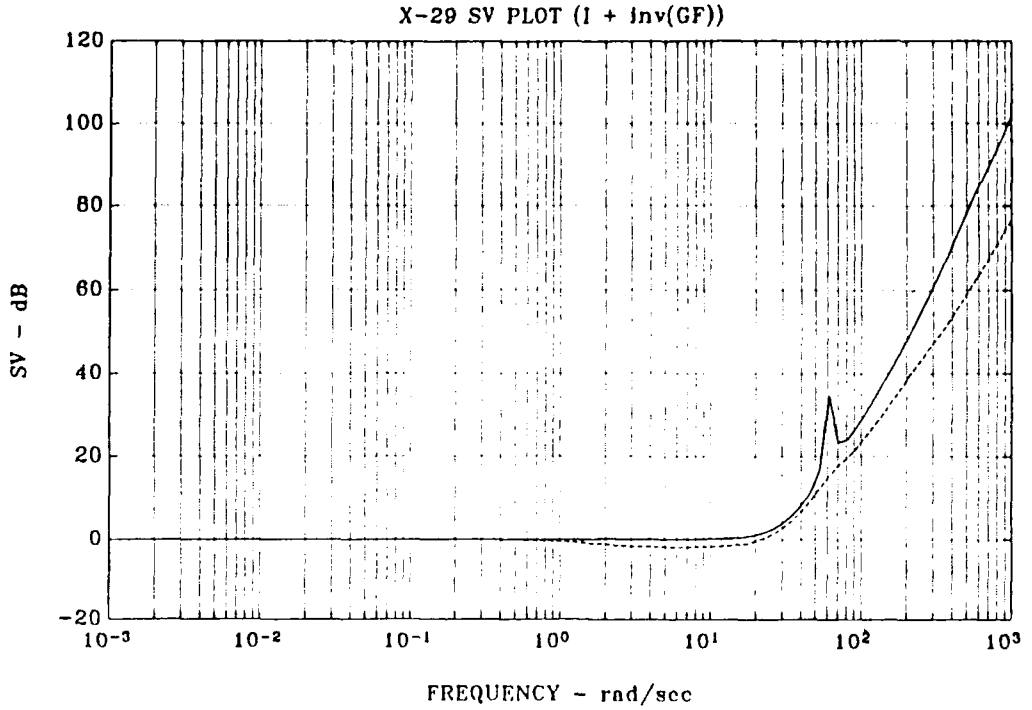

Figure 4.22 Singular Value Plot $\mathbf{I}+(\mathbf{G}(s)\mathbf{F}(s))^{-1}$, H_∞ Compensated X-29

can provide a measure of the aircraft's gain and phase margins with respect to multiplicative modeling errors using the universal gain and phase margin curve (Figure 4.23) [Ref. 6:pp. 54-55]. As shown in the universal curve, a minimum singular value of one, i.e., 0 dB, provides gain and phase margins of -6 dB to infinity and ±60 deg, respectively, or that stability margin guaranteed by the LQ regulator problem. It is seen from Figure 4.23 that any singular value less than one is associated with suboptimal gain and phase margins. Returning to Figure 4.22, it is seen that $\sigma_{min}[\mathbf{I} + (\mathbf{G}(j\omega)\mathbf{F}(j\omega))^{-1}]$ drops to approximately -2 dB at frequencies between 1 rad/sec and 20 rad/sec. Entering the vertical axis

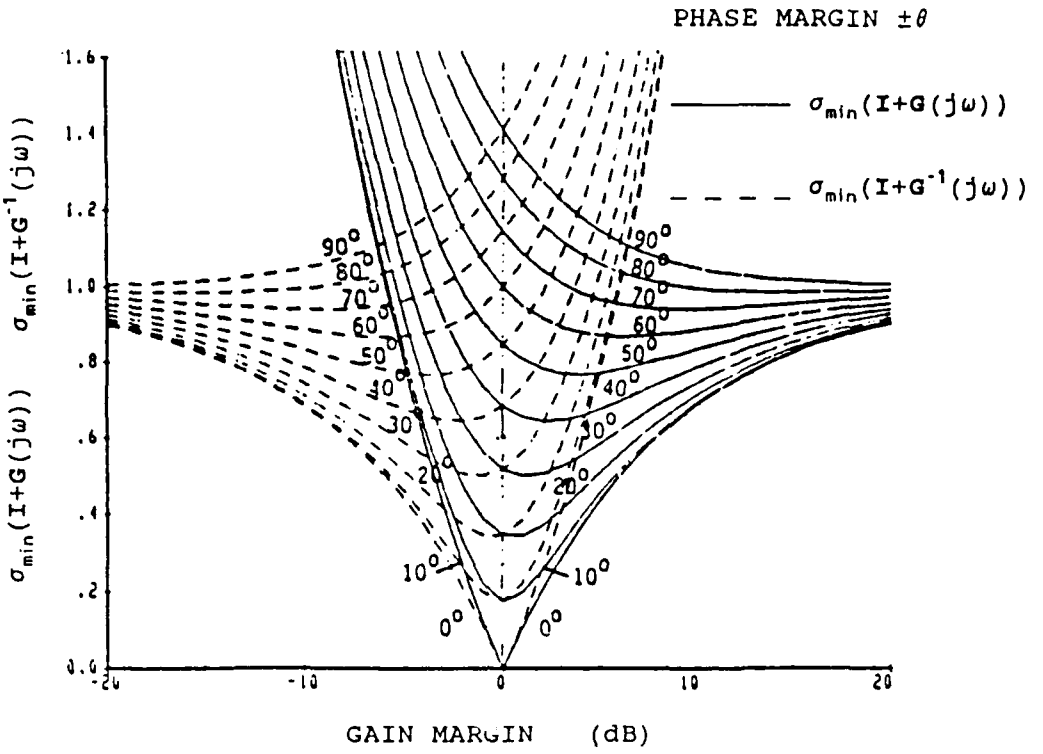

Figure 4.23 Universal Gain and Phase Margin Curve

of the universal curve at a singular value of .79, i.e., -2 dB, the gain and phase margins of the compensated X-29 near the 0 dB crossover frequency are -14 dB to +5 dB and ±47 deg, respectively. This is more stable than the -8 dB to +4 dB, ±35 deg gain and phase margins typically designed into a fighter aircraft.

The singular value plots of the input additive and input multiplicative return difference matrices are shown in Figures 4.24 and 4.25, respectively. These singular value plots show that the H_∞ solution to the X-29 small gain problem does not satisfy the performance objectives or the stability constraints at the X-29 plant input. An exceptionally poor

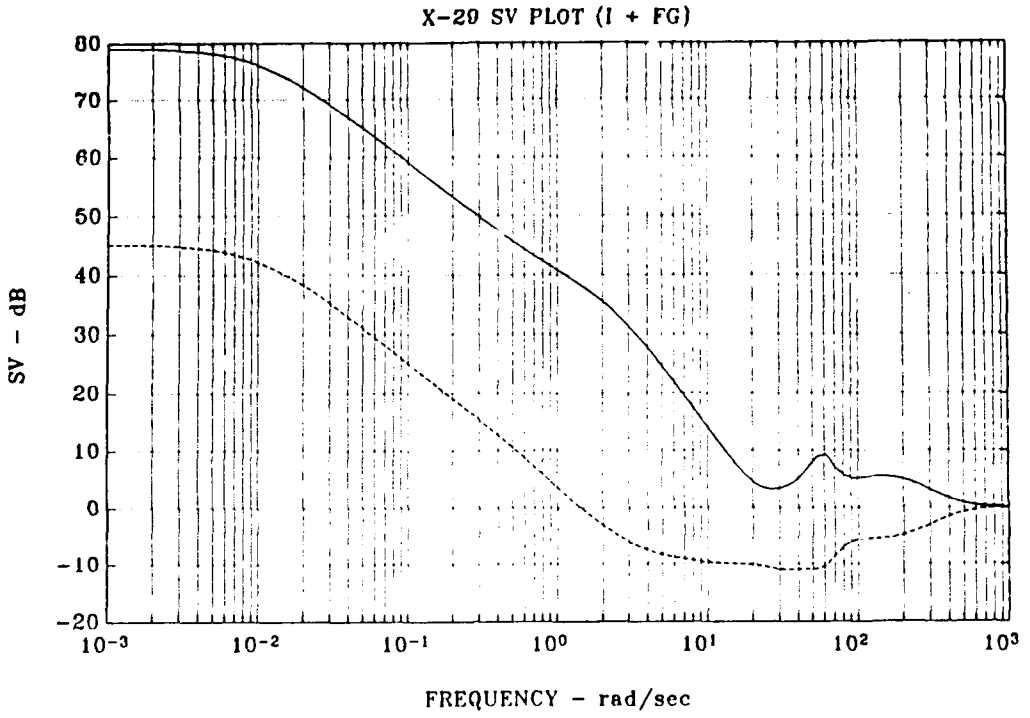

Figure 4.24 Singular Value Plot $\mathbf{I+F(s)G(s)}$, H_∞ Compensated X-29

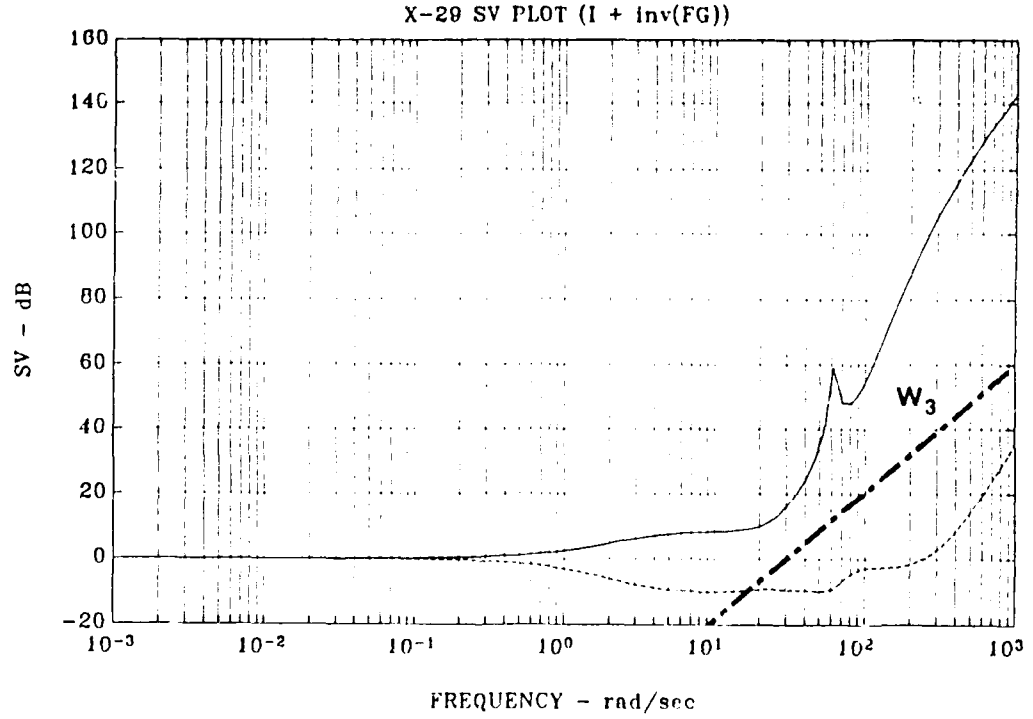

Figure 4.25 Singular Value Plot $\mathbf{I+(F(s)G(s))}^{-1}$, H_∞ Compensated X-29

disturbance attenuation and low sensitivity to uncertainties are indicated by a small $\sigma_{min}[\mathbf{I} + \mathbf{F}(j\omega)\mathbf{G}(j\omega)]$, especially between the frequencies of 2 rad/sec and 300 rad/sec (Figure 4.24). A $\sigma_{min}[1 + (\mathbf{F}(j\omega)\mathbf{G}(j\omega))^{-1}]$ of -11 dB equates to a gain and phase margin of -3 dB to 2 dB and ±15 deg, respectively, over much of the bandwidth between 2 rad/sec and 60 rad/sec (Figure 4.25). Further, since

$$\sigma_{min}[\mathbf{I} + (\mathbf{F}(j\omega)\mathbf{G}(j\omega))^{-1}] < |W_3^{-1}(j\omega)|,$$

the required condition for stability, Equation (2.25), is violated meaning a relative modeling error exists that can destabilize the aircraft at its inputs. It can be concluded that H_∞ control synthesis does not guarantee that the performance and stability robustness requirements of Equations (2.27) and (2.25) will be satisfied at the plant $\mathbf{G}(s)$ inputs.

A .01745 rad (1 deg) step input was applied separately for one second to each of the two reference commands, and the aircraft responses and control deflections plotted. Following standard convention, a positive α or q corresponds to a nose-up response, and a positive control deflection is trailing edge down for all three control surfaces. Positive canard deflection δ_c, negative flap deflection δ_f, and negative strake deflection δ_s each induce a nose-up response, i.e., positive α and q.

The closed loop, compensated X-29 model (Figure 4.19) exhibits precision flight path control modes as a result of

the multiple, independently controlled surface configuration. Figure 4.26 presents a graphic representation of these precision control modes in terms of angle-of-attack α, pitch attitude θ, flight path angle γ, and the aircraft principal and stability axes x_p and x_s, respectively. (Note that the flight path angle γ is in no way related to the γ constant used in the H_2 and H_∞ design specifications.) The three precision longitudinal modes observed are [Ref. 3]:

1. Vertical Translation: The aircraft vertical velocity is controlled at a constant θ by varying α, i.e., the aircraft flight path angle γ or velocity vector is controlled while x_s remains fixed.

2. Direct Lift Control: The aircraft flight path angle γ is controlled at a constant α by varying θ, i.e., the aircraft flight path angle γ or velocity vector remains along the aircraft stability axis x_s as x_s rotates.

3. Pitch Pointing: The aircraft pitch attitude θ is controlled at a constant flight path angle γ, i.e., the aircraft flight path angle γ or velocity vector remains fixed while x_s rotates ($\theta = \alpha$).

The α and q responses of the compensated X-29 are presented for inputs 1 and 2 in Figures 4.27 and 4.28, respectively. The compensated X-29 responds to input 1 (r_1) with a positive α and negligible change in q, i.e., order of magnitude is 10^{-3}, (Figure 4.27) which is the vertical translation mode discussed above. That is, input one decouples q and θ from α. The compensated aircraft exhibits a fast response to input 1 with an α rise time of .125 sec. The direct lift control mode is effected by input 2 (r_2) as shown in Figure 4.28. The aircraft responds to input 2 with a positive q while its α response is negligible, i.e., order

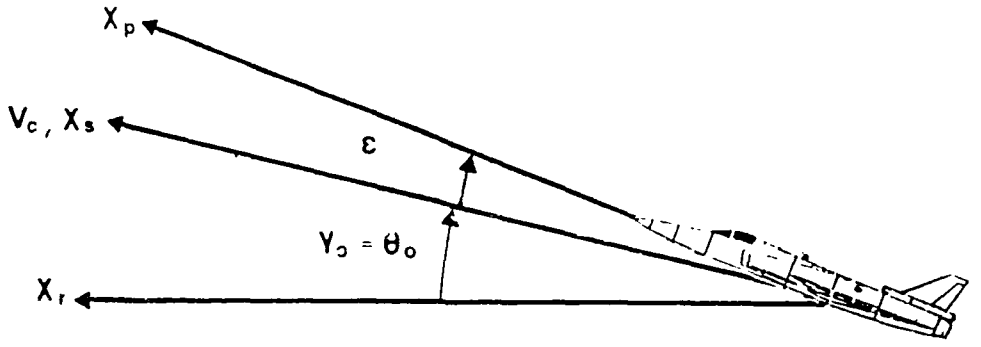

Reference Condition

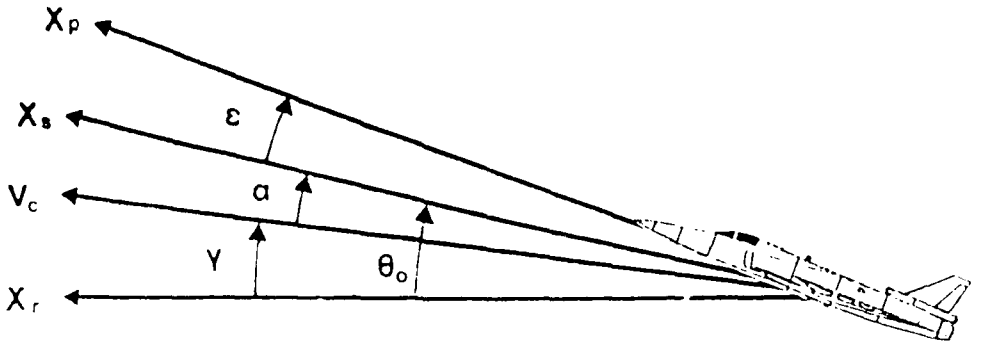

Vertical Translation

Figure 4.26 Advanced Control Modes

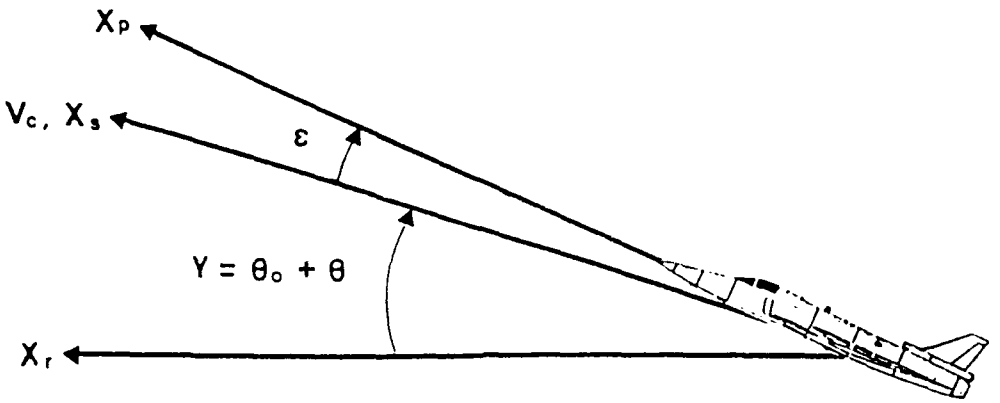

Direct Lift Control

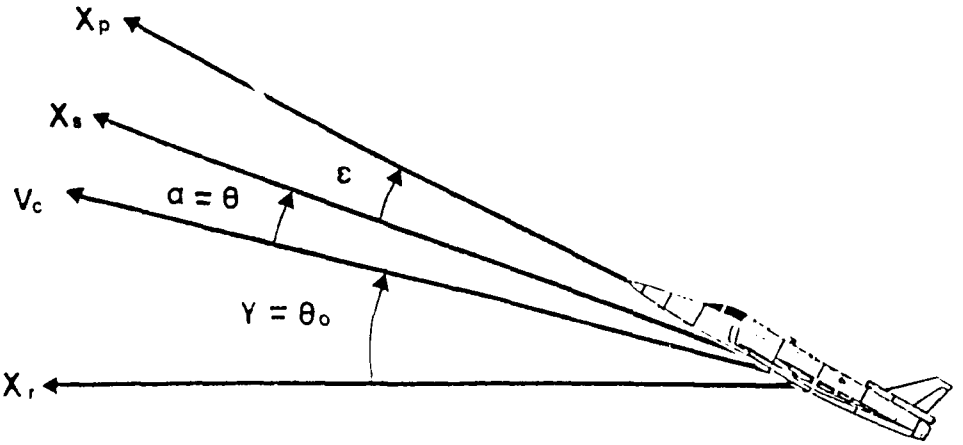

Pitch Pointing

Figure 4.26 (Cont) Advanced Control Modes

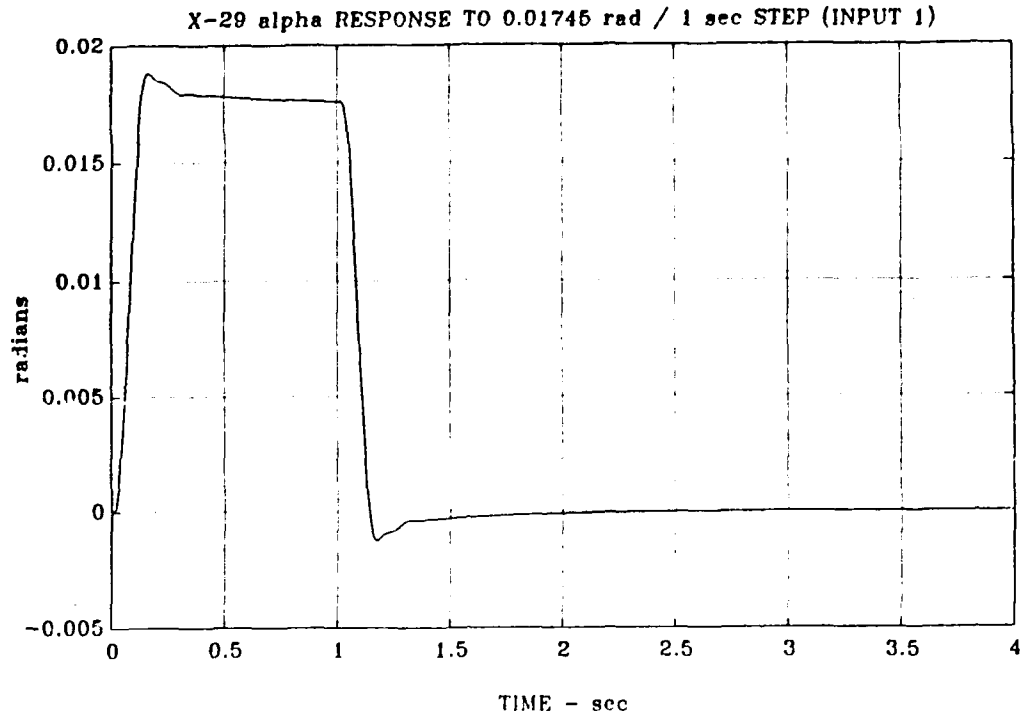

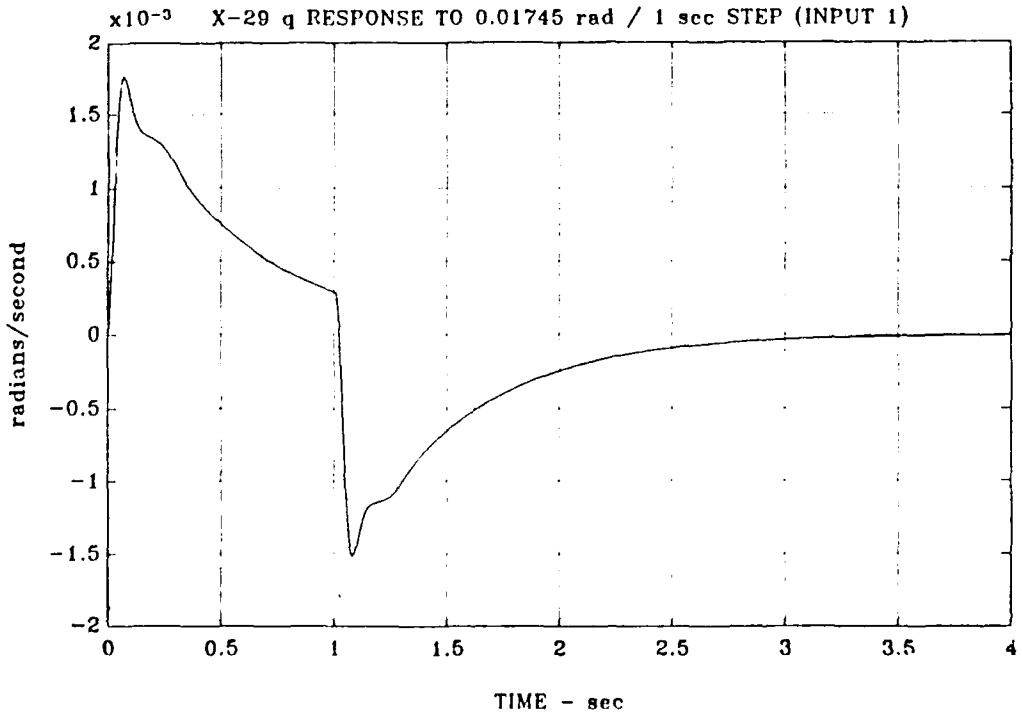

Figure 4.27 Compensated X-29 α and q Responses to Input 1

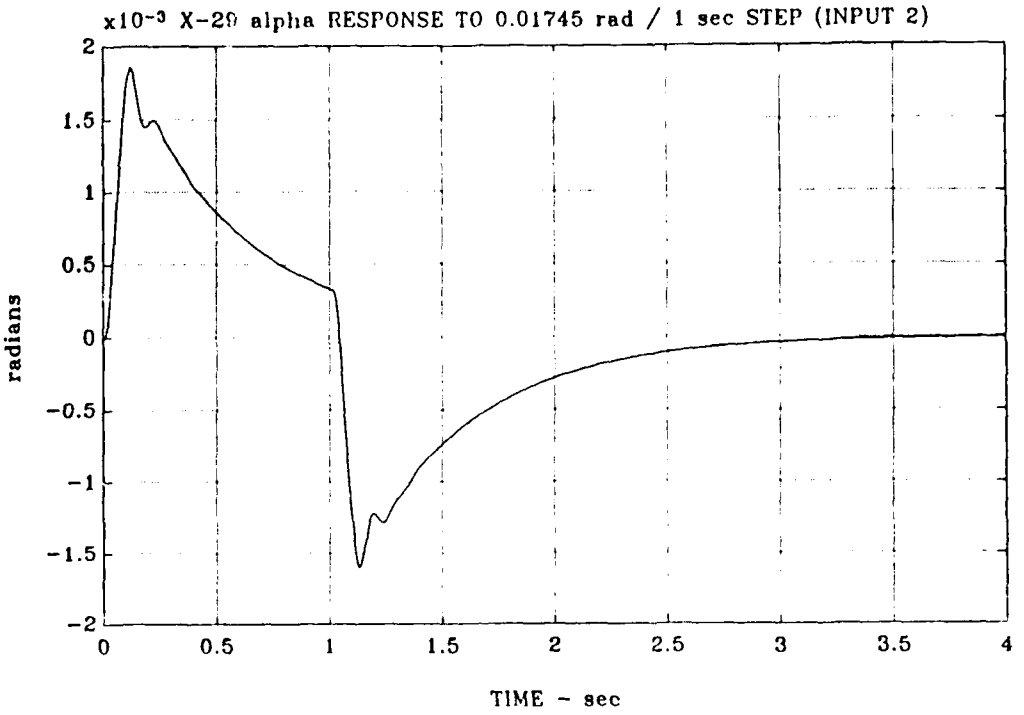

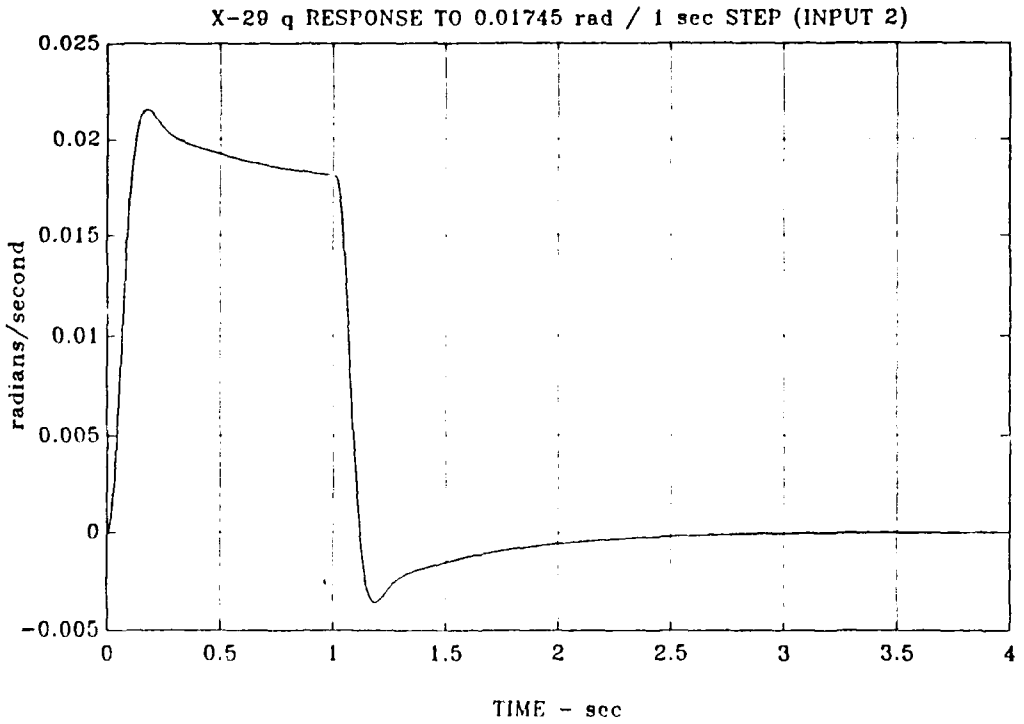

Figure 4.28 Compensated X-29 α and q Responses to Input 2

of magnitude is 10^{-3}. As with input 1, a decoupling of the aircraft responses, α and q, is observed with input 2. The aircraft q response is equally fast with a rise time of approximately .095 sec. Figures 4.29 and 4.30 show the compensated X-29 control surface deflections δ_c, δ_f, and δ_s for inputs 1 and 2, respectively. From these figures it is determined that the flap and strake control inputs, δ_f and δ_s respectively, control the aircraft's α response while the canard δ_c controls the q (and θ) response. A simultaneous injection of inputs 1 and 2 is necessary to effect the pitch pointing precision control mode.

The control deflections δ_c, δ_f, and δ_s for the vertical translation mode (input 1) have peak magnitudes between 1.4 rad and 3 rad which exceed the X-29's control surface deflection limits of;

1. canards (leading edge): 30 deg up / 60 deg down,
2. flaps (trailing edge): 10 deg up / 25 deg down,
3. strakes (trailing edge): 30 deg up and down.

The control deflections are significantly less for the direct lift control mode (input 2) with peak magnitudes between .15 rad and .6 rad, and are more closely aligned with the control surface deflection limits listed above. A similar difference in control rates between inputs 1 and 2 is observed in Figures 4.31 and 4.32 which present the compensated X-29 control rates $\dot{\delta}_c$, $\dot{\delta}_f$, and $\dot{\delta}_s$ for inputs 1 and 2, respectively. The peak

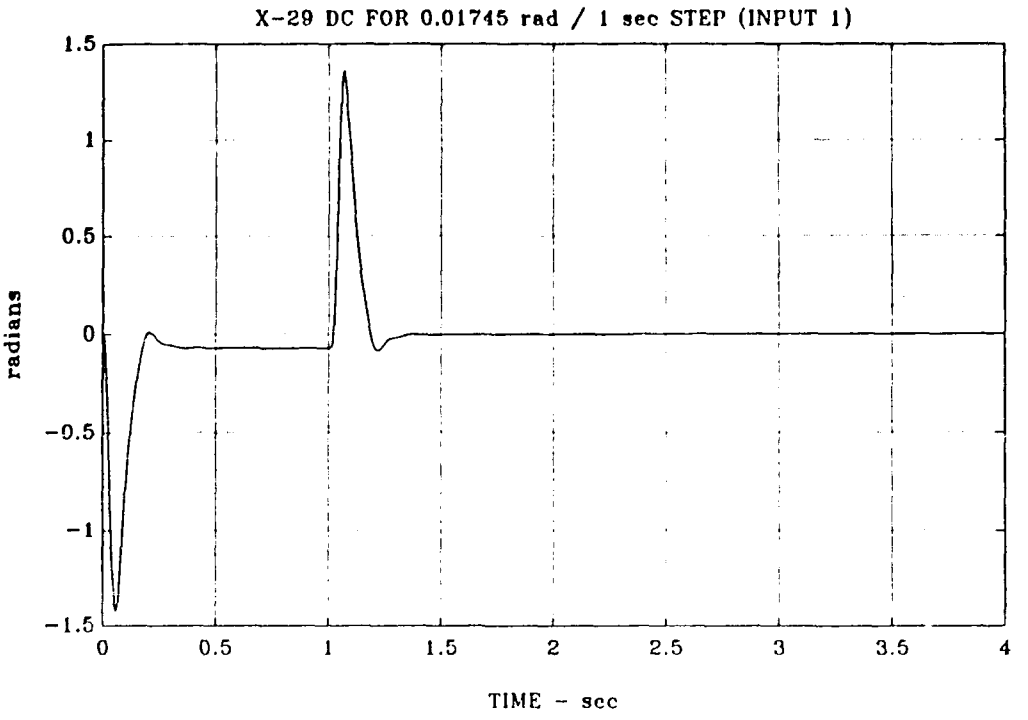

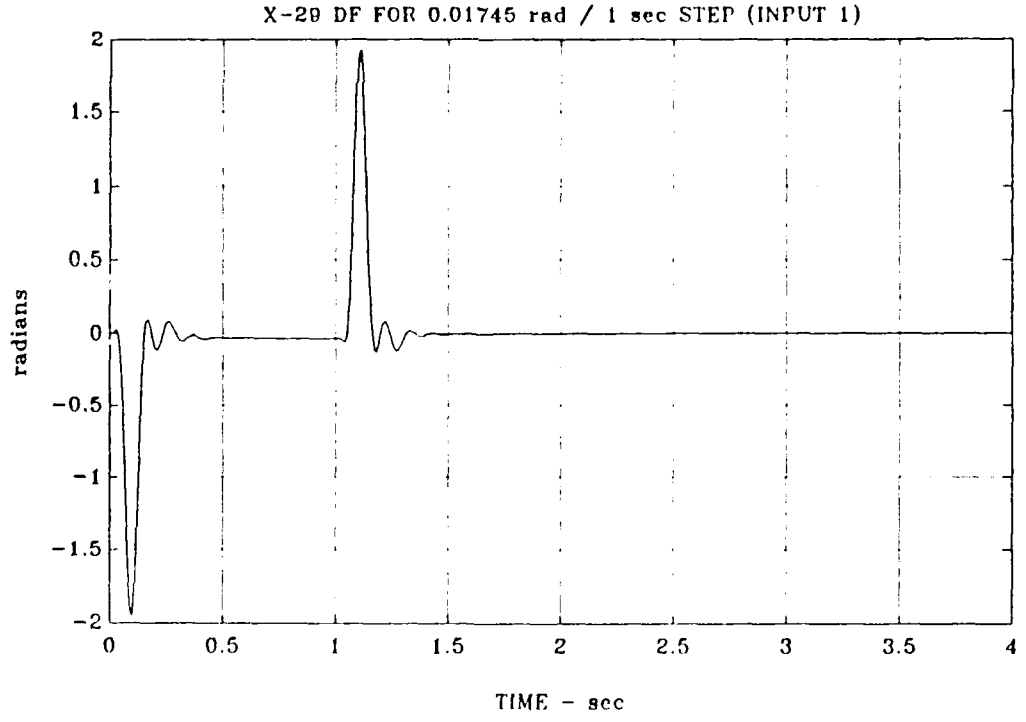

Figure 4.29 Compensated X-29 Control Deflections δ_c, δ_f, and δ_s for Input 1

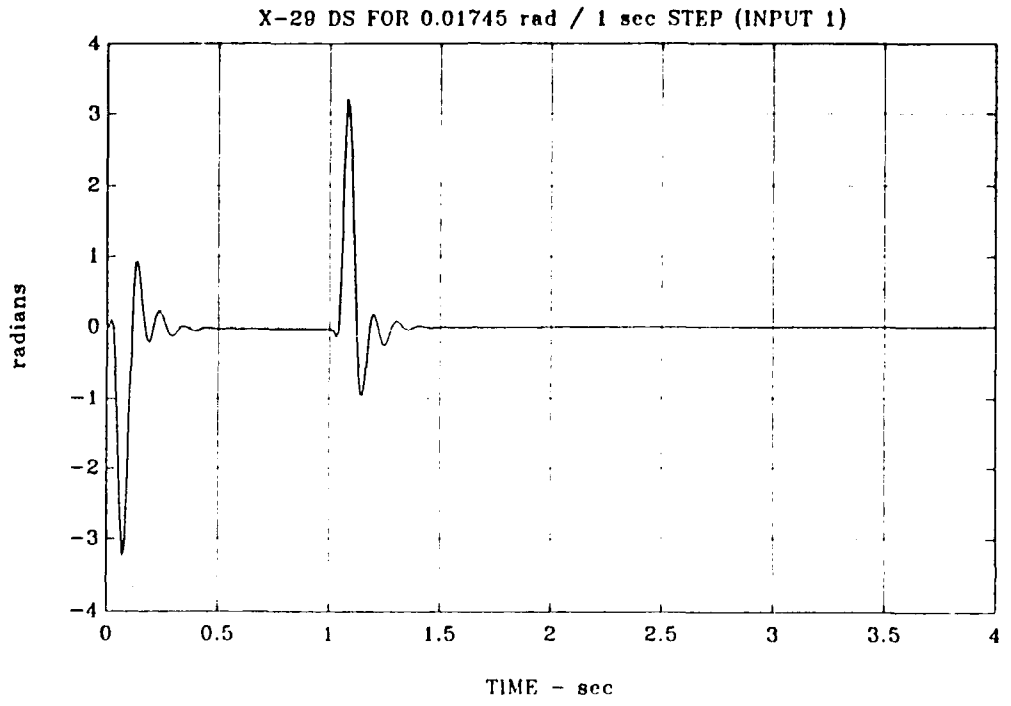

Figure 4.29 (Cont) Compensated X-29 Control Deflections δ_c, δ_f, and δ_s for for Input 1

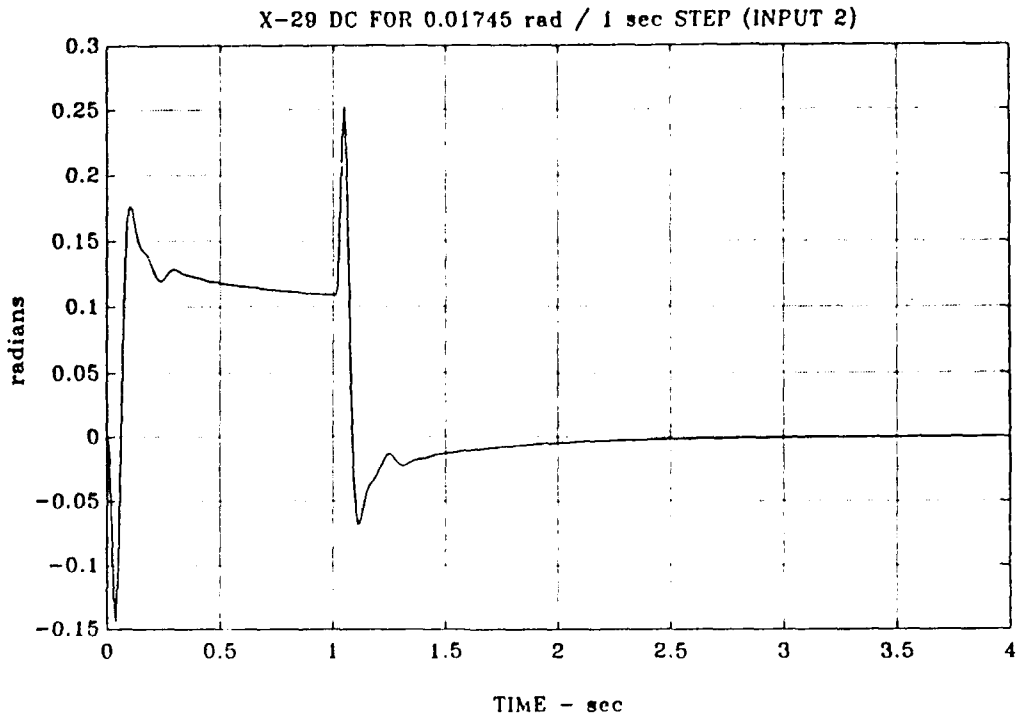

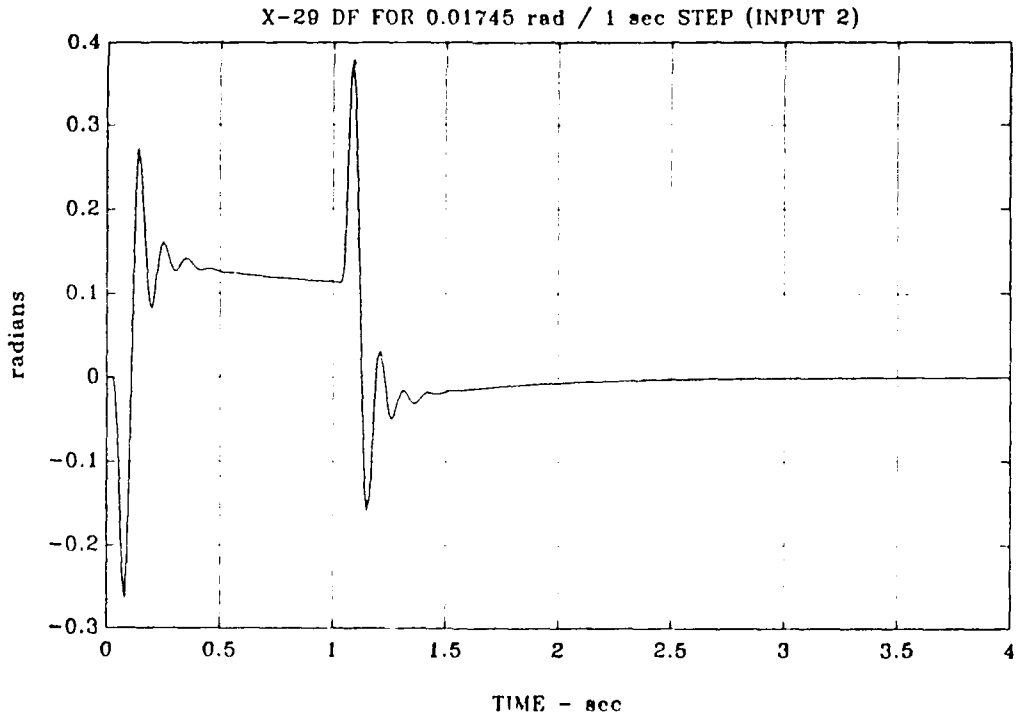

Figure 4.30 Compensated X-29 Control Deflections δ_c, δ_f, and δ_s for for Input 2

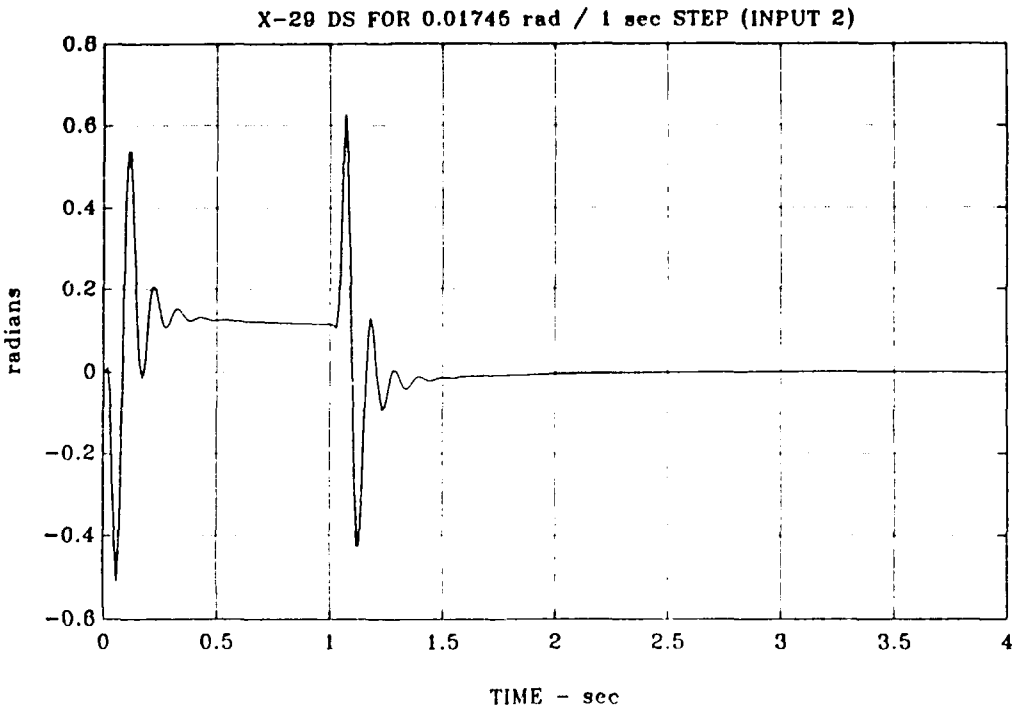

Figure 4.30 (Cont) Compensated X-29 Control Deflections δ_c, δ_f, and δ_s for for Input 2

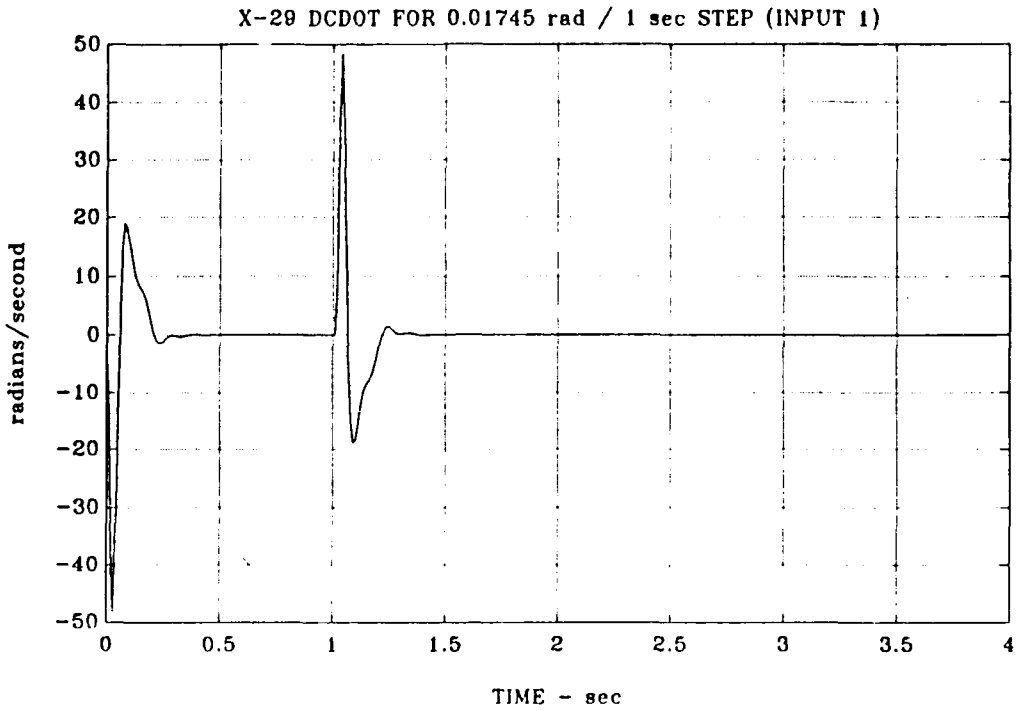

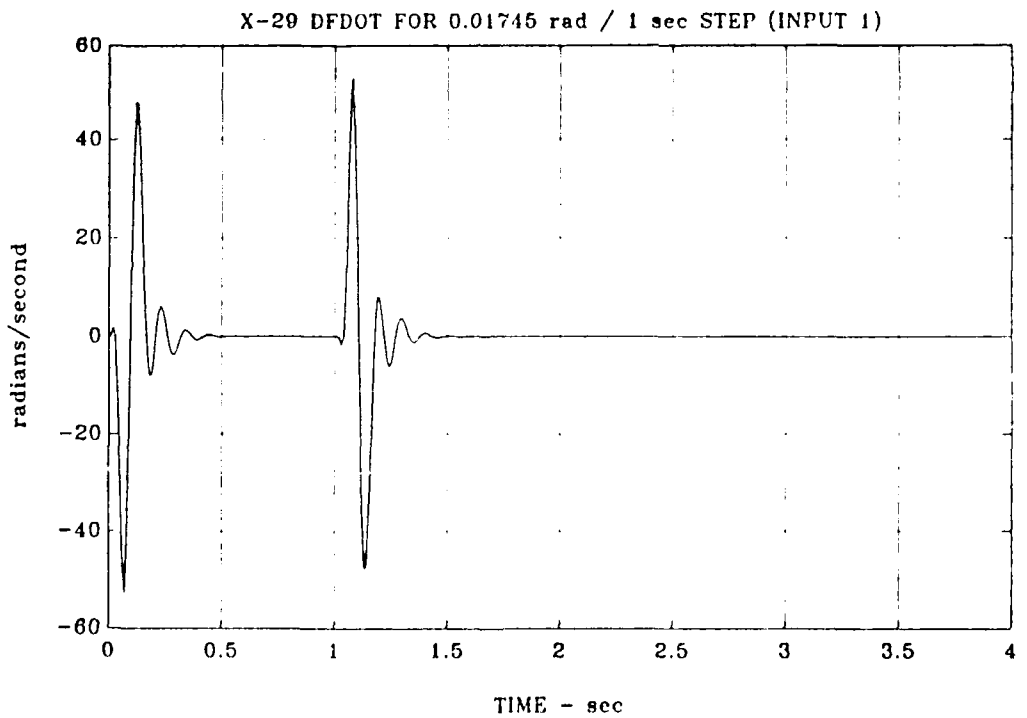

Figure 4.31 Compensated X-29 Control Rates $\dot{\delta}_c$, $\dot{\delta}_f$, and $\dot{\delta}_s$ for Input 1

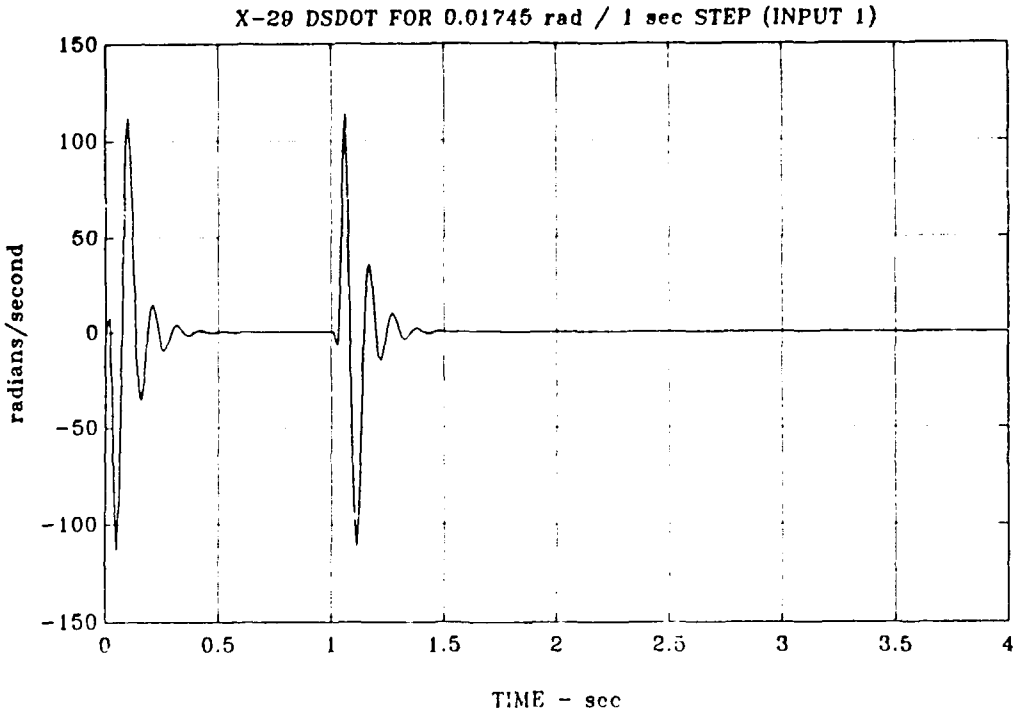

Figure 4.31 (Cont) Compensated X-29 Control Rates $\dot{\delta}_c$, $\dot{\delta}_f$, and $\dot{\delta}_s$ for Input 1

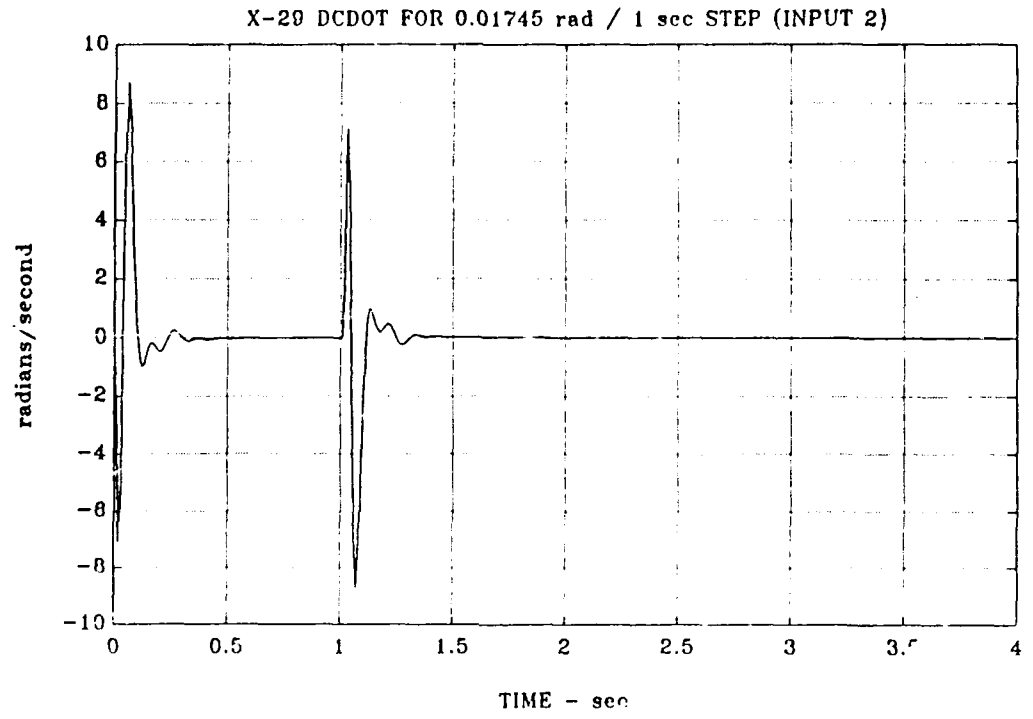

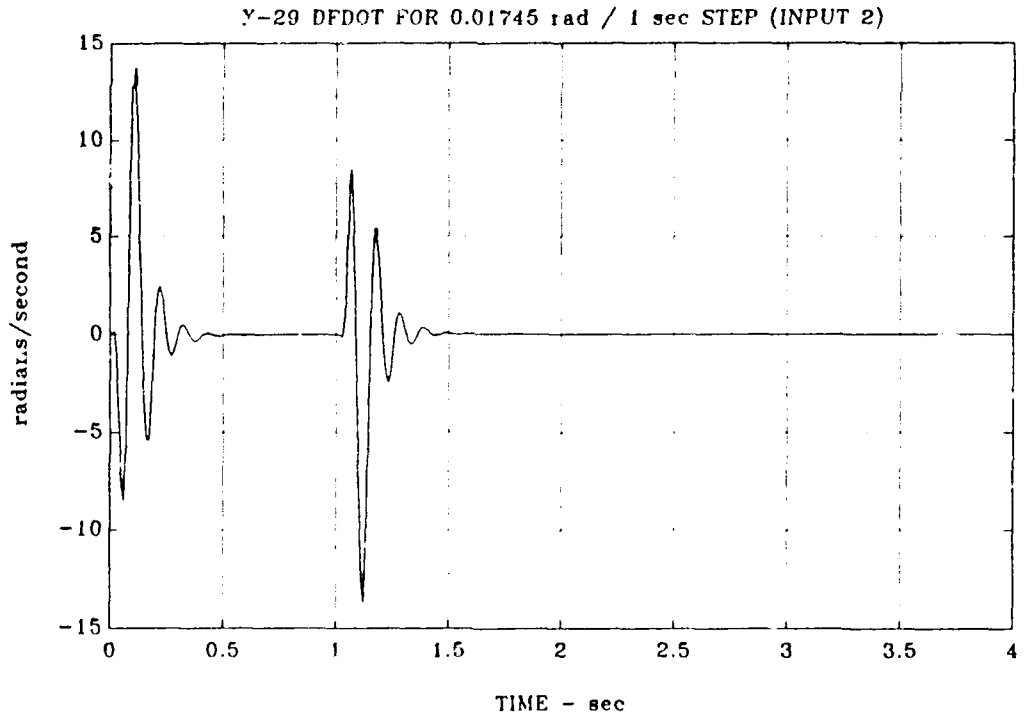

Figure 4.32 Compensated X-29 Control Rates $\dot{\delta}_c$, $\dot{\delta}_f$, and $\dot{\delta}_s$ for Input 2

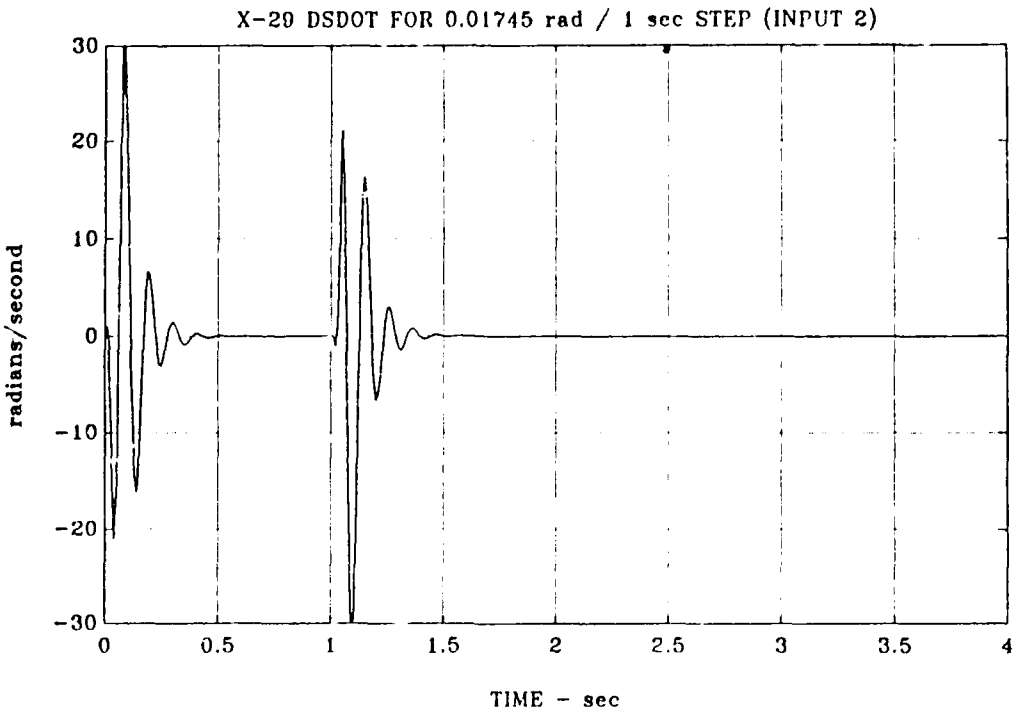

Figure 4.32 (Cont) Compensated X-29 Control Rates $\dot{\delta}_c$, $\dot{\delta}_f$, and $\dot{\delta}_s$ for Input 2

control rates for both inputs 1 and 2, ranging from approximately 8 rad/sec to over 100 rad/sec, greatly exceed the X-29 actuator, minimum design requirements of;

1. canards: 1.75 rad/sec (100 deg/sec),
2. flaps: .87 rad/sec (50 deg/sec),
3. strakes: .52 rad/sec (30 deg/sec).

E. LIMITED-PERFORMANCE H_∞ CONTROLLER DESIGN

The H_∞ synthesis of a stabilizing controller for the X-29 was reworked to bring the control surface deflections and control rates more into line with physical capabilities. A

secondary objective was to retain the system robustness achieved with the initial H_∞ controller. To accomplish these objectives, a greater weighting or penalty was applied to the control input vector **u** of Figure 3.2. This was effected by increasing the magnitude of the $W_2(s)$ ϵ term to .025. Additionally, the upper corner frequency of the $W_1^{-1}(s)$ weighting function was moved from 100 rad/sec to 10 rad/sec to restrain the sensitivity function overshoot near the 0 dB crossover frequency. The weighting function assignments for the limited-performance controller design are:

$$(\gamma W_1)^{-1}(s) = \gamma^{-1} * \frac{.01(100s + 1)}{.1s + 1} * \mathbf{I}_{(2 \times 2)}$$

$$W_2(s) = \left[\begin{array}{c|c} \mathbf{A} & \mathbf{B} \\ \hline \mathbf{C} & \mathbf{D} \end{array}\right] = -.025 * \mathbf{I}_{(4 \times 4)}$$

$$W_3^{-1}(s) = \frac{1000}{s^2} * \mathbf{I}_{(2 \times 2)}. \qquad (4.5)$$

A plot of the $W_1^{-1}(s)$ and $W_3^{-1}(s)$ weighting functions is shown in Figure 4.33.

To avoid confusion, the initial H_∞ controller design will be referred to as the optimal-performance case. This is not meant to imply that the solution is the result of a cost function minimization as with the LQ regulator problem. Rather it implies the compensated X-29 performance is optimal

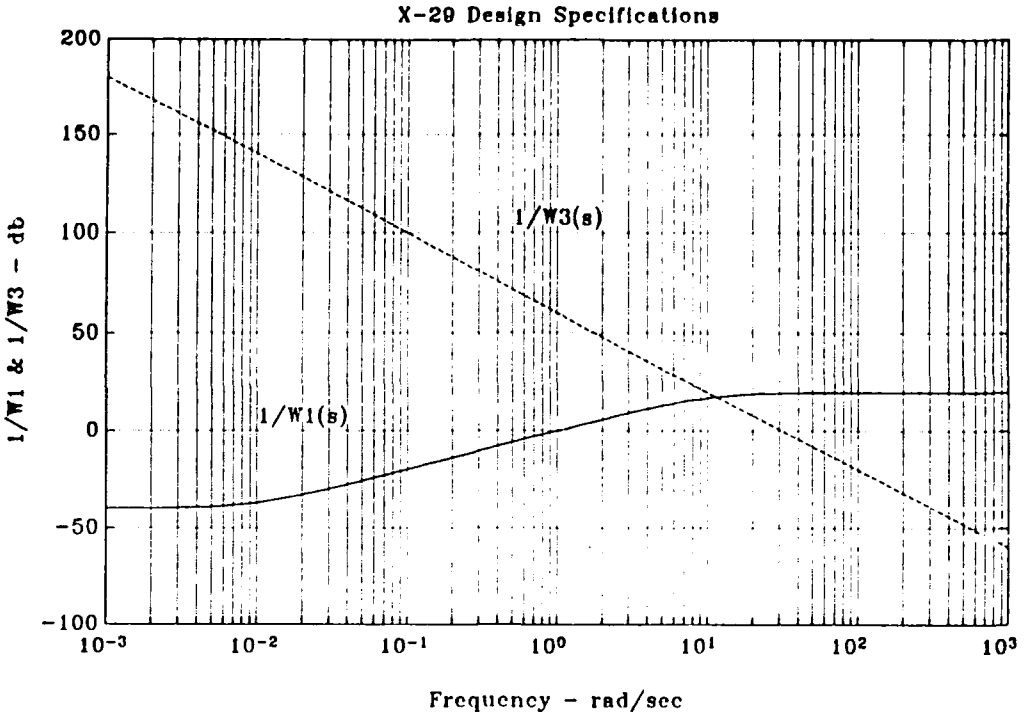

Figure 4.33 Limited-Performance X-29 H_∞ Design Specifications

with respect to the design specifications. The reworked controller design will be termed the limited-performance case.

With a maximum achievable γ of 2.62, the limited-performance H_∞ solution is only able to push the $\|T_{y_1u_1}\|_\infty$ cost function singular values to within 5 dB of the "all pass limit" (Figure 4.34) as compared to .5 dB for the optimal-performance H_∞ solution (Figure 4.8). The singular value plots of the sensitivity function $\mathbf{S}(s)$ and the complementary sensitivity function $\mathbf{T}(s)$ for the limited-performance X-29

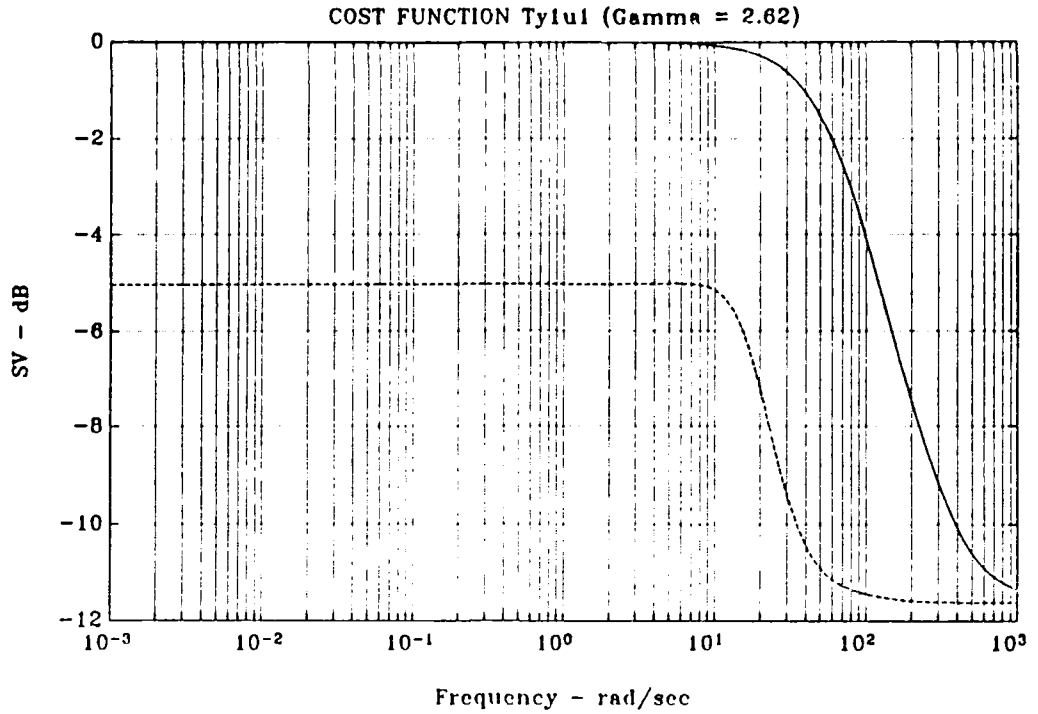

Figure 4.34 H_∞ Cost Function $\|T_{y1u1}\|_\infty$ for γ=2.62, Limited-Performance X-29

are presented in Figures 4.35 and 4.36, respectively. These figures are from the H_∞ solution for a γ of 2.62. Comparison of Figures 4.35 and 4.36 with Figures 4.11 and 4.14 shows that the feedback properties of the limited-performance X-29 are not as robust as those of the optimal-performance aircraft. The limited-performance X-29 is characterized by smaller disturbance attenuation, larger sensitivity to plant variations and modeling errors, a smaller control bandwidth, and a smaller closed loop bandwidth.

The state space realization of the 29th order, closed loop limited-performance model is presented in Appendix B, and the closed loop poles are listed in Table 4.4. Note that, once

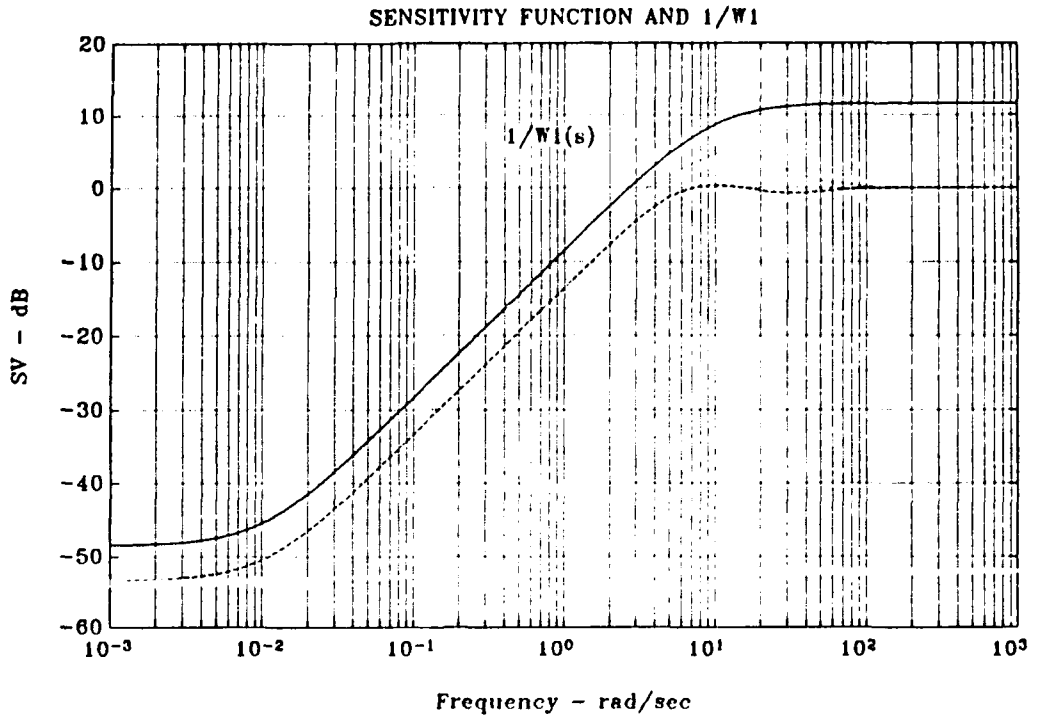

Figure 4.35 Sensitivity Function **S**(s) for H_∞ Solution, γ=2.62, Limited-Performance X-29

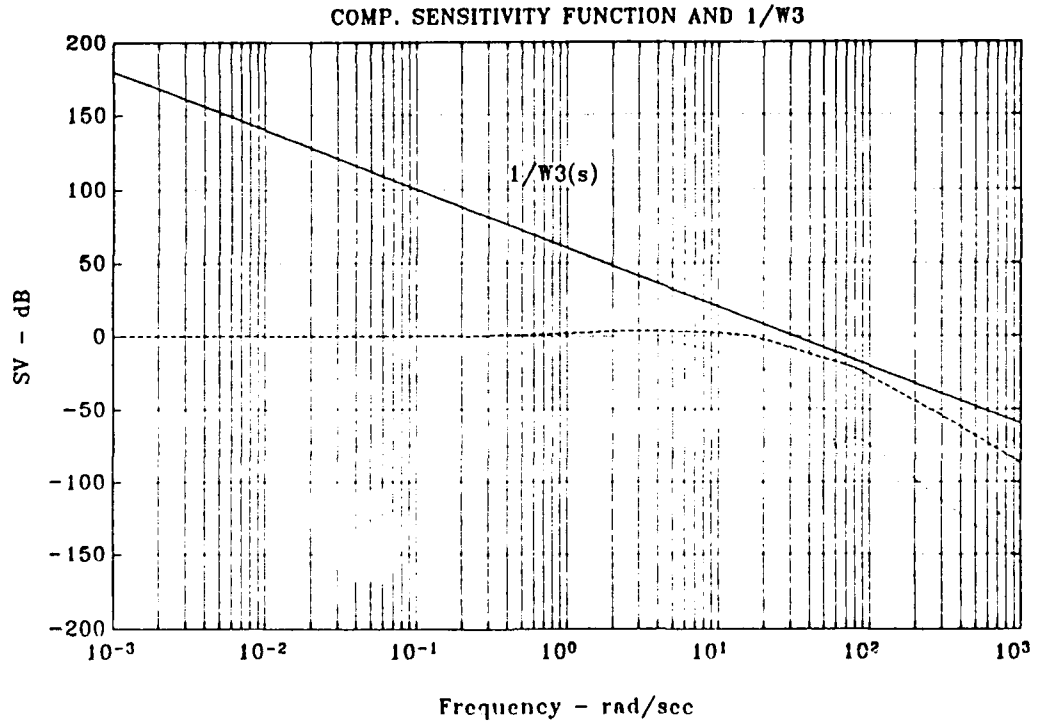

Figure 4.36 Complementary Sensitivity Function **T**(S) for H_∞ Solution, γ=2.62, Limited-Performance X-29

TABLE 4.4

CLOSED LOOP POLES OF THE LIMITED-PERFORMANCE X-29

$$
\begin{array}{l}
-2.2747e{+}02 \pm 2.3201e{+}02i \\
-1.3612e{+}02 \\
-1.4415e{+}02 \\
-1.4494e{+}02 \\
-1.4476e{+}02 \\
-1.0023e{+}02 \\
-5.1688e{+}01 \pm 7.7445e{+}01i \\
-7.2313e{+}01 \\
-3.7606e{+}01 \pm 5.2777e{+}01i \\
-5.1716e{+}01 \pm 5.0560e{+}01i \\
-5.3298e{+}01 \pm 4.7220e{+}01i \\
-5.2512e{+}01 \pm 4.8306e{+}01i \\
-5.0505e{+}01 \\
-3.6342e{+}01 \\
-1.1889e{+}01 \pm 1.2160e{+}01i \\
-1.9539e{+}00 \\
-2.7204e{+}00 \\
-3.7372e{+}00 \\
-9.6752e{+}00 \\
-2.0387e{+}01 \pm 1.1180e{+}00i \\
-2.1180e{+}01
\end{array}
$$

again, the unstable short period pole of the open loop system was mirrored into the left-half plane of the closed loop system, i.e., -1.9539.

Review of the output return difference matrices confirms the above characterizations of the limited-performance aircraft (Figures 4.37 and 4.38). The singular value plot of $\sigma_{min}[\mathbf{I} + \mathbf{G}(j\omega)\mathbf{F}(j\omega)]$ (Figure 4.37) clearly shows a smaller loop gain as compared to that of the optimal-performance X-29 (Figure 4.21). Referring to Figure 4.38, $\sigma_{min}[\mathbf{I} + (\mathbf{G}(j\omega)\mathbf{F}(j\omega))^{-1}]$ drops to approximately -3.45 dB, a .67 singular value, between 1 rad/sec and 10 rad/sec. Using the universal gain and phase margin curve of Figure 4.23, this equates to a gain and phase

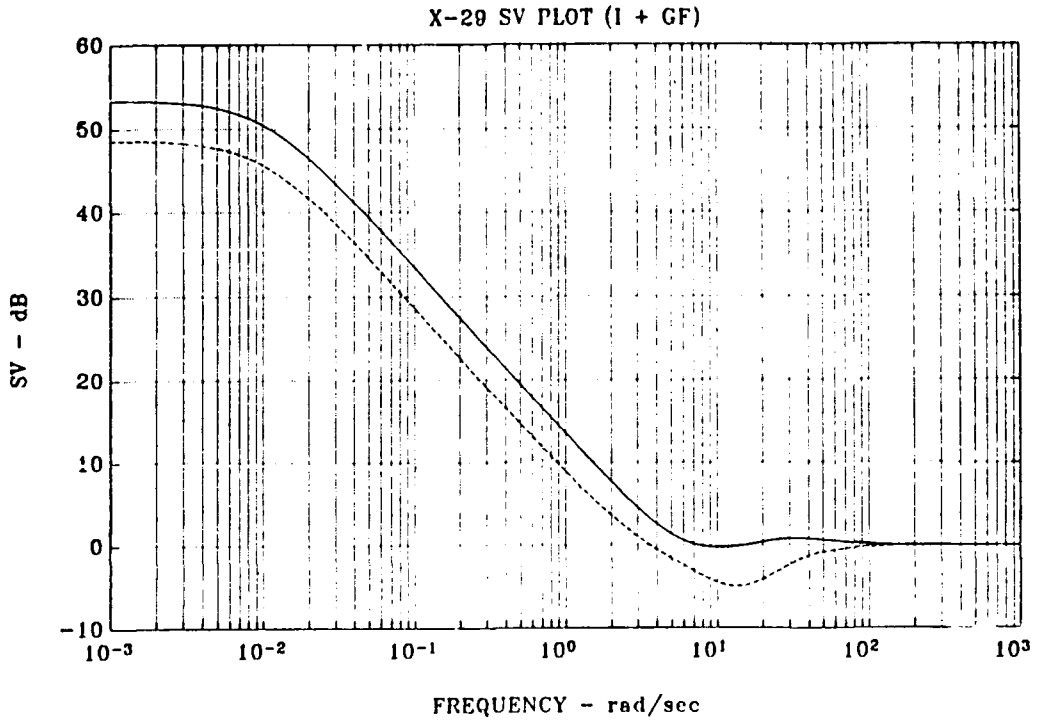

Figure 4.37 Singular Value Plot I + G(s)F(s), Limited-Performance X-29

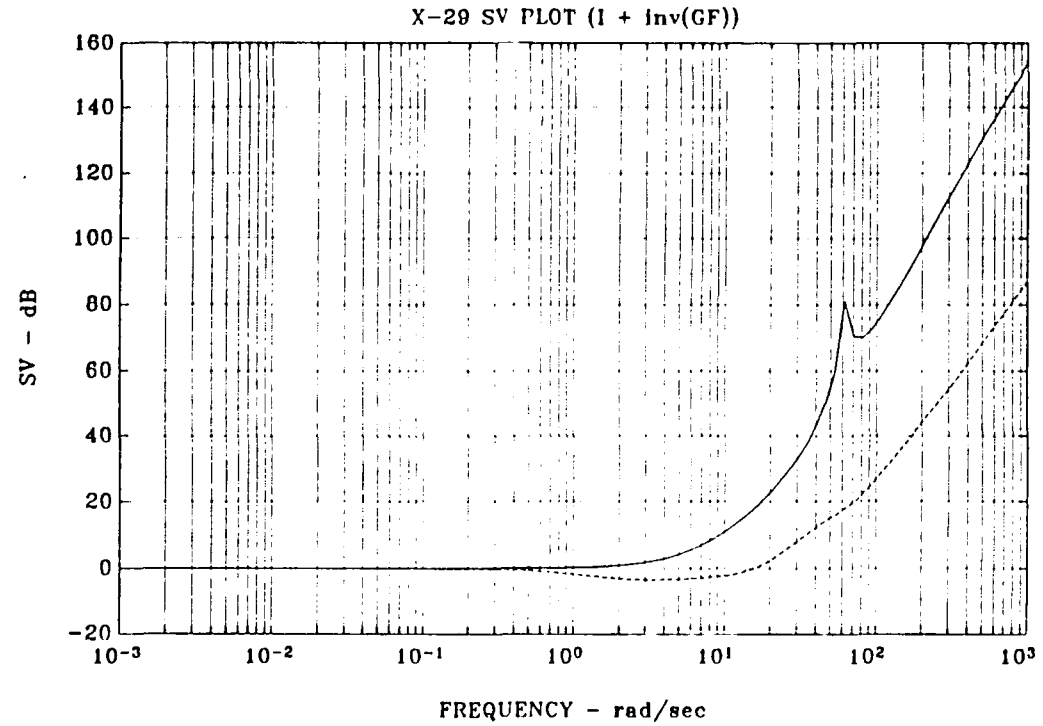

Figure 4.38 Singular Value Plot I + $(G(s)F(s))^{-1}$, Limited-Performance X-29

margin of -10 dB to +5 dB and ±39 deg, respectively. Therefore, the stability margins of the limited-performance X-29, with respect to multiplicative modeling errors, is closer to the values desired of a fighter aircraft, i,e., -8 dB to +4 dB, ±35 deg gain and phase margin, respectively.

The singular value plot of the input, additive return difference matrix (Figure 4.39) shows that the limited-performance H_∞ solution also did not satisfy the desired performance objectives at the X-29 plant inputs. That is, $\sigma_{min}[\mathbf{I} + \mathbf{F}(j\omega)\mathbf{G}(j\omega)]$ is small, especially between .8 rad/sec and 30 rad/sec. However, the singular value plot of the input, inverse-return difference matrix (Figure 4.40) shows that the required stability constraints are met at the X-29 plant inputs, i.e.,

$$\sigma_{min}[\mathbf{I} + (\mathbf{F}(j\omega)\mathbf{G}(j\omega))^{-1}] > |W_3(j\omega)|.$$

Although the stability constraints are satisfied, the relative stability with respect to multiplicative modeling errors is very low between .7 rad/sec and 15 rad/sec. This is evidenced by the large sub-0 dB values of $\sigma_{min}[\mathbf{I} + (\mathbf{F}(j\omega)\mathbf{G}(j\omega))^{-1}]$. A minimum singular value of -13 dB at 4 rad/sec equates to a gain and phase margin of -2 dB to 2 dB and ±12 deg, respectively.

Identical step inputs were applied to the limited-performance X-29 model as were previously applied to the

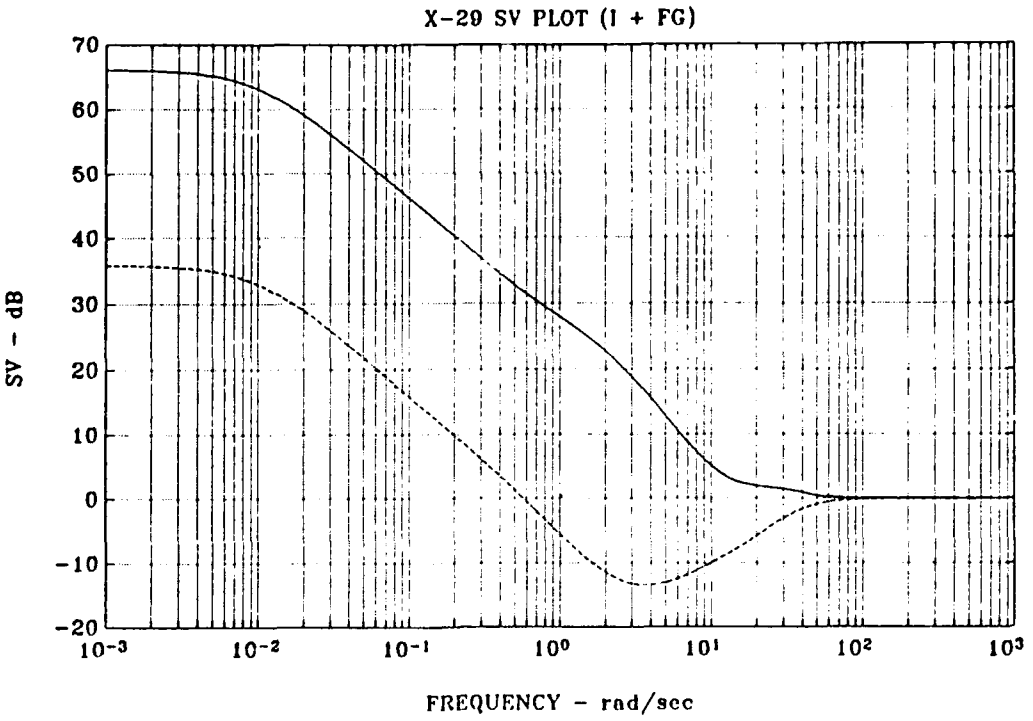

Figure 4.39 Singular Value Plot I + F(s)G(s), Limited-Performance X-29

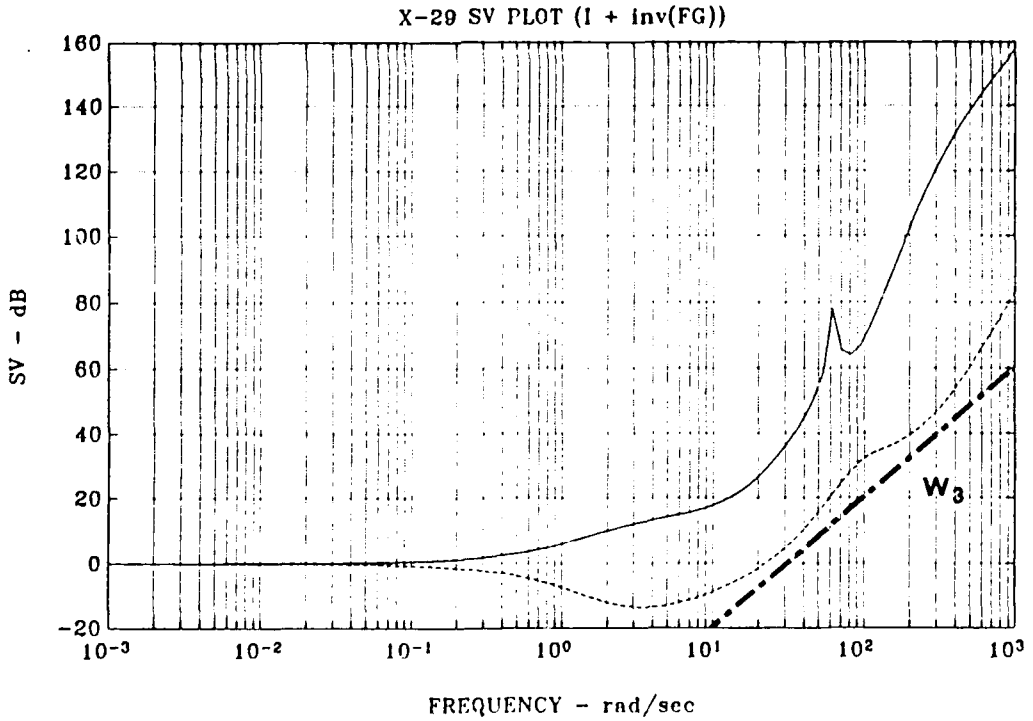

Figure 4.40 Singular Value Plot I + $(F(s)G(s))^{-1}$, Limited-Performance X-29

optimal-performance model. Figures 4.41 and 4.42 show the α and q responses of the limited-performance X-29 for inputs 1 and 2, respectively. As with the optimal-performance X-29, the limited-performance X-29 responds to input 1 (r_1) with a positive α while input 2 (r_2) effects a positive q response. However, the decoupling of the α and q responses is not as pronounced as observed in the optimal-performance X-29. This indicates that the precision flight path modes are not achieved in the limited-performance X-29 to the extent observed in the optimal-performance case. The limited-performance X-29 responses to the step inputs are slower with rise times of .5 sec and .22 sec for α and q, respectively. This is a result of the smaller closed loop bandwidth observed in the complementary sensitivity function.

The control deflections δ_c, δ_f, and δ_s for the limited-performance X-29 (Figures 4.43 and 4.44) are considerably smaller than observed for the optimal-performance case. The peak magnitudes of the deflections for inputs 1 and 2 vary from .1 rad to .33 rad and, with the exception of negative flap deflection for input 1, are well within the X-29 control surface deflection limits. It is also seen that the input 1 and 2 deflections are more closely matched. Similar observations are made for the control rates $\dot{\delta}_c$, $\dot{\delta}_f$, and $\dot{\delta}_s$ for inputs 1 and 2 shown in Figures 4.45 and 4.46, respectively.

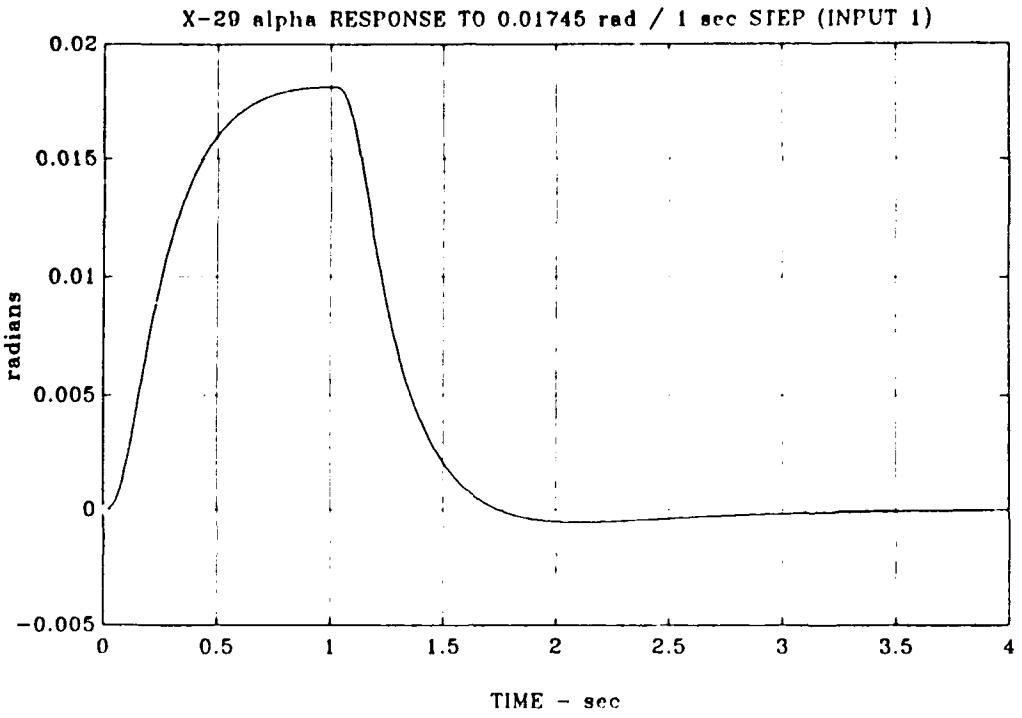

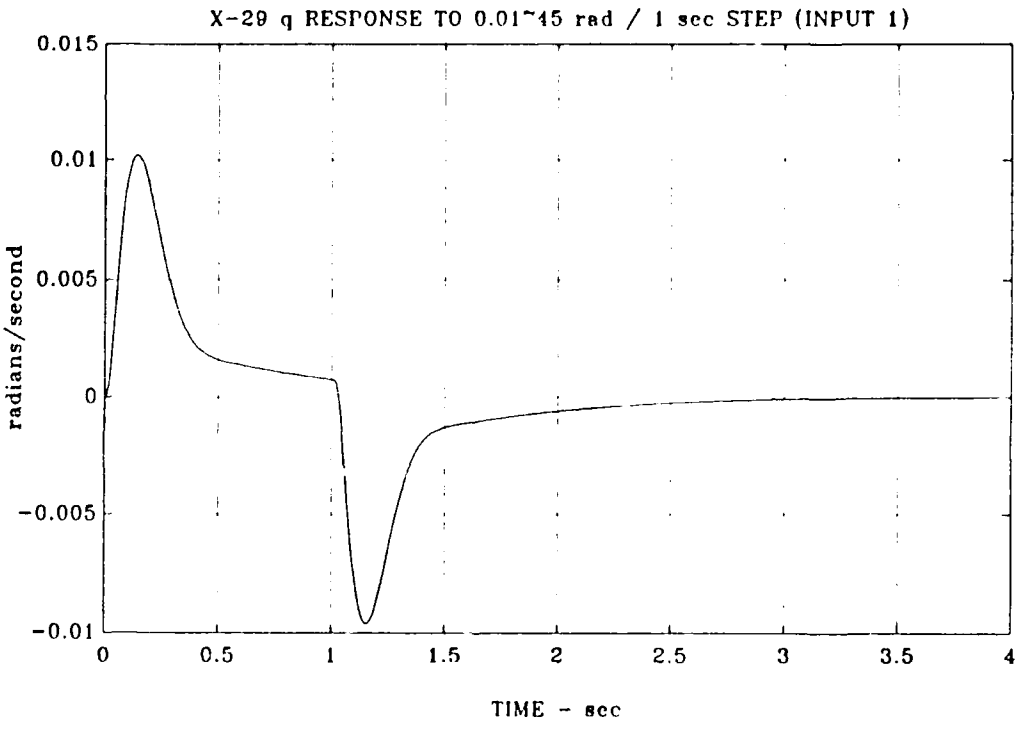

Figure 4.41 Limited-Performance X-29 α and q Responses to Input 1

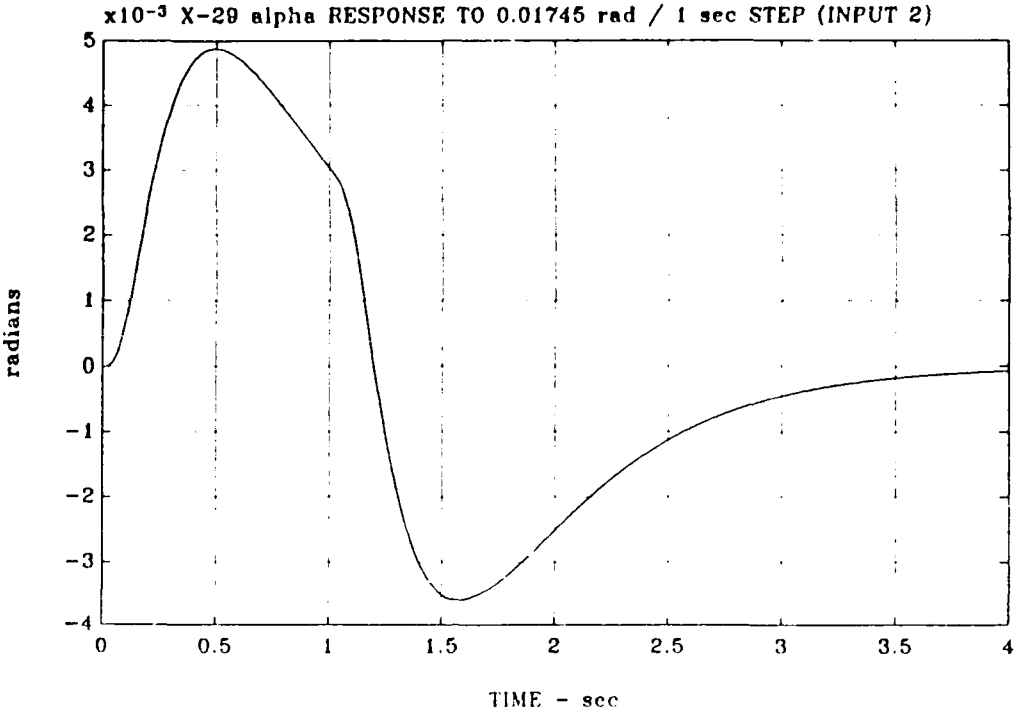

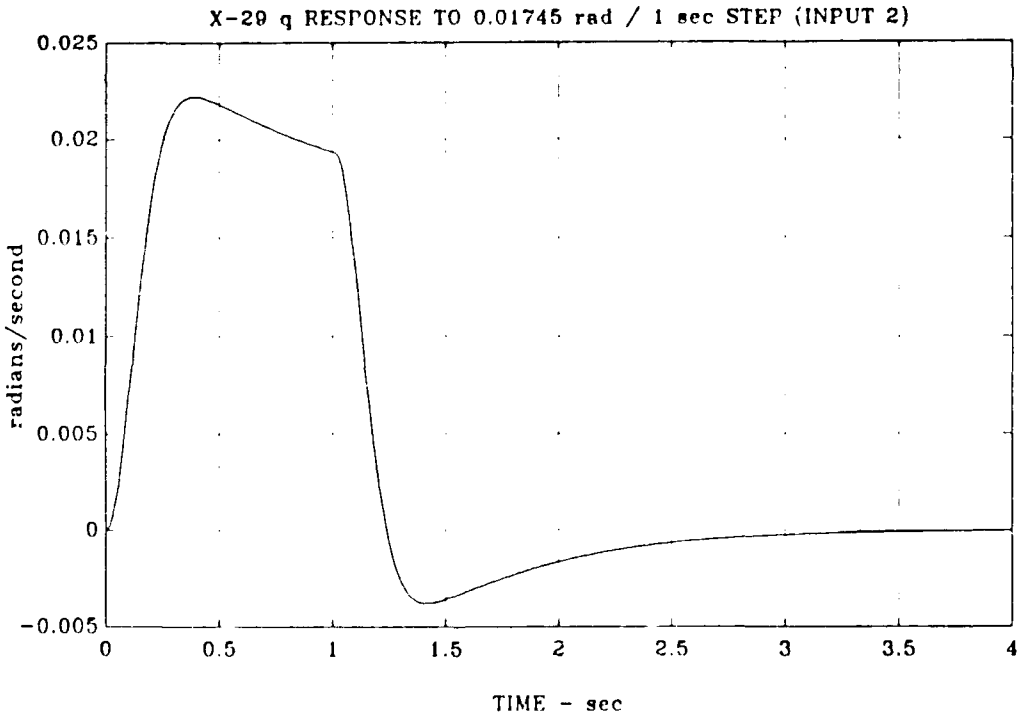

Figure 4.42 Limited-Performance X-29 α and q Responses to Input 2

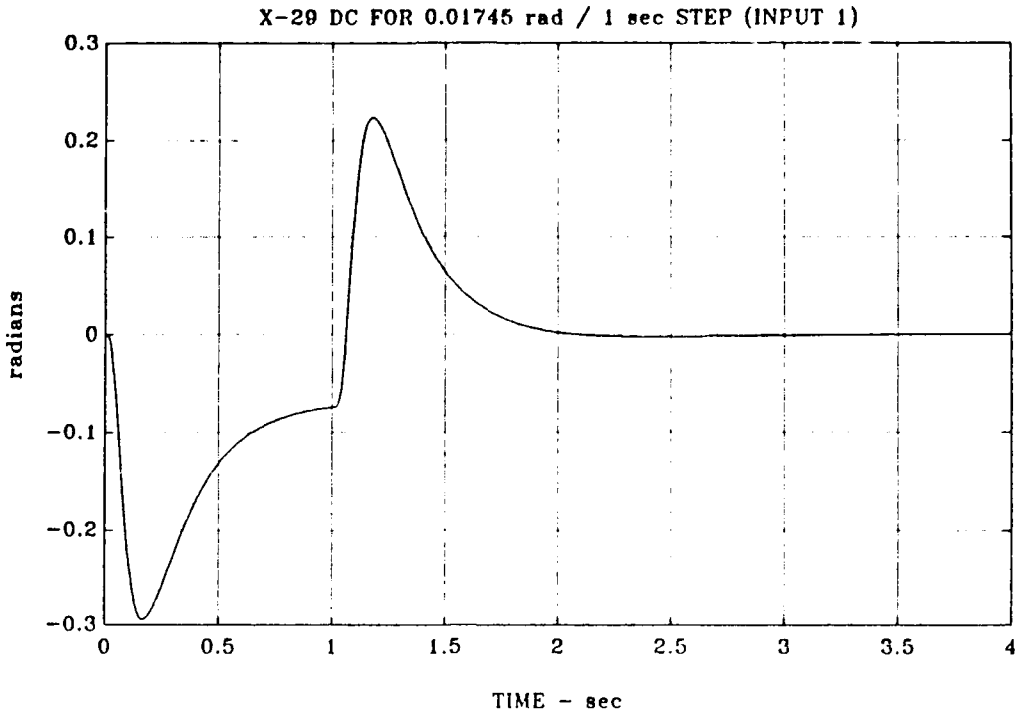

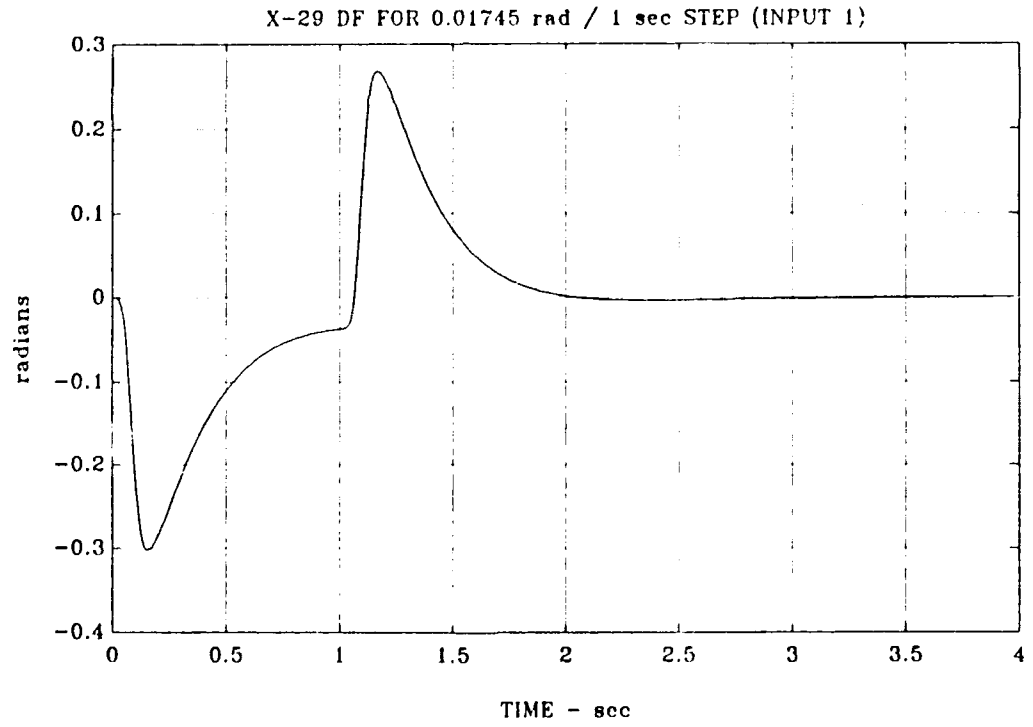

Figure 4.43 Limited-Performance X-29 Control Deflections δ_c, δ_f, and δ_s for Input 1

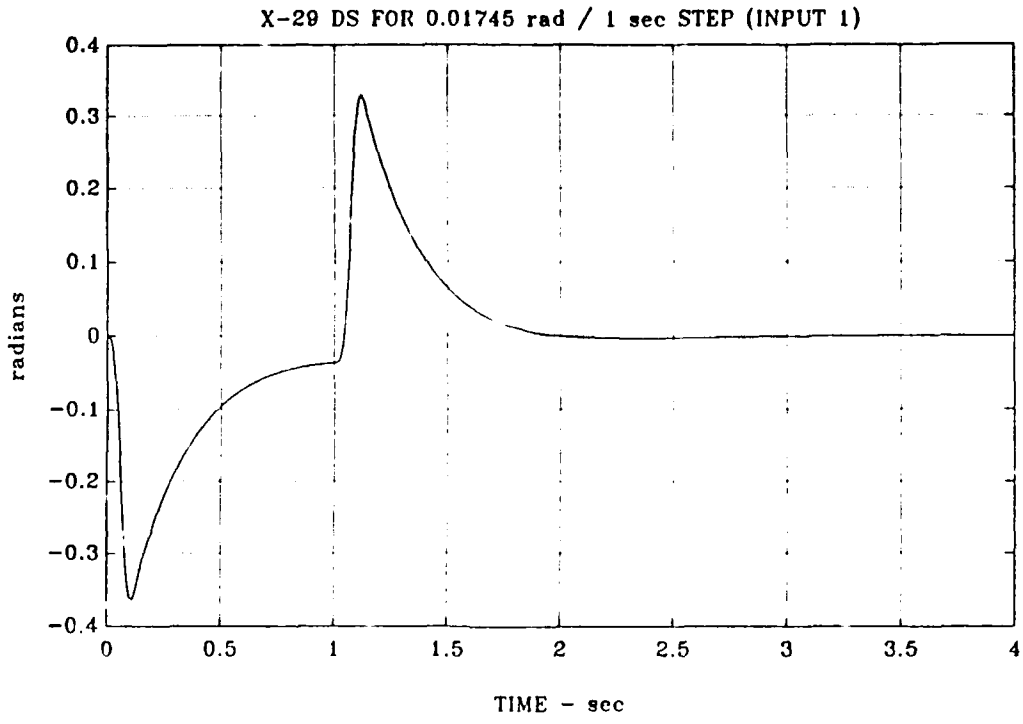

Figure 4.43 (Cont) Limited-Performance X-29 Control Deflections δ_c, δ_f, and δ_s for Input 1

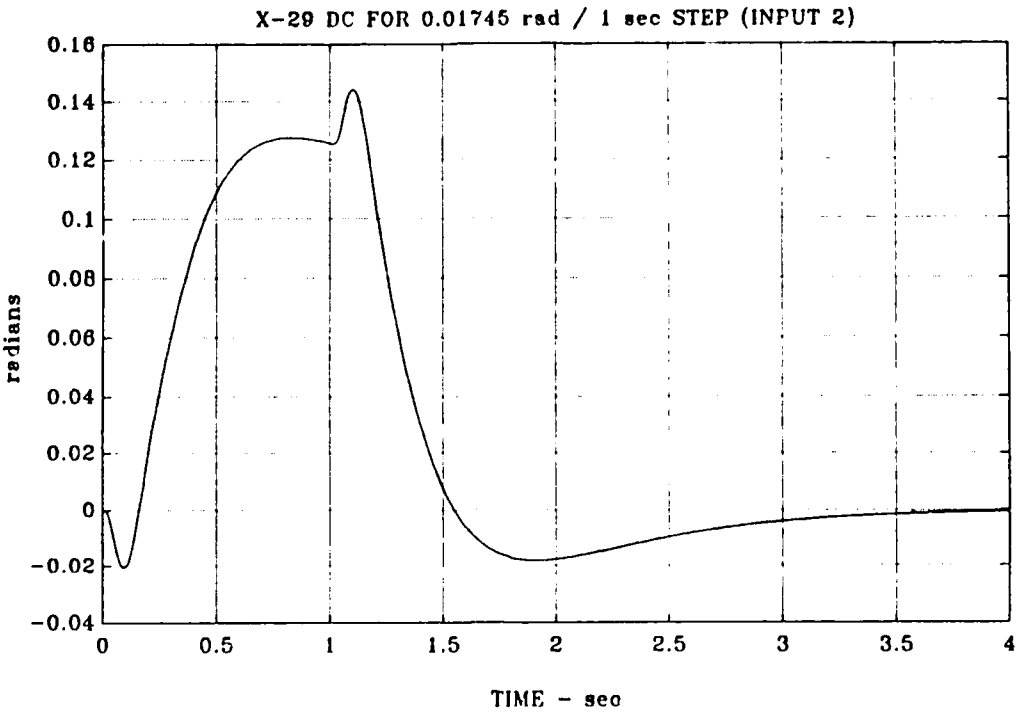

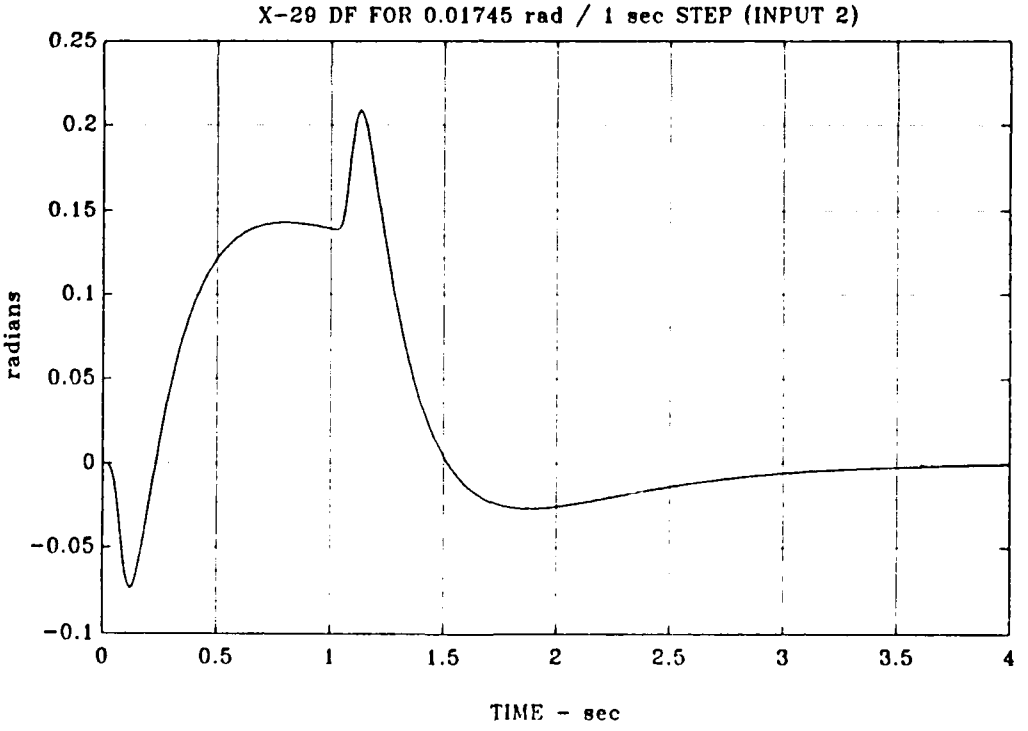

Figure 4.44 Limited-Performance X-29 Control Deflections δ_c, δ_f, and δ_s for Input 2

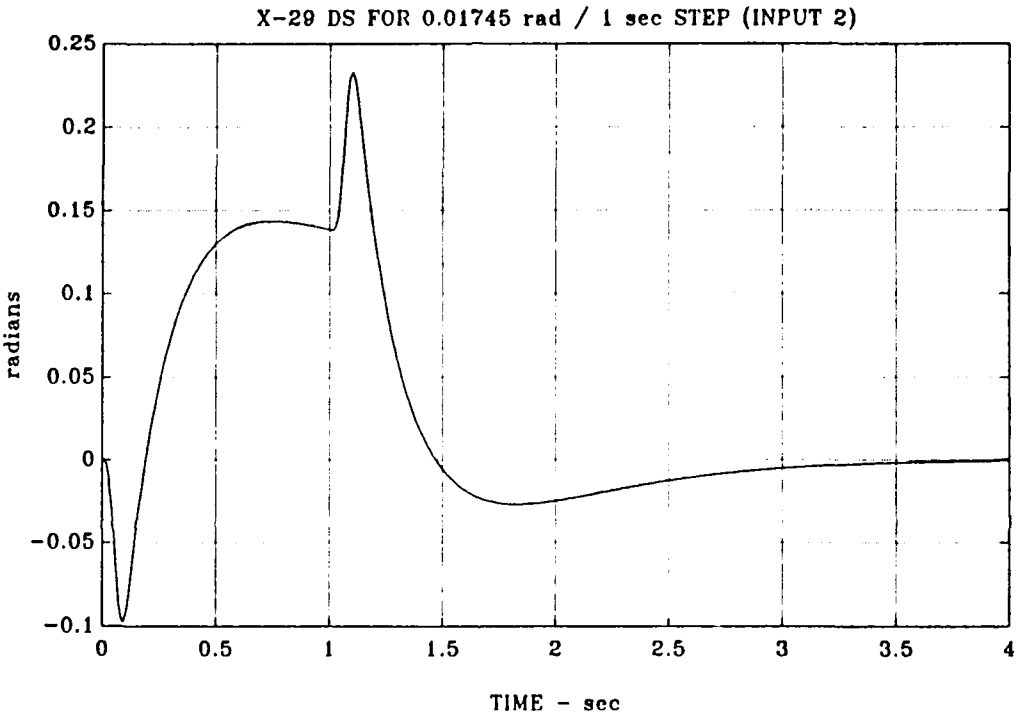

Figure 4.44 (Cont) Limited-Performance X-29 Control Deflections δ_c, δ_f, and δ_s for Input 2

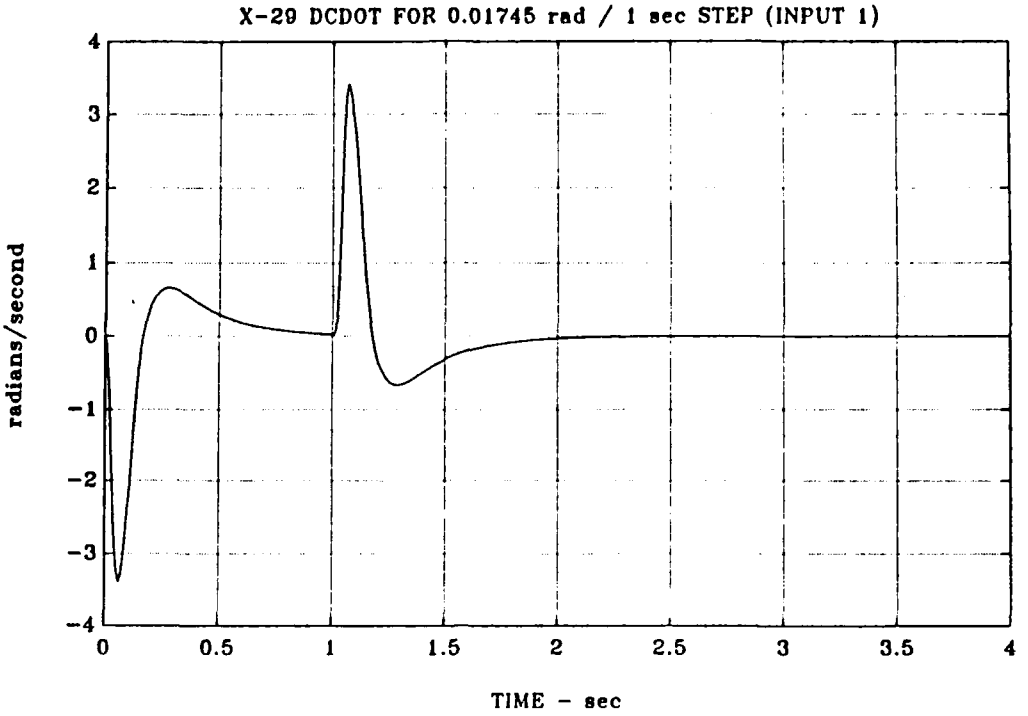

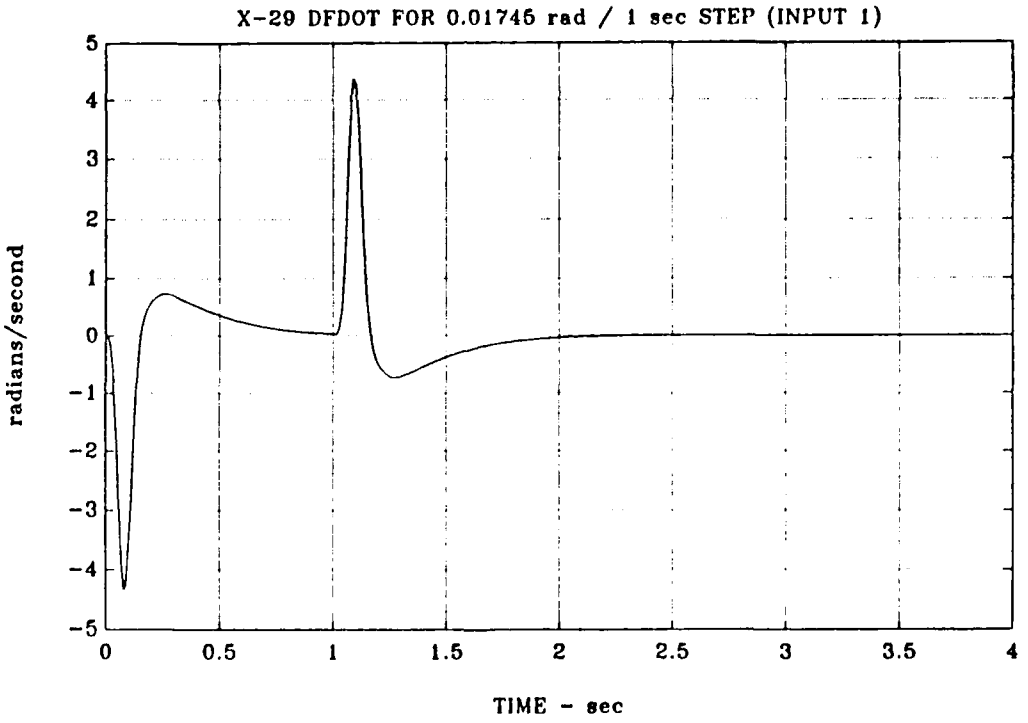

Figure 4.45 Limited-Performance X-29 Control Rates $\dot{\delta}_c$, $\dot{\delta}_f$, and $\dot{\delta}_s$ for Input 1

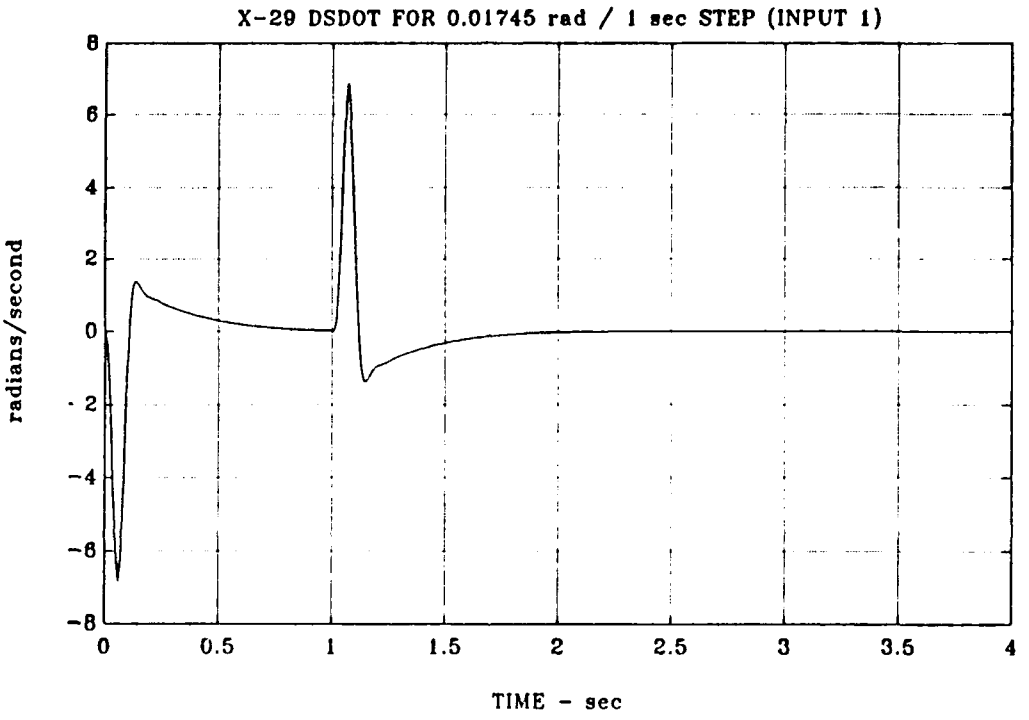

Figure 4.45 (Cont) Limited-Performance X-29 Control Rates $\dot{\delta}_c$, $\dot{\delta}_f$, and $\dot{\delta}_s$ for Input 1

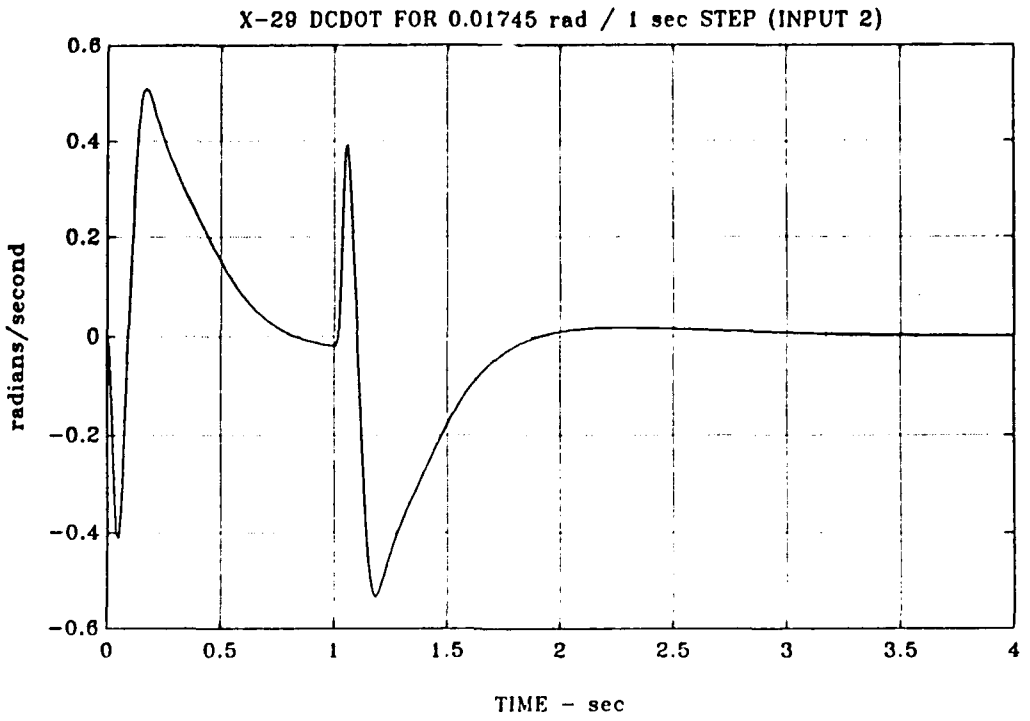

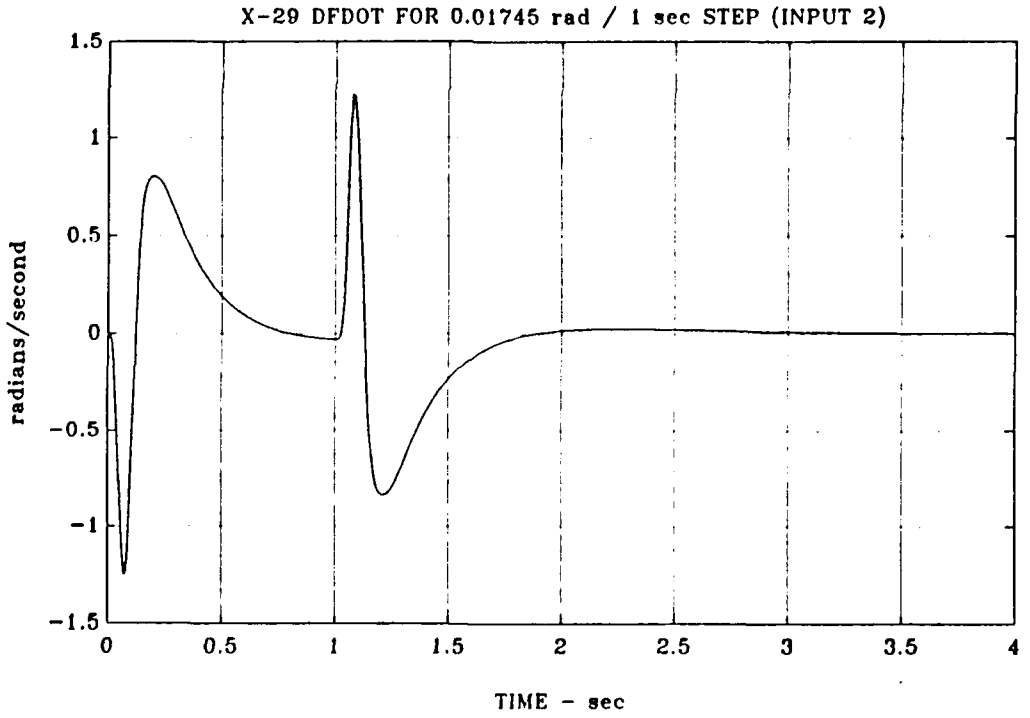

Figure 4.46 Limited-Performance X-29 Control Rates $\dot{\delta}_c$, $\dot{\delta}_f$, and $\dot{\delta}_s$ for Input 2

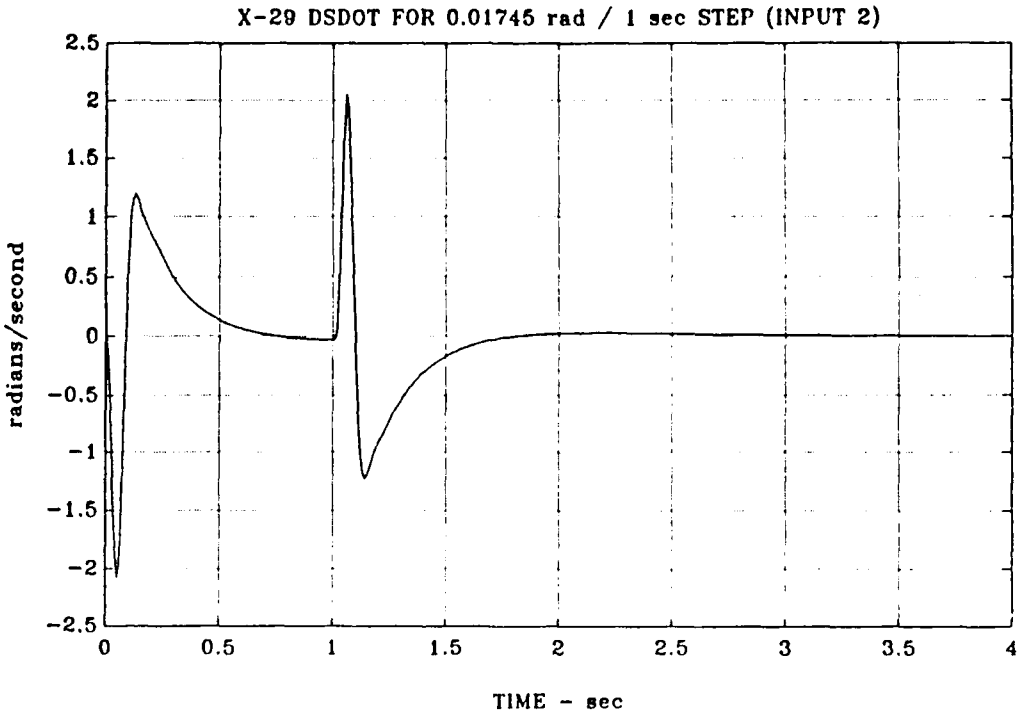

Figure 4.46 (Cont) Limited-Performance X-29 Control Rates $\dot{\delta}_c$, $\dot{\delta}_f$, and $\dot{\delta}_s$ for Input 2

That is, the peak control rates of the limited-performance X-29 range from .4 rad/sec to approximately 7 rad/sec which, with the exception of $\dot{\delta}_c$ for input 2, exceed the actuators' capabilities.

Although the primary objective of the limited-performance H_∞ controller was achieved, i.e., the control deflections and control rates were reduced, it is obvious from the results that the performance robustness of the compensated X-29 was reduced. Considering the results of the optimal-performance and limited-performance H_∞ solutions, there is a direct relationship between the level of system performance attained

and the weighting of the control inputs **u** (Figure 3.2). Small control weightings permit a greater influx of energy into the plant **G**(s) and improve system performance, i.e., larger loop gains and a larger control bandwidth. The constraint for this particular example is the physical plant's inability to accommodate the energy levels necessary to attain the desired levels of performance. That is, actuator performance is inadequate for the compensated X-29 to achieve the performance levels specified in the H_∞ small gain problem. The limited-performance solution works around this constraint by penalizing the control input **u** more heavily and accepting a reduced system performance.

V. CONCLUSIONS AND RECOMMENDATIONS

H_∞ control theory provided a systematic and effective procedure to synthesize a stabilizing controller for the statically unstable X-29. The framework of H_∞ control theory ensured that the performance and stability design specifications, i.e., the γW_1 and W_3 weightings, were satisfied. As a result, the H_∞ optimal-performance X-29 demonstrates (at the plant outputs) good disturbance attenuation, low sensitivity to plant variations and modeling errors over a control bandwidth of 9 rad/sec, and sufficient stability margin to tolerate perturbations from the unmodeled flexible mode dynamics.

Additionally, H_∞ control theory demonstrated an ability to cope with a true multivariable design problem such as the multiple, independently controlled surfaces characteristic of a super-maneuverable aircraft. The H_∞ optimal-performance X-29 demonstrates a quick response to command inputs along with a decoupling of its angle-of-attack and pitch modes. This latter attribute is necessary to effect the advanced control modes in which aircraft flight path and pitch attitude are independently controlled. However, the results also show that the control surface actuators are saturated by the high input energy necessary to realize the performance specifications. That is, the control surface deflections and

control rates required to effect the desired performance attributes exceed the present actuators' performance capabilities.

It was shown that a work-around to the problem of actuator saturation is an increased penalty on the control input **u**. The magnitude of the control surface deflections and control rates for the limited-performance X-29 model are more in line with physical capabilities at the expense of reduced performance robustness. Therefore, it is apparent that physical plant capabilities are an additional constraint in achieving the desired levels of performance, and must be included in the H_∞ problem formulation.

While H_∞ control theory ensured satisfaction of the design specifications at the X-29 plant outputs, the theory did not ensure these specifications were met at the plant inputs. This occurred since the feedback property specifications are formulated in terms of the sensitivity function $(\mathbf{I} + \mathbf{G}(s)\mathbf{F}(s))^{-1}$ and complementary sensitivity function $\mathbf{G}(s)\mathbf{F}(s)(\mathbf{I} + \mathbf{G}(s)\mathbf{F}(s))^{-1}$ which are structured in terms of the plant outputs.

It is recommended that the synthesis of an H_∞ stabilizing controller for the X-29 be repeated with actuator performance considerations included in the H_∞ problem formulation. This can be accomplished by including the control inputs δ_c, δ_f, and δ_s and/or the control rates $\dot{\delta}_c$, $\dot{\delta}_f$, and $\dot{\delta}_s$ in the output vector $\mathbf{y}_1$ (Figure 3.1). The objective of this formulation is

to design a stabilizing controller that will not saturate the control surface actuators, yet have the compensated X-29 match the performance and stability robustness achieved with the optimal-performance case.

Additionally, it is recommended that a second order $W_1(s)$ weighting function be considered in the H_∞ problem formulation in order to further suppress the sensitivity function $\mathbf{S}(s)$ at frequencies immediately below its 0 dB crossover frequency.

APPENDIX A

X-29 MATLAB SCRIPT FILES

```
%x29h2.m
diary x29h2.dat
format short e
disp('    ')
disp('     This script file is designed to solve the H2 control ')
disp('     problem for the X-29.  The 14th order FDLTI model, in state ')
disp('     space form, is that of the X-29 aircraft and actuator dynamics.')
disp('     Two states are those of the aircraft dynamics, i.e., alpha ')
disp('     and q.  The remaining 12 states are the dynamics of the ')
disp('     three, fourth order actuators, i.e., the canard, flaperon, and ')
disp('     strake actuators.  The order of the unbalanced states is as ')
disp('     follows:')
disp('       alpha, q, dc, df, ds, dcdot, dfdot, dsdot, dcdbldot,')
disp('       dfdbldot, dsdbldot, dctrpldot, dftrpldot, dstrpldot')
disp('     Given the open loop transfer function G(s)=Cinv(Is-A)B+D, a ')
disp('     stabilizing controller F(s) will be found such that the H2 norm')
disp('     of Tylul is minimized.  ')
disp('     H2 optimal control synthesis is performed to determine attainable')
disp('     performance levels.  Once completed, an Hinf control ')
disp('     synthesis is performed.')
disp('    ')
pause
clc
disp('     The scaled X-29 aircraft and actuator state space representation')
disp('    ')
ag=[-.4181d+00  .9960d+00  -.2269d-01  -.1213d+00  -.1948d-01  -.9493d-03...
     .4427d-04  -.6712d-04  .1451d-05  -.2162d-04  -.3540d-05  0.0  0.0  0.0;
     .5474d+01  -.3424d+00   .2585d+01  -.1386d+01  -.1058d+01  .3898d-02 ...
    -.1164d-01  -.6397d-02  -.2509d-03  -.5362d-03  -.2912d-03  0.0 0.0 0.0;
    0.0  0.0  0.0  0.0  0.0  1.0  0.0  0.0  0.0  0.0  0.0  0.0  0.0  0.0;
    0.0  0.0  0.0  0.0  0.0  0.0  1.0  0.0  0.0  0.0  0.0  0.0  0.0  0.0;
    0.0  0.0  0.0  0.0  0.0  0.0  0.0  1.0  0.0  0.0  0.0  0.0  0.0  0.0;
    0.0  0.0  0.0  0.0  0.0  0.0  0.0  0.0  1.0  0.0  0.0  0.0  0.0  0.0;
    0.0  0.0  0.0  0.0  0.0  0.0  0.0  0.0  0.0  1.0  0.0  0.0  0.0  0.0;
    0.0  0.0  0.0  0.0  0.0  0.0  0.0  0.0  0.0  0.0  0.0  1.0e+04  0.0  0.0;
    0.0  0.0  0.0  0.0  0.0  0.0  0.0  0.0  0.0  0.0  0.0  0.0  1.0e+04  0.0;
    0.0  0.0  0.0  0.0  0.0  0.0  0.0  0.0  0.0  0.0  0.0  0.0  0.0  1.0e+04;
    0.0  0.0  -.1479d+04  0.0  0.0  -.1143d+03  0.0  0.0  -.2529d+01  0.0 ...
    0.0  -.2697d+03  0.0  0.0;
    0.0  0.0  0.0  -.1491d+04  0.0  0.0  -.1149d+03  0.0  0.0  -.2536d+01 ...
    0.0  0.0  -.2701d+03  0.0;
    0.0  0.0  0.0  0.0  -.5302d+05  0.0  0.0  -.1816d+04  0.0  0.0 ...
    -.1790d+02  0.0  0.0  -.6053d+03]
```

```
bg=[0.0  0.0;
    0.0  0.0;
    0.0  0.0;
    0.0  0.0;
    0.0  0.0;
    0.0  0.0;
    0.0  0.0;
    0.0  0.0;
    0.0  0.0;
    0.0  0.0;
    0.0  0.0;
    .1479d+04 0.0;
    0.0  .1491d+04;
    0.0  .5308d+05]

cg=[1.0  0.0  0.0  0.0  0.0  0.0  0.0  0.0  0.0  0.0  0.0  0.0  0.0  0.0;
    0.0  1.0  0.0  0.0  0.0  0.0  0.0  0.0  0.0  0.0  0.0  0.0  0.0  0.0]


dg=zeros(2)
pause
disp('    ')
disp('    Balanced realization of the X-29 state space representation')
disp('    ')
[agbl,bgbl,cgbl,g,t]=obalreal(ag,bg,cg)
ag=agbl; bg=bgbl; cg=cgbl;
disp('    ')
disp('     Calculate the poles and transmission zeros of the open loop plant')
disp('    ')
poleg=eig(ag),  tzerog=tzero(ag,bg,cg,dg)
disp('    ')
disp('    ')
disp('     Determine the condition number of ag')
disp('    ')
disp('    ')
condag=cond(ag),  rcondag=rcond(ag)
disp('    ')
disp('    ')
pause
disp('    ')
```

```
disp('                    << Design Specifications >>  ')
disp('    ')
disp('      1). Robustness Spec. : -40 dB roll-off, -20 db @ 100 Rad/Sec.')
disp('          Associated Weighting:')
disp('    ')
disp('                      -1       1000 ')
disp('                W3(s) =   ------ * I       (fixd)')
disp('                                 2 ')
disp('                               s       2x2')
disp('    ')
disp('    ')
disp('      2). Performance Spec.: minimizing the sensitivity function')
disp('                             as much as possible.')
disp('          Associated Weighting:')
disp('    ')
disp('                                                ')
disp('                      -1       -1  (100s + 1)    ')
disp('                W1(s) = Gam  * ----------- *  I')
disp('                                      100          2x2')
disp('    ')
disp('          where "Gam" in this design is iteratively updated from 1')
w=logspace(-3,3,100);
k=1000;  mn=[2 2]; tau=0.0;
nuw3i = [0.0 k]; dnw3i = [1.0 0 0];
svw3i = bode(nuw3i,dnw3i,w); svw3i = 20*log10(svw3i);
nuw1i = [100.0 1.0]; dnw1i =[0 100.0];
svw1i = bode(nuw1i,dnw1i,w); svw1i = 20*log10(svw1i);
aw2=-.001*eye(2); bw2=zeros(2); cw2=zeros(2); dw2=-.001*eye(2);
disp('    ')
disp('    ')
disp('                   (strike a key to see the plot of the weightings ...)')
pause
semilogx(w,svw1i,w,svw3i)
grid
title('X-29 Design Specifications')
xlabel('Frequency - Rad/Sec')
ylabel('1/W1 & 1/W3 - dB')
text(.01,0,'1/W1(s)')
text(.5,100,'1/W3(s)')
meta x29specs
pause
clc
```

```
disp('                        << Problem Formulation >>')
disp('    ')
disp('    Form an augmented plant P(s) with these two weighting functions:')
disp('    ')
disp('                1). Gam*W1 penalizing error signal "e"')
disp('    ')
disp('                2). W3 penalizing plant output "y"')
disp('    ')
disp('    and find a stabilizing controller F(s) such that the H2 norm')
disp('    of TF Tylu1 is minimized, i.e.')
disp('    ')
disp('                          min |Tylu1|    < 1,')
disp('                          F(s)        2')
disp('    ')
disp('      where ')
disp('                          |                  -1|')
disp('                Tylu1 = | Gam*W1*(I + GF)  |   = | Gam * W1 * S   |')
disp('                          |                  -1|     |  W3 * (I - S)  |')
disp('                          |  W3*GF*(I + GF)  |')
disp('    ')
disp('    ')
disp('    ')
disp('                                  (strike a key to continue ...)')
pause
clc
disp('    ')
disp('    ')
disp('                                << DESIGN PROCEDUPE >>')
disp('    ')
disp('             * * * * * * * * * * * * * * * * * * * * * * * * * * * * *')
disp('             *    [Step 1]. Do plant augmentation (run AUGMENT.M or    *')
disp('             *              AUGX29.M)                                   *')
disp('             *                                                          *')
disp('             *    [Step 2]. Do H2 synthesis (run H2LQG.M)               *')
disp('             *                                                          *')
disp('             *    [Step 3]. Redo the plant augmentation for a           *')
disp('             *              new "Gam" and rerun H2LQG.M                 *')
disp('             *                                                          *')
disp('             *    [Step 4]. Redo the plant augmentation for a           *')
disp('             *              higher "Gam" then run HINF.M                *')
disp('             * * * * * * * * * * * * * * * * * * * * * * * * * * * * *')
disp('    ')
disp('    ')
disp('                                  (strike a key to continue ...)')
pause
clc
disp('    ')
disp('    ')
disp('    ')
```

```
disp('            Assign the cost coefficients "Gam" with Gam=1 ')
disp('    ')
disp('            serving as the baseline design ....')
pack
gama=[1.0,6.7];
ngama=length(gama);
for i=1:ngama
Gam=gama(1,i)
k=1000
disp('    ')
disp('             ------------------------------------------------------------')
disp('              augment    % Plant augmentation of the X-29 dynamics')
disp('             ------------------------------------------------------------')
disp('    ')
disp('    ')
augx29
disp('    ')
disp('    ')
disp('                                    (strike a key to continue ...)')
pause
clc
disp('    ')
disp('    ')
%disp('     Do state space balancing on the augmented plant if needed')
%disp('    ')
%disp('    ')
%[abal,bbal,cbal,g,t]=obalreal(A,[B1 B2],[C1;C2])
%A=abal, B1=bbal(:,1:2), B2=bbal(:,3:4), C1=cbal(1:6,:), C2=cbal(7:8,:)
disp('    ')
disp('    ')
disp('    The transmission zeros, poles and condition number of the augmented')
disp('    plant follow.  In addition, determine if (A,B1) & (A,B2) are ')
disp('    stabilizable and if (C1,A) & (C2,A) are detectable.')
disp('    ')
disp('    ')
tzeroaug=tzero(A,[B1 B2],[C1;C2],[D11 D12;D21 D22])
poleaugA=eig(A)
condaugA=cond(A)
rcondaugA=rcond(A)
eps=eps
toldef=10*max(size(A))*norm(A,1)*eps
tol=100*eps*norm([A B1])
[A1c,B1c,C1c,t,k]=ctrbf(A,B1,C1,tol)
tol=100*eps*norm([A B2])
[A2c,B2c,C2c,t,k]=ctrbf(A,B2,C2,tol)
tol=100*eps*norm([A;C1])
[A1o,B1o,C1o,t,k]=obsvf(A,B1,C1,tol)
tol=100*eps*norm([A;C2])
[A2o,B2o,C2o,t,k]=obsvf(A,B2,C2,tol)
pause
disp('    ')
disp('    ')
```

```
disp('    ------------------------------------------------------------')
disp('     h2lqg     % Running script file H2LQG.M for H2 optimization')
disp('    ------------------------------------------------------------')
aretype='Schur'
h2lqg
disp('    ')
disp('    ')
disp('                                   (strike a key to continue ...)')
clear functions
pause
pltopt           % Preparing singular values for plotting
end
disp('    ')
disp('    ')
disp('                                   (strike a key to continue ...)')
pause
disp('    ')
disp('    ')
disp('    State space representation of controller (acp, bcp, ccp, dcp) ')
disp('    and CLTF Tylul (acl, bcl, ccl, dcl) and poles, controllability, ')
disp('    observability, and condition number of the controller. ')
disp('    ')
disp('    ')
acp,bcp,ccp,dcp
polec=eig(acp)
tol=100*eps*norm([acp bcp])
[acpc,bcpc,ccpc,t,k]=ctrbf(acp,bcp,ccp,tol)
tol=100*eps*norm([acp;ccp])
[acpo,bcpo,ccpo,t,k]=obsvf(acp,bcp,ccp,tol)
condacp=cond(acp),  rcondacp=rcond(acp)
acl,bcl,ccl,dcl
polet=eig(acl)
disp('    ')
disp('    ')
disp('                                   (strike a key to continue ...)')
pause
disp('    ')
disp('    ')
disp('    Open loop state space representation of controller/plant series')
disp('    ')
[algf,blgf,clgf,dlgf]=series(acp,bcp,ccp,dcp,ag,bg,cg,dg)
polol=eig(algf)
disp('    ')
disp('    ')
disp('                                   (strike a key to continue ...)')
pause
disp('    ')
disp('    ')
```

```
disp('    Closed loop state space representation of controller/plant series,')
disp('    controllability, observability, and condition number of the closed')
disp('    loop acgf matrix. ')
disp('   ')
disp('   ')
[acgf,bcgf,ccgf,dcgf]=feedbk(algf,blgf,clgf,dlgf,2)
tol=100*eps*norm([acgf bcgf])
[acgfc,bcgfc,ccgfc,t,k]=ctrbf(acgf,bcgf,ccgf,tol)
tol=100*eps*norm([acgf;ccgf])
[acgfo,bcgfo,ccgfo,t,k]=obsvf(acgf,bcgf,ccgf,tol)
condacgf=cond(acgf)
disp('   ')
disp('   ')
disp('                                    (strike a key to continue ...)')
pause
disp('   ')
disp('    Poles of the closed loop system')
disp('   ')
polcl=eig(acgf)
end
```

```
%x29hinf.m
diary x29hinf.dat
format short e
disp('   ')
disp('   ')
disp('     This script file is designed to solve the Hinf control ')
disp('     problem for the X-29.  The 14th order FDLTI model, in state ')
disp('     space form, is that of the X-29 aircraft and actuator dynamics.')
disp('     Two states are those of the aircraft dynamics, i.e., alpha ')
disp('     and q.  The remaining 12 states are the dynamics of the ')
disp('     three, fourth order actuators, i.e., the canard, flaperon, and ')
disp('     strake actuators.  The order of the unbalanced states is as ')
disp('     follows:')
disp('   ')
disp('       alpha, q, dc, df, ds, dcdot, dfdot, dsdot, dcdbldot,')
disp('       dfdbldot, dsdbldot, dctrpldot, dftrpldot, dstrpldot')
disp('   ')
disp('     Given the open loop transfer function G(s)=Cinv(Is-A)B+D, a ')
disp('     stabilizing controller F(s) will be found such that the Hinf norm')
disp('     of Tylul is less than or equal to one.  ')
disp('   ')
disp('   ')
pause
clc
disp('     X-29 aircraft and actuator state space representation')
disp('   ')
disp('   ')
ag=[-.4181d+00  .9960d+00  -.2269d-01  -.1213d+00  -.1948d-01  -.9493d-03 ...
     .4427d-04  -.6712d-04  .1451d-05  -.2162d-04  -.3540d-05  0.0  0.0  0.0;
     .5474d+01  -.3424d+00   .2585d+01  -.1386d+01  -.1058d+01  .3898d-02 ...
    -.1164d-01  -.6397d-02  -.2509d-03  -.5362d-03  -.2912d-03  0.0 0.0 0.0;
    0.0  0.0  0.0  0.0  0.0  1.0  0.0  0.0  0.0  0.0  0.0  0.0  0.0  0.0;
    0.0  0.0  0.0  0.0  0.0  0.0  1.0  0.0  0.0  0.0  0.0  0.0  0.0  0.0;
    0.0  0.0  0.0  0.0  0.0  0.0  0.0  1.0  0.0  0.0  0.0  0.0  0.0  0.0;
    0.0  0.0  0.0  0.0  0.0  0.0  0.0  0.0  1.0  0.0  0.0  0.0  0.0  0.0;
    0.0  0.0  0.0  0.0  0.0  0.0  0.0  0.0  0.0  1.0  0.0  0.0  0.0  0.0;
    0.0  0.0  0.0  0.0  0.0  0.0  0.0  0.0  0.0  0.0  1.0  0.0  0.0  0.0;
    0.0  0.0  0.0  0.0  0.0  0.0  0.0  0.0  0.0  0.0  0.0  1.0e+04  0.0  0.0;
    0.0  0.0  0.0  0.0  0.0  0.0  0.0  0.0  0.0  0.0  0.0  0.0  1.0e+04  0.0;
    0.0  0.0  0.0  0.0  0.0  0.0  0.0  0.0  0.0  0.0  0.0  0.0  0.0  1.0e+04;
    0.0  0.0  -.1479d+04  0.0  0.0  -.1143d+03  0.0  0.0  -.2529d+01  0.0 ...
    0.0  -.2697d+03  0.0  0.0;
    0.0  0.0  0.0  -.1491d+04  0.0  0.0  -.1149d+03  0.0  0.0  -.2536d+01 ...
    0.0  0.0  -.2701d+03  0.0;
    0.0  0.0  0.0  0.0  -.5302d+05  0.0  0.0  -.1816d+04  0.0  0.0 ...
    -.1790d+02  0.0  0.0  -.6053d+03]
```

```
bg=[0.0  0.0;
    0.0  0.0;
    0.0  0.0;
    0.0  0.0;
    0.0  0.0;
    0.0  0.0;
    0.0  0.0;
    0.0  0.0;
    0.0  0.0;
    0.0  0.0;
    0.0  0.0;
    .1479d+04  0.0;
    0.0  .1491d+04;
    0.0  .5308d+05]

cg=[1.0  0.0  0.0  0.0  0.0  0.0  0.0  0.0  0.0  0.0  0.0  0.0  0.0  0.0;
    0.0  1.0  0.0  0.0  0.0  0.0  0.0  0.0  0.0  0.0  0.0  0.0  0.0  0.0]


dg=zeros(2)
pause
disp('   ')
disp('    Balanced realization of the X-29 state space representation')
disp('   ,
[agbl,bgbl,cgbl,g,t]=obalreal(ag,bg,cg)
ag=agbl; bg=bgbl; cg=cgbl;
disp('   ')
disp('     Calculate the poles and transmission zeros of the balanced open')
disp('     loop plant')
disp('   ')
poleg=eig(ag),  tzerog=tzero(ag,bg,cg,dg)
disp('   ')
disp('   ')
disp('     Determine determine the condition number of ag')
disp('   ')
disp('   ')
condag=cond(ag),  rcondag=rcond(ag)
disp('   ')
disp('   ')
pause
disp('   ')
```

```
disp('                    << Design Specifications >>  ')
disp('    ')
disp('      1). Robustness Spec. : -40 dB roll-off, -20 db @ 100 Rad/Sec.')
disp('          Associated Weighting:')
disp('    ')
disp('                      -1       1000 ')
disp('                W3(s) =   ------ * I       (fixd)')
disp('                                 2     2x2')
disp('                               s       ')
disp('    ')
disp('    ')
disp('      2). Performance Spec.: minimizing the sensitivity function')
disp('                             as much as possible.')
disp('          Associated Weighting:')
disp('    ')
disp('                                                ')
disp('                      -1       -1 .01(100s + 1)   ')
disp('                W1(s) = Gam  * ----------- *  I')
disp('                                                  2x2')
disp('                                    (.01s + 1)     ')
disp('    ')
disp('          where "Gam" in this design is iteratively updated from 1')
w=logspace(-3,3,100);
k=1000;  mn=[2 2]; tau=0.0;
nuw3i = [0.0 k]; dnw3i = [1.0 0 0];
svw3i = bode(nuw3i,dnw3i,w); svw3i = 20*log10(svw3i);
nuw1i = [1.0 0.01]; dnw1i =[0.01 1.0];
svw1i = bode(nuw1i,dnw1i,w); svw1i = 20*log10(svw1i);
aw2=-0.001*eye(2); bw2=zeros(2); cw2=zeros(2); dw2=-0.001*eye(2);
disp('    ')
disp('    ')
disp('                   (strike a key to see the plot of the weightings ...)')
pause
semilogx(w,svw1i,w,svw3i)
grid
title('X-29 Design Specifications')
xlabel('Frequency - Rad/Sec')
ylabel('1/W1 & 1/W3 - db')
text(.01,0,'1/W1(s)')
text(.5,100,'1/W3(s)')
meta x29specs
pause
```

```
clc
disp('                        << Problem Formulation >>')
disp('    ')
disp('    Form an augmented plant P(s) with these two weighting functions:')
disp('    ')
disp('                1). Gam*W1 penalizing error signal "e"')
disp('    ')
disp('                2). W3 penalizing plant output "y"')
disp('    ')
disp('    and find a stabilizing controller F(s) such that the Hinf norm')
disp('    of TF Tylu1 is less than or equal to one, i.e.')
disp('    ')
disp('                              |Tylu1|    < or = 1,')
disp('                         F(s)        inf')
disp('    ')
disp('      where ')
disp('                             |                  -1|')
disp('                Tylu1 = | Gam*W1*(I + GF)  |   = | Gam * W1 * S   |')
disp('                             |                  -1|     |  W3 * (I - S) |')
disp('                             |  W3*GF*(I + GF) |')
disp('    ')
disp('    ')
disp('    ')
disp('                                  (strike a key to continue ...)')
pause
clc
disp('    ')
disp('    ')
disp('                                << DESIGN PROCEDURE >>')
disp('    ')
disp('              * * * * * * * * * * * * * * * * * * * * * * * * * * * * * *')
disp('              *    [Step 1]. Do plant augmentation (run AUGMENT.M or    *')
disp('              *              AUGX29.M)                                    *')
disp('              *                                                           *')
disp('              *    [Step 2]. Balance the augmented plant for better     *')
disp('              *              numerical condition if necessary             *')
disp('              *                                                           *')
disp('              *    [Step 3]. Do Hinf synthesis with "Gam" = 1           *')
disp('              *                                                           *')
disp('              *    [Step 4]. Redo the plant augmentation for a          *')
disp('              *              higher "Gam" and rerun HINF.M                *')
disp('              * * * * * * * * * * * * * * * * * * * * * * * * * * * * * *')
disp('    ')
disp('    ')
disp('                                  (strike a key to continue ...)')
pause
clc
disp('    ')
disp('    ')
disp('    ')
```

```
disp('           Assign the cost coefficients "Gam" with Gam=1 ')
disp('   ')
disp('           serving as the baseline design ....')
gama=[12.5];
ngama=length(gama);
for i=1:ngama
Gam=gama(1,i)
k=1000
disp('   ')
disp('            ------------------------------------------------------')
disp('             augment    % Plant augmentation of the X-29 dynamics')
disp('            ------------------------------------------------------')
disp('   ')
disp('   ')
augx29
disp('   ')
disp('   ')
disp('                                  (strike a key to continue ...)')
pause
clc
disp('   ')
disp('   ')
%disp('     Do state space balancing on the augmented plant if needed')
%disp('   ')
%disp('   ')
%[abal,bbal,cbal,g,t]=obalreal(A,[B1 B2],[C1;C2])
%A=abal, B1=bbal(:,1:2), B2=bbal(:,3:4), C1=cbal(1:6,:), C2=cbal(7:8,:)
disp('   ')
disp('   ')
disp('    The transmission zeros, poles and condition number of the augmented')
disp('    plant follow.  In addition, determine if (A,B1) & (A,B2) are ')
disp('    stabilizable and if (C1,A) & (C2,A) are detectable.')
disp('   ')
disp('   ')
tzeroaug=tzero(A,[B1 B2],[C1;C2],[D11 D12;D21 D22]), poleaugA=eig(A)
condaugA=cond(A), rcondaugA=rcond(A)
eps=eps
toldef=10*max(size(A))*norm(A,1)*eps
tol=100*eps*norm([A B1])
[A1c,B1c,C1c,t,k]=ctrbf(A,B1,C1,tol)
tol=100*eps*norm([A B2])
[A2c,B2c,C2c,t,k]=ctrbf(A,B2,C2,tol)
tol=100*eps*norm([A;C1])
[A1o,B1o,C1o,t,k]=obsvf(A,B1,C1,tol)
tol=100*eps*norm([A;C2])
[A2o,B2o,C2o,t,k]=obsvf(A,B2,C2,tol)
pause
disp('   ')
disp('   ')
```

```
disp('    ------------------------------------------------------------')
disp('     hinf     % Running script file HINF.M for Hinf optimization')
disp('    ------------------------------------------------------------')
aretype='Schur'
hinf
disp('   ')
disp('   ')
disp('                                    (strike a key to continue ...)')
clear functions
pause
disp('   ')
disp('   ')
disp('    State space representation of the full order controller')
disp('    (acp, bcp, ccp, dcp) with its poles and condition number')
disp('   ')
acp,bcp,ccp,dcp
polec=eig(acp)
condacp=cond(acp)
disp('   ')
disp('    Minimal realization of the controller')
disp('   ')
toldef=10*max(size(acp))*norm(acp,1)*eps
tol=100*eps*norm([acp bcp;ccp dcp])
[acpm,bcpm,ccpm,dcpm]=minreal(acp,bcp,ccp,dcp)
disp('   ')
disp('    Balanced realization & model reduction of the minimal controller')
disp('   ')
[acpbl,bcpbl,ccpbl,g,t]=obalreal(acpm,bcpm,ccpm)
elim=[10]
[acpr,bcpr,ccpr,dcpr]=modred(acpbl,bcpbl,ccpbl,dcpm,elim)
disp('   ')
disp('    Poles, controllability, observability, and condition of the ')
disp('    balanced, reduced order controller')
disp('   ')
poleacpr=eig(acpr)
tol=100*eps*norm([acpr bcpr])
[acpc,bcpc,ccpc,t,k]=ctrbf(acpr,bcpr,ccpr,tol)
tol=100*eps*norm([acpr;ccpr])
[acpo,bcpo,ccpo,t,k]=obsvf(acpr,bcpr,ccpr,tol)
condacpr=cond(acpr),  rcondacpr=rcond(acpr)
acp=acpr; bcp=bcpr; ccp=ccpr; dcp=dcpr;
disp('   ')
disp('    CLTF Tylul (acl, bcl, ccl, dcl) and its poles (reduced order)')
[acl,bcl,ccl,dcl]=lftf(sysp,dimp,acp,bcp,ccp,dcp)
polet=eig(acl)
pause
disp('   ')
disp('   ')
```

```
pltopt          % Preparing singular values for plotting
end
disp('   ')
disp('   ')
disp('                                    (strike a key to continue ...)')
pause
disp('   ')
disp('   ')
disp('    Open loop state space representation of controller/plant series')
disp('   ')
[algf,blgf,clgf,dlgf]=series(acp,bcp,ccp,dcp,ag,bg,cg,dg)
disp('   ')
disp('   ')
disp('                                    (strike a key to continue ...)')
pause
disp('   ')
disp('   ')
disp('    Closed loop state space representation of controller/plant series,')
disp('    controllability, observability, and condition number of the closed')
disp('    loop acgf matrix. ')
disp('   ')
disp('   ')
[acgf,bcgf,ccgf,dcgf]=feedbk(algf,blgf,clgf,dlgf,2)
tol=100*eps*norm([acgf bcgf])
[acgfc,bcgfc,ccgfc,t,k]=ctrbf(acgf,bcgf,ccgf,tol)
tol=100*eps*norm([acgf;ccgf])
[acgfo,bcgfo,ccgfo,t,k]=obsvf(acgf,bcgf,ccgf,tol)
condacgf=cond(acgf)
disp('   ')
disp('   ')
disp('                                    (strike a key to continue ...)')
pause
disp('   ')
disp('    Poles of the closed loop system')
disp('   ')
polcl=eig(acgf)
end
```

```
% augx29.m
% Plant Augmentation for the X-29 H2 and Hinf problem as W3 is not a
% proper transfer function.  Includes contingency for adding W2 to
% ensure d12 is full column rank.  This script file is designed for
% the X-29 system without theta as a state, ie, 2 inputs & 2 outputs.
% This script file is a modified version of the aughimat.m M-file taken
% from the Matlab Robust-Control Tool Box [Ref 7].
disp('   ')
disp('   ')
disp('                 << Plant Augmentation >>')
Gam=gama(1,i)
%Gam = input('            Input the cost coefficient "Gam" = ');
cgb = 1/k*[cg(1,:)*ag*ag;cg(2,:)*ag*ag*ag*tau+cg(2,:)*ag*ag]
dgb = 1/k*[cg(1,:)*ag*bg;cg(2,:)*ag*ag*bg*tau]
nw1 = Gam*[dnw1i;0 0;0 0;dnw1i]
dw1 = nuw1i
sysw2=[aw2 bw2;cw2 dw2]; xw2=2;
[A,B1,B2,C1,C2,D11,D12,D21,D22]=augx29p1(ag,bg,cg,cgb,dg,dgb,nw1,dw1,sysw2,xw2
,mn)
disp('   ')
disp('     - - - State-Space (A,B1,B2,C1,C2,D11,D12,D21,D22) is ready for')
disp('           the Small-Gain problem - - -')
%
% ------ End of AUGX29.M ----- % ^Z
```

```
%augx29pl.m
function
[a,b1,b2,c1,c2,d11,d12,d21,d22]=augx29pl(ag,bg,cga,cgb,dga,dgb,num,den,sys,x,mn)
%
% [A,B1,B2,C1,C2,D11,D12,D21,D22]=AUGX29PL(AG,BG,CG,CGB,DG,DGB,NUM,DEN,SYS,X,MN)
%     produces the augmented plant for the X-29 h2 and hinf problem for
%     an improper W3 weighting and W2 added to make d12 full column rank.
%     This script file is a modified version of the augpl.m function taken
%     from the Matlab Robust-Control Tool Box [Ref 7].
%
%        Weighted Plant :
%              .
%            Xg = Ag Xg + Bg Ug
%
%          |Yga| = |Cga| Xg + |Dga| Ug
%          |Ygb|   |Cgb|       |Dgb|
%
%        Weighting W1 :                    Weighting W2 :
%           .                                 .
%           Xw1 = Aw1 Xw1 + Bw1 Uw1           Xw2 = Aw2 Xw2 + Bw2 Uw2
%
%           Yw1 = Cw1 Xw1 + Dw1 Uw1           Yw2 = Cw2 Xw2 + Dw2 Uw2
%
%        Over all augmented plant :
%           .
%          |Xg |   | Ag       0       0 | |Xg |   |0    Bg     | |U1|
%          | . | = |                    | |Xw1| + |            | |U2|
%          |Xw1|   |-Bw1Cga   Aw1     0 | |Xw2|   |Bw1 -Bw1Dga|
%          | . |   |                    |           |          |
%          |Xw2|   |  0       0     Aw2 |           |0    Bw2  |
%
%          |Y1a|   |-Dw1Cga   Cw1     0 | |Xg |   |Dw1 -Dw1Dga| |U1|
%          |Y1b|   |  0         0   Cw2 | |Xw1|   |0     Dw2 | |U2=Ug|
%          |Y1c| = | Cgb        0     0 | |Xw2| + |0     Dgb |
%          |Y2 |   |-Cga        0     0 |         |I    -Dga |


% State Space of Weighting W1 & W2:
%
[aw1,bw1,cw1,dw1] = tfm2ss(num,den,mn(1),mn(2))
[aw2,bw2,cw2,dw2] = sys2ss(sys,x)
%
% State Space of Augmented Plant :
%
% ----- A matrix :
%
[rag,cag] = size(ag);
[raw1,caw1] = size(aw1);
[raw2,caw2] = size(aw2);
a = [ag zeros(rag,caw1) zeros(rag,caw2);-bw1*cga aw1 zeros(raw1,caw2);
     zeros(raw2,cag) zeros(raw2,caw1) aw2];
```

```
%
% ----- B matrix :
%
[rbg,cbg] = size(bg);
[rbw1,cbw1] = size(bw1);
[rbw2,cbw2] = size(bw2);
b1 = [zeros(rbg,cbw1);bw1;zeros(rbw2,cbw1)];
b2 = [bg;-bw1*dga;bw2];
%
% ----- C matrix :
%
[rcgb,ccgb] = size(cgb);
[rcw1,ccw1] = size(cw1);
[rcw2,ccw2] = size(cw2);
c1 = [-dw1*cga cw1 zeros(rcw1,ccw2);zeros(rcw2,ccgb) zeros(rcw2,ccw1) cw2;
      cgb zeros(rcgb,ccw1) zeros(rcgb,ccw2)];
[rcga,ccga] = size(cga);
c2 = [-cga zeros(rcga,ccw1) zeros(rcga,ccw2)];
%
% ----- D matrix :
%
[rdgb,cdgb] = size(dgb);
[rdw1,cdw1] = size(dw1);
[rdw2,cdw2] = size(dw2);
d11 = [dw1;zeros(rdw2,cdw1);zeros(rdgb,cdw1)];
d12 = [-dw1*dga;dw2;dgb];
[rdga,cdga] = size(dga);
d21 = eye(rdga);
d22 = -dga;
%
% ------ End of AUGX29PL.M ----  %
```

```
%x29analy.m
diary x29analy.dat
format short e
disp('    ')
disp('    ')
disp('    This script file analyzes the results of Hinf synthesis of the')
disp('    X-29 MIMO model by plotting resultant system return difference')
disp('    singular values, calculating the closed loop poles/zeros,and ')
disp('    mak ng Bode plots')
disp('    ')
disp('    ')
disp('    The unaugmented state space plant representation')
disp('    ')
disp('    ')
ag,bg,cg,dg
disp('    ')
disp('    ')
pause
disp('    State space representation of the controller')
disp('    ')
disp('    ')
acp,bcp,ccp,dcp
disp('    ')
disp('    ')
pause
disp('    Open loop state space representation of controller/')
disp('    plant series')
disp('    ')
disp('    ')
algf,blgf,clgf,dlgf
[alfg,blfg,clfg,dlfg]=series(ag,bg,cg,dg,acp,bcp,ccp,dcp)
disp('    ')
disp('    ')
disp('    Compute singular value plot of return difference matrices')
disp('    ')
disp('    ')
w=logspace(-3,3,100);
svg=sigma(ag,bg,cg,dg,3,w);  svg=20*log10(svg);
semilogx(w,svg)
title('X-29 SV PLOT (I + G)')
xlabel('FREQUENCY - rad/sec')
ylabel('SV - dB')
grid
meta x29sv1
pause
svgf=sigma(algf,blgf,clgf,dlgf,3,w); svgf=20*log10(svgf);
semilogx(w,svgf)
title('X-29 SV PLOT (I + GF)');
xlabel('FREQUENCY - rad/sec')
ylabel('SV - dB')
grid
meta x29sv2
```

```
pause
svfg=sigma(alfg,blfg,clfg,dlfg,3,w);  svfg=20*log10(svfg);
semilogx(w,svfg)
title('X-29 SV PLOT (I + FG)')
xlabel('FREQUENCY - rad/sec')
ylabel('SV - dB')
grid
meta x29sv3
pause
svgf=sigma(algf,blgf,clgf,dlgf,4,w); svgf=20*log10(svgf);
semilogx(w,svgf)
title('X-29 SV PLOT (I + inv(GF))')
xlabel('FREQUENCY - rad/sec')
ylabel('SV - dB')
grid
meta x29sv4
pause
svfg=sigma(alfg,blfg,clfg,dlfg,4,w);  svfg=20*log10(svfg);
semilogx(w,svfg)
title('X-29 SV PLOT (I + inv(FG))')
xlabel('FREQUENCY - rad/sec')
ylabel('SV - dB')
grid
meta x29sv5
pause
svloop=sigma(algf,blgf,clgf,dlgf,1,w); svloop=20*log10(svloop);
semilogx(w,svloop)
title('X-29 SV PLOT (GF)')
xlabel('FREQUENCY - rad/sec')
ylabel('SV - dB')
grid
meta x29sv6
pause
disp('    ')
disp('    ')
disp('    Closed loop state space representation of controller/plant series')
disp('    ')
disp('    ')
acgf,bcgf,ccgf,dcgf
tzerocgf=tzero(acgf,bcgf,ccgf,dcgf)
disp('    ')
disp('    ')
pause
```

```
disp('    Poles and zeros of the closed loop controller/plant system ')
disp('    (acgf, bcgf, ccgf, dgcf) ')
disp('    ')
disp('    ')
disp('    output alpha/q vs input 1 ')
disp('    ')
[z,p,k]=ss2zp(acgf,bcgf,ccgf,dcgf,1)
pause
disp('    ')
disp('    output alpha/q vs input 2 ')
disp('    ')
[z,p,k]=ss2zp(acgf,bcgf,ccgf,dcgf,2)
pause
disp('    ')
disp('    ')
disp('    Open loop Bode plots of outputs vs inputs')
disp('    ')
disp('    ')
[mag1,phase1]=bode(algf,blgf,clgf,dlgf,1,w); mag1=20*log10(mag1);
[mag2,phase2]=bode(algf,blgf,clgf,dlgf,2,w); mag2=20*log10(mag2);
semilogx(w,mag1(:,1))
title('X-29 OPEN LOOP BODE PLOT INPUT 1 / alpha  (GF)')
xlabel('FREQUENCY - rad/sec')
ylabel('GAIN - dB')
grid
meta x29bode1
pause
semilogx(w,mag1(:,2))
title('X-29 OPEN LOOP BODE PLOT INPUT 1 / q  (GF)')
xlabel('FREQUENCY - rad/sec')
ylabel('GAIN - dB')
grid
meta x29bode2
pause
semilogx(w,mag2(:,1))
title('X-29 OPEN LOOP BODE PLOT INPUT 2 / alpha  (GF)')
xlabel('FREQUENCY - rad/sec')
ylabel('GAIN - dB')
grid
meta x29bode3
pause
semilogx(w,mag2(:,2))
title('X-29 OPEN LOOP BODE PLOT INPUT 2 / q  (GF)')
xlabel('FREQUENCY - rad/sec')
ylabel('GAIN - dB')
grid
meta x29bode4
disp('    ')
disp('    ')
```

```
disp('    Closed loop Bode plots of outputs vs inputs')
disp('    ')
disp('    ')
[mag1,phase1]=bode(acgf,bcgf,ccgf,dcgf,1,w); mag1=20*log10(mag1);
[mag2,phase2]=bode(acgf,bcgf,ccgf,dcgf,2,w); mag2=20*log10(mag2);
semilogx(w,mag1(:,1))
title('X-29 CLOSED LOOP BODE PLOT INPUT 1 / alpha  ')
xlabel('FREQUENCY - rad/sec')
ylabel('GAIN - dB')
grid
meta x29bode5
pause
semilogx(w,mag1(:,2))
title('X-29 CLOSED LOOP BODE PLOT INPUT 1 / q  ')
xlabel('FREQUENCY - rad/sec')
ylabel('GAIN - dB')
grid
meta x29bode6
pause
semilogx(w,mag2(:,1))
title('X-29 CLOSED LOOP BODE PLOT INPUT 2 / alpha  ')
xlabel('FREQUENCY - rad/sec')
ylabel('GAIN - dB')
grid
meta x29bode7
pause
semilogx(w,mag2(:,2))
title('X-29 CLOSED LOOP BODE PLOT INPUT 2 / q  ')
xlabel('FREQUENCY - rad/sec')
ylabel('GAIN - dB')
grid
meta x29bode8
pause
end
```

```
%x29resp.m
diary x29resp.dat
format short e
disp('    ')
disp('    ')
disp('    This script file is designed to calculate and plot the time')
disp('    response of the augmented X-29 (controller/plant closed loop')
disp('    series) to a 1 degree / 1 second step input from each of')
disp('    the two inputs separately.')
disp('    ')
disp('    ')
disp('    Setting up the time vectors')
disp('    ')
time=[0:0.01:4]
%stas=[1 0 0 0 0;0 1 0 0 0;0 0 1 0 0;0 0 0 1 0;0 0 0 0 1]
%ccgfwc=[zeros(5,18) stas zeros(5,6)]
%dcgfwc=zeros(5,2)
stas=[1 0 0 0 0 0 0 0;0 1 0 0 0 0 0 0;0 0 1 0 0 0 0 0;0 0 0 1 0 0 0 0;...
0 0 0 0 1 0 0 0;0 0 0 0 0 1 0 0;0 0 0 0 0 0 1 0;0 0 0 0 0 0 0 1]
ccgfwc=[zeros(8,15) stas zeros(8,6)]
dcgfwc=zeros(8,2)
disp('    ')
disp('    Plotting alpha, q, dc, df, ds, dcdot, dfdot, and dsdot')
disp('    responses to a 0.01745 rad / 1 second step from input one')
disp('    ')
u=[0.01745*ones(1,101) zeros(1,300);zeros(1,401)]'
[y]=lsim(acgf,bcgf,ccgfwc,dcgfwc,u,time)
%[y]=lsim(acgf,bcgf,ccgf,dcgf,u,time)
plot(time,y(:,1))
title('X-29 alpha RESPONSE TO 0.01745 rad / 1 sec STEP (INPUT 1)')
xlabel('TIME - sec')
ylabel('radians')
grid
meta x29rsp11
pause
plot(time,y(:,2))
title('X-29 q RESPONSE TO 0.01745 rad / 1 sec STEP (INPUT 1)')
xlabel('TIME - sec')
ylabel('radians/second')
grid
meta x29rsp12
pause
plot(time,y(:,3))
title('X-29 DC FOR 0.01745 rad / 1 sec STEP (INPUT 1)')
xlabel('TIME - sec')
ylabel('radians')
grid
meta x29rsp13
pause
```

```
plot(time,y(:,4))
title('X-29 DF FOR 0.01745 rad / 1 sec STEP (INPUT 1)')
xlabel('TIME - sec')
ylabel('radians')
grid
meta x29rsp14
pause
plot(time,y(:,5))
title('X-29 DS FOR 0.01745 rad / 1 sec STEP (INPUT 1)')
xlabel('TIME - sec')
ylabel('radians')
grid
meta x29rsp15
pause
plot(time,y(:,6))
title('X-29 DCDOT FOR 0.01745 rad / 1 sec STEP (INPUT 1)')
xlabel('TIME - sec')
ylabel('radians/second')
grid
meta x29rsp16
pause
plot(time,y(:,7))
title('X-29 DFDOT FOR 0.01745 rad / 1 sec STEP (INPUT 1)')
xlabel('TIME - sec')
ylabel('radians/second')
grid
meta x29rsp17
pause
plot(time,y(:,8))
title('X-29 DSDOT FOR 0.01745 rad / 1 sec STEP (INPUT 1)')
xlabel('TIME - sec')
ylabel('radians/second')
grid
meta x29rsp18
pause
disp('    ')
disp('    Plotting alpha, q, dc, df, ds, dcdot, dfdot, and dsdot')
disp('    responses to a 0.01745 rad / 1 second step from input two')
disp('    ')
u=[zeros(1,401);0.01745*ones(1,101) zeros(1,300)]'
[y]=lsim(acgf,bcgf,ccgfwc,dcgfwc,u,time)
%[y]=lsim(acgf,bcgf,ccgf,dcgf,u,time)
plot(time,y(:,1))
title('X-29 alpha RESPONSE TO 0.01745 rad / 1 sec STEP (INPUT 2)')
xlabel('TIME - sec')
ylabel('radians')
grid
meta x29rsp21
pause
```

```
plot(time,y(:,2))
title('X-29 q RESPONSE TO 0.01745 rad / 1 sec STEP (INPUT 2)')
xlabel('TIME - sec')
ylabel('radians/second')
grid
meta x29rsp22
pause
plot(time,y(:,3))
title('X-29 DC FOR 0.01745 rad / 1 sec STEP (INPUT 2)')
xlabel('TIME - sec')
ylabel('radians')
grid
meta x29rsp23
pause
plot(time,y(:,4))
title('X-29 DF FOR 0.01745 rad / 1 sec STEP (INPUT 2)')
xlabel('TIME - sec')
ylabel('radians')
grid
meta x29rsp24
pause
plot(time,y(:,5))
title('X-29 DS FOR 0.01745 rad / 1 sec STEP (INPUT 2)')
xlabel('TIME - sec')
ylabel('radians')
grid
meta x29rsp25
pause
plot(time,y(:,6))
title('X-29 DCDOT FOR 0.01745 rad / 1 sec STEP (INPUT 2)')
xlabel('TIME - sec')
ylabel('radians/second')
grid
meta x29rsp26
pause
plot(time,y(:,7))
title('X-29 DFDOT FOR 0.01745 rad / 1 sec STEP (INPUT 2)')
xlabel('TIME - sec')
ylabel('radians/second')
grid
meta x29rsp27
pause
plot(time,y(:,8))
title('X-29 DSDOT FOR 0.01745 rad / 1 sec STEP (INPUT 2)')
xlabel('TIME - sec')
ylabel('radians/second')
grid
meta x29rsp28
end
```

```
%x29schmr.m
diary x29schmr.dat
format short e
disp('    ')
disp('    ')
disp('    This script file employs Schur Model Reduction ')
disp('    to reduce the order of the minimal, balanced hinf controller.  ')
disp('    The reduced order controller is then combined in series with the ')
disp('    balanced X-29 plant.  The reduced order model and minimal, balanced')
disp('    model SV Bode plots are compared and the error system plotted.')
disp('    Additionally, the reduced order controller/balanced plant series')
disp('    is compared with the minimal, balanced controller/plant series.')
disp('    ')
disp('    ')
disp('    State space representation of the minimal, balanced hinf controller')
disp('    ')
acp,bcp,ccp,dcp
poleacp=eig(acp)
condacp=cond(acp)
disp('    ')
disp('    ')
disp('   Schur Model Reduction of the hinf controller')
disp('    ')
[acph,bcph,ccph,dcph,totbnd,hsv]=schmr(acp,bcp,ccp,dcp,1,10)
poleacph=eig(acph)
condacph=cond(acph)
disp('    ')
disp('   Computing the SV Bode plot of the minimal & reduced order controllers')
disp('    ')
w=logspace(-3,3,100);
svcp=sigma(acp,bcp,ccp,dcp,1,w); svcp=20*log10(svcp);
svcph=sigma(acph,bcph,ccph,dcph,1,w); svcph=20*log10(svcph);
[acpher,bcpher,ccpher,dcpher]=addss(acp,bcp,ccp,dcp,acph,bcph,-ccph,-dcph);
sver=sigma(acpher,bcpher,ccpher,dcpher,1,w); sver=20*log10(sver);
totbnd=20*log10(totbnd)*ones(w);
semilogx(w,svcp)
title('15th ORDER X-29 CONTROLLER')
xlabel('FREQUENCY - rad/sec')
ylabel('SV - dB')
grid
meta x29schr1
pause
semilogx(w,svcp,w,svcph)
title('10th & 15th ORDER X-29 CONTROLLERS')
xlabel('FREQUENCY - rad/sec')
ylabel('SV - dB')
grid
meta x29schr2
pause
```

```
semilogx(w,totbnd,w,sver)
title('10th ORDER X-29 CONTROLLER ERROR & ERROR BOUND')
xlabel('FREQUENCY - rad/sec')
ylabel('SV - dB')
text(.02,6,'error bound')
grid
meta x29schr3
pause
disp('    ')
disp('   State space representation of the minimal, balanced controller/plant')
disp('    series and ROM controller/balanced plant series (open loop)')
disp('    ')
algf,blgf,clgf,dlgf
polealgf=eig(algf)
condalgf=cond(algf)
[algfrc,blgfrc,clgfrc,dlgfrc]=series(acph,bcph,ccph,dcph,ag,bg,cg,dg)
polealgfrc=eig(algfrc)
condalgfrc=cond(algfrc)
disp('    ')
disp('   Computing the SV Bode plot of the minimal, balanced controller/plant')
disp('    series and the ROM controller/balanced plant series.')
disp('    ')
svlgf=sigma(algf,blgf,clgf,dlgf,1,w); svlgf=20*log10(svlgf);
svrc=sigma(algfrc,blgfrc,clgfrc,dlgfrc,1,w); svrc=20*log10(svrc);
[algfer,blgfer,clgfer,dlgfer]=addss(algf,blgf,clgf,dlgf,algfrc,blgfrc,...
-clgfrc,-dlgfrc);
svlgfer=sigma(algfer,blgfer,clgfer,dlgfer,1,w); svlgfer=20*log10(svlgfer);
semilogx(w,svlgf,w,svrc)
title('10th & 15th ORDER X-29 CONTROLLERS IN SERIES WITH X-29 PLANT')
xlabel('FREQUENCY - rad/sec')
ylabel('SV - dB')
grid
meta x29schr4
pause
semilogx(w,svlgfer)
title('10th ORDER X-29 CONTROLLER/PLANT SERIES ERROR')
xlabel('FREQUENCY - rad/sec')
ylabel('SV - dB')
grid
meta x29schr5
end
```

APPENDIX B

X-29 MODEL STATE SPACE REALIZATIONS

Open loop state space representation of the uncompensated X-29 model.

ag =

Columns 1 through 6

-4.1810e-01	9.9600e-01	-2.2690e-02	-1.2130e-01	-1.9480e-02	-9.4930e-04
5.4740e+00	-3.4240e-01	2.5850e+00	-1.3860e+00	-1.0560e+00	3.8980e-03
0	0	0	0	0	1.0000e+00
0	0	0	0	0	0
0	0	0	0	0	0
0	0	0	0	0	0
0	0	0	0	0	0
0	0	0	0	0	0
0	0	0	0	0	0
0	0	0	0	0	0
0	0	0	0	0	0
0	0	-1.4790e+03	0	0	-1.1430e+02
0	0	0	-1.4910e+03	0	0
0	0	0	0	-5.3020e+04	0

Columns 7 through 12

4.4270e-05	-6.7120e-05	1.4510e-06	-2.1620e-05	-3.5400e-06	0
-1.1640e-02	-6.3970e-03	-2.5090e-04	-5.3620e-04	-2.9120e-04	0
0	0	0	0	0	0
1.0000e+00	0	0	0	0	0
0	1.0000e+00	0	0	0	0
0	0	1.0000e+00	0	0	0
0	0	0	1.0000e+00	0	0
0	0	0	0	1.0000e+00	0
0	0	0	0	0	1.0000e+04
0	0	0	0	0	0
0	0	0	0	0	0
0	0	-2.5290e+00	0	0	-2.6970e+02
-1.1490e+02	0	0	-2.5360e+00	0	0
0	-1.8160e+03	0	0	-1.7900e+01	0

```
  Columns 13 through 14

            0            0
            0            0
            0            0
            0            0
            0            0
            0            0
            0            0
            0            0
            0            0
   1.0000e+04            0
            0   1.0000e+04
            0            0
  -2.7010e+02            0
            0  -6.0530e+02


bg =

            0            0
            0            0
            0            0
            0            0
            0            0
            0            0
            0            0
            0            0
            0            0
            0            0
            0            0
   1.4790e+03            0
            0   1.4910e+03
            0   5.3080e+04


cg =

  Columns 1 through 12

    1     0     0     0     0     0     0     0     0     0     0     0
    0     1     0     0     0     0     0     0     0     0     0     0

  Columns 13 through 14

    0     0
    0     0


dg =
      0     0
      0     0
```

Closed loop state space representation of the H_∞ compensated X-29, i.e., optimal-performance model.

acgf =

Columns 1 through 6

-1.0380e-02	2.5396e-04	-2.0139e-02	3.3550e-01	6.9246e-01	-7.5674e-02
-7.4356e-04	-1.0502e-02	-3.6887e-01	-2.2137e+00	-1.9108e+00	-3.3622e-01
-9.6973e-02	1.5535e-01	-2.5920e+00	-1.1063e+02	-6.1722e+01	-4.9836e+00
6.6210e-01	1.2903e+00	1.1697e+02	-1.5192e+02	-1.7331e+02	-6.7749e+01
8.7596e-01	1.1040e+00	8.0559e+01	-2.7211e+02	-3.5450e+02	-1.4092e+02
-1.0283e-01	2.6001e-01	-1.9307e+00	8.7694e+01	1.8904e+02	-8.6324e+00
1.6027e-01	3.0656e-01	9.7828e+00	-6.1279e+01	-1.1054e+02	1.4974e+01
-1.1326e-01	7.9258e-02	-5.0472e+00	5.0715e+01	8.8977e+01	-1.7586e+01
2.0666e-02	8.9411e-02	1.4269e+00	-9.0525e+00	-1.7498e+01	-1.1775e-01
-2.9553e-02	2.4729e-02	-1.2592e+00	1.3117e+01	2.2217e+01	-4.2756e+00
6.6863e-03	3.3912e-02	4.9473e-01	-2.8382e+00	-5.6200e+00	-1.2383e-01
2.6231e-03	3.0885e-03	1.3971e-01	-1.1509e+00	-2.0618e+00	2.3346e-01
6.2838e-03	4.2536e-03	3.1809e-01	-2.7681e+00	-4.8951e+00	6.4728e-01
-2.3165e-03	1.5649e-03	-1.0068e-01	1.0309e+00	1.7591e+00	-3.2588e-01
-2.9225e-04	-8.3162e-04	-1.8149e-02	1.2658e-01	2.3676e-01	-1.2454e-02
1.9047e+00	8.3656e-01	1.3368e+01	2.6068e+01	-1.0156e+01	1.7859e+01
1.6249e+00	-6.9125e+00	-8.4058e+01	-5.2856e+02	-5.2865e+02	-7.8929e+01
-5.9083e+00	7.4810e+00	8.4663e+01	6.4688e+02	7.1853e+02	6.9016e+01
-4.0509e+00	3.3677e+00	3.5998e+01	3.1630e+02	3.7254e+02	2.5569e+01
-4.2915e+00	-3.9162e-01	-1.1427e+01	4.9115e+01	1.2470e+02	-2.1801e+01
5.5297e+00	3.0377e+00	4.6432e+01	1.1967e+02	1.2039e+01	5.9368e+01
-2.4640e+00	7.1488e-01	5.2026e+00	9.6072e+01	1.3567e+02	-9.1372e-01
-9.0592e-01	-1.0399e+00	-1.4394e+01	-5.8765e+01	-3.8942e+01	-1.6421e+01
1.8418e+00	4.5560e-01	8.5033e+00	-3.1257e-01	-3.3913e+01	1.2907e+01
-2.6872e+00	-7.4178e-01	-1.3371e+01	-5.1094e+00	4.4225e+01	-1.9782e+01
4.9869e-01	1.6324e-01	2.8015e+00	2.7956e+00	-6.4631e+00	3.9870e+00
2.7973e-01	1.2875e-01	2.0369e+00	4.2538e+00	-1.0900e+00	2.6956e+00
-1.8133e-01	9.1365e-02	8.6801e-01	9.8691e+00	1.2627e+01	4.1132e-01
3.7460e-02	1.4831e-02	2.4260e-01	3.9552e-01	-3.1035e-01	3.3121e-01

Columns 7 through 12

7.3362e-02	1.0724e-01	5.6964e-03	-3.1043e-02	-2.5046e-03	2.2455e-03
-4.7184e-01	1.3951e-01	9.9626e-02	2.1029e-02	-3.6276e-02	4.2633e-03
-7.9436e+00	4.4151e+00	1.8861e+00	-9.1523e-02	-6.9471e-01	1.1167e-01
-7.2469e+01	-8.9555e+00	1.2570e+01	1.0305e+01	-4.3749e+00	4.5774e-02
-1.0508e+02	-4.8144e+01	1.3934e+01	2.2625e+01	-4.6125e+00	-6.6097e-01
-1.4401e+01	1.6726e+01	4.4932e+00	-1.8884e+00	-1.6597e+00	3.6889e-01
-8.7251e+01	-3.1218e+01	3.5283e+01	1.7517e+01	-1.0706e+01	5.6280e-01
8.7848e+01	-8.6275e+01	-3.9404e+01	3.9886e+01	1.2111e+01	-3.9614e+00
-3.6523e+01	2.3802e+01	-2.8890e+01	-7.8925e+00	2.3488e+01	-2.9093e+00
1.8198e+01	-4.9880e+01	1.1589e+01	-5.9065e+01	8.0195e-01	6.3343e+00
-1.0989e+01	2.5817e+00	-2.3453e+01	5.7327e+00	-3.5512e+01	1.2254e+01
-2.6019e+00	3.0928e+00	-3.2759e+00	7.3988e+00	-1.2501e+01	-9.3120e+00
-5.6900e+00	7.9380e+00	-6.4217e+00	2.0670e+01	-2.1244e+01	-6.7622e+01
1.5521e+00	-3.5151e+00	8.8043e-01	-9.0745e+00	2.0510e+00	1.3813e+01
3.7429e-01	-2.5131e-01	6.0387e-01	-6.0252e-01	2.0077e+00	2.4844e+00
1.1270e+01	-1.5754e+01	-4.6012e+00	2.0579e+00	1.7023e+00	-3.8322e-01
-1.5310e+02	3.9986e+01	3.2641e+01	8.8556e+00	-1.1758e+01	1.2624e+00
1.8002e+02	-2.1721e+01	-3.4040e+01	-1.5764e+01	1.2173e+01	-9.1123e-01
8.5846e+01	-2.5523e+00	-1.4893e+01	-9.1686e+00	5.2950e+00	-2.5765e-01
6.4678e+00	2.5033e+01	3.2072e+00	-6.0269e+00	-1.2489e+00	5.5221e-01
4.5711e+01	-5.0002e+01	-1.5278e+01	5.4075e+00	5.9970e+00	-1.2395e+00
2.3763e+01	7.7899e+00	-2.6644e+00	-4.3353e+00	9.1071e-01	1.2121e-01
-1.9057e+01	1.1990e+01	5.2666e+00	-3.8111e-01	-1.9217e+00	3.1606e-01
3.3588e+00	-1.2758e+01	-2.7551e+00	2.3189e+00	1.0341e+00	-2.9692e-01
-6.5445e+00	1.9154e+01	4.3892e+00	-3.3116e+00	-1.6422e+00	4.4927e-01
1.7603e+00	-3.7337e+00	-9.3719e-01	5.9074e-01	3.4906e-01	-8.8705e-02
1.7807e+00	-2.3549e+00	-7.0399e-01	2.9675e-01	2.6021e-01	-5.7508e-02
2.5756e+00	3.0174e-01	-3.8191e-01	-3.5512e-01	1.3415e-01	8.4243e-04
1.8703e-01	-2.9846e-01	-8.2715e-02	4.1984e-02	3.0670e-02	-7.1986e-03

Columns 13 through 18

-5.3501e-03	2.0318e-03	1.7690e-04	-9.5355e+00	3.4391e+00	4.5069e+00
9.4699e-03	3.5463e-03	-9.9307e-04	7.6335e-02	7.7386e+00	7.6895e+00
8.8814e-02	9.5436e-02	-1.5234e-02	-4.3986e+01	4.4315e+01	4.9092e+01
2.5904e+00	-1.6803e-03	-1.7911e-01	3.1638e+02	-1.0033e+02	-1.3583e+02
4.9202e+00	-6.5175e-01	-2.7845e-01	4.1820e+02	-1.9565e+02	-2.4224e+02
-1.0100e-01	3.2152e-01	-2.3626e-02	-5.2255e+01	-4.8502e+01	-4.2299e+01
5.0603e+00	4.0275e-01	-3.8818e-01	6.9366e+01	-1.1341e+02	-1.2071e+02
4.5223e+00	-3.4922e+00	1.8122e-02	-5.3946e+01	-2.1608e+01	-1.5353e+01
-3.8990e+00	-2.5071e+00	5.1219e-01	7.8527e+00	-3.4635e+01	-3.5348e+01
-2.2728e+01	6.1784e+00	9.5196e-01	-1.4194e+01	-6.7545e+00	-5.1031e+00
1.4122e+01	8.7487e+00	-1.6967e+00	2.4494e+00	-1.2916e+01	-1.3127e+01
4.9965e+01	-1.7175e+01	5.0142e-01	1.1575e+00	-1.3352e+00	-1.4601e+00
-9.5020e+01	2.1892e+01	1.0389e+01	2.8333e+00	-2.0479e+00	-2.3598e+00
6.1890e+01	-1.2681e+02	6.6685e+00	-1.1049e+00	-3.9118e-01	-2.6334e-01
9.9712e+00	-1.9078e+01	-1.4357e+02	-1.1957e-01	3.2707e-01	3.3898e-01
1.1827e-01	-3.3412e-01	2.3620e-02	-3.6424e-02	-1.9965e+00	1.5995e-01
3.4434e+00	1.0399e+00	-3.3733e-01	-1.5021e+00	-1.7400e+00	-2.6733e+00
-4.7831e+00	-7.1415e-01	3.9905e-01	-1.0712e+00	2.2889e+00	-1.4713e+01
-2.5074e+00	-1.8361e-01	1.9103e-01	-1.9232e-01	8.9650e-01	-1.5627e+01
-9.2095e-01	4.9337e-01	1.6779e-02	2.9619e-01	-3.5656e-01	-6.6464e-01
7.6436e-02	-1.0758e+00	9.7119e-02	-7.1159e-01	1.2877e+00	-8.3136e+00
-9.4065e-01	1.2001e-01	5.3684e-02	2.2932e-02	1.1616e-01	-3.8392e+00
2.2512e-01	2.7045e-01	-4.1326e-02	1.8364e-01	-3.8875e-01	3.4413e+00
2.6923e-01	-2.6170e-01	6.2769e-03	-1.5060e-01	2.4093e-01	-8.2107e-01
-3.5903e-01	3.9521e-01	-1.2770e-02	2.4407e-01	-3.8251e-01	1.4705e+00
5.5418e-02	-7.7786e-02	3.5689e-03	-5.2288e-02	7.8130e-02	-3.6707e-01
1.4788e-02	-5.0093e-02	3.7449e-03	-3.1193e-02	5.7132e-02	-3.4273e-01
-8.6209e-02	2.0978e-03	5.7673e-03	-2.4991e-03	2.0851e-02	-4.2393e-01
3.0370e-03	-6.2893e-03	3.8849e-04	-4.6699e-03	6.7562e-03	-3.6901e-02

Columns 19 through 24

-2.8169e+00	-4.4292e+00	2.5190e+00	-2.6330e-01	1.5369e-01	-1.9085e+00
-3.5970e+00	-8.8914e-02	3.6727e+00	-1.1671e+00	1.1007e+00	-4.9087e-01
-2.6254e+01	-2.0887e+01	2.5148e+01	-5.4978e+00	4.7458e+00	-1.0658e+01
8.7045e+01	1.4674e+02	-7.7029e+01	6.6623e+00	-3.1450e+00	6.2425e+01
1.4443e+02	1.9497e+02	-1.3179e+02	1.8295e+01	-1.3100e+01	8.6622e+01
1.5952e+01	-2.3194e+01	-1.8221e+01	8.6966e+00	-8.7138e+00	-6.0691e+00
6.1686e+01	3.3636e+01	-6.0354e+01	1.5222e+01	-1.3659e+01	1.9644e+01
3.2024e+00	-2.4400e+01	-5.2758e+00	4.6927e+00	-4.9571e+00	-8.1206e+00
1.7142e+01	4.1569e+00	-1.7197e+01	5.0048e+00	-4.6390e+00	3.6444e+00
1.3408e+00	-6.4030e+00	-1.8965e+00	1.3957e+00	-1.4560e+00	-2.0670e+00
6.3315e+00	1.3305e+00	-6.3686e+00	1.8791e+00	-1.7467e+00	1.2745e+00
7.6968e-01	5.5234e-01	-7.4218e-01	1.7013e-01	-1.4888e-01	2.9148e-01
1.3152e+00	1.3325e+00	-1.2364e+00	2.3270e-01	-1.9124e-01	6.3395e-01
4.1646e-02	-5.0056e-01	-8.3625e-02	8.8378e-02	-9.4238e-02	-1.6967e-01
-1.6766e-01	-6.0088e-02	1.6661e-01	-4.6050e-02	4.2216e-02	-4.2438e-02
-7.3858e-02	5.4248e-02	8.0145e-02	-3.2383e-02	3.1757e-02	9.4644e-03
1.2795e+00	4.3523e-01	-1.2763e+00	3.5565e-01	-3.2666e-01	3.1595e-01
1.5508e+01	9.3482e-01	-1.4353e+01	4.5759e+00	-4.2979e+00	2.1484e+00
-4.5349e+01	-9.8406e+00	1.0983e+02	-2.5846e+01	2.4917e+01	-1.5217e+01
-1.2548e+00	-1.5613e+01	-7.2403e+00	1.2733e+00	1.7900e+00	-1.4103e+01
-7.4415e+01	5.5042e+01	-1.8958e+02	1.4305e+02	-1.6158e+02	7.4043e+01
-2.2661e+01	-1.3867e+01	-6.3472e+01	-4.5635e+01	1.7203e+02	-5.2529e+01
1.7982e+01	-1.1310e+01	1.6003e+02	-1.0863e+02	-5.1421e+01	1.9684e+01
-2.8087e+00	1.5640e+01	-9.0324e+01	4.0505e+01	5.3125e+01	-6.7007e+01
6.0983e+00	-2.2100e+01	1.3275e+02	-4.7354e+01	-7.4804e+01	1.7661e+02
-1.7819e+00	4.1876e+00	-2.5282e+01	4.8131e+00	1.9246e+01	-3.8141e+01
-1.8477e+00	2.5316e+00	-1.7125e+01	5.4035e-01	1.4710e+01	-2.4872e+01
-2.7233e+00	-8.2321e-01	-3.6217e+00	-8.5471e+00	5.9972e+00	1.1996e+00
-1.9364e-01	3.2615e-01	-2.0869e+00	1.8733e-01	1.7541e+00	-3.2227e+00

Columns 25 through 29

7.6745e-01	3.9425e-03	-4.4244e-01	-2.4640e-01	-3.0173e-02
1.2606e+00	-2.5128e-01	-2.1089e-03	5.5342e-02	-1.8258e-02
8.1808e+00	-9.0223e-01	-2.0616e+00	-9.4110e-01	-2.0696e-01
-2.3217e+01	-5.7644e-01	1.4670e+01	8.2701e+00	9.6831e-01
-4.0969e+01	1.2770e+00	1.9437e+01	1.0498e+01	1.4301e+00
-6.7799e+00	2.2004e+00	-2.3756e+00	-1.8131e+00	-4.9158e-03
-2.0000e+01	2.8308e+00	3.2828e+00	1.1850e+00	4.3004e-01
-2.3565e+00	1.3508e+00	-2.4731e+00	-1.6762e+00	-7.2878e-02
-5.8195e+00	1.0256e+00	3.8750e-01	-1.5636e-02	1.0061e-01
-7.9439e-01	3.9001e-01	-6.4995e-01	-4.4838e-01	-1.6629e-02
-2.1598e+00	3.8825e-01	1.2241e-01	-1.9394e-02	3.6413e-02
-2.4286e-01	2.9213e-02	5.4373e-02	2.3603e-02	5.8488e-03
-3.9539e-01	3.2021e-02	1.3221e-01	6.6164e-02	1.1409e-02
-3.9883e-02	2.6004e-02	-5.0690e-02	-3.3977e-02	-1.6150e-03
5.5939e-02	-9.1366e-03	-5.7545e-03	-1.1385e-03	-1.0547e-03
2.8776e-02	-7.7507e-03	5.6167e-03	4.8600e-03	-1.7207e-04
-4.2090e-01	7.0974e-02	4.1538e-02	7.0883e-03	7.9756e-03
-4.9759e+00	9.7110e-01	6.5646e-02	-1.8196e-01	7.4508e-02
3.1196e+01	-5.9282e+00	-9.0624e-01	8.3131e-01	-4.9034e-01
5.1872e+00	1.8317e-01	-3.14[illegible]7e+00	-1.7869e+00	-2.0083e-01
-1.3929e+02	2.5207e+01	3.1780e+00	-3.8659e+00	2.0019e+00
1.0694e+02	-1.9838e+01	-1.1774e-01	4.3850e+00	-1.4247e+00
-1.0021e+02	2.2620e+01	-6.1728e-01	-5.5200e+00	1.6696e+00
5.1785e+01	-1.6217e+01	-2.1071e+01	-7.6674e+00	-2.9695e+00
-3.0613e+02	9.6944e+01	6.6540e+00	-1.9641e+01	9.3531e+00
1.0064e+02	-5.7549e+01	3.7812e+01	2.9900e+01	-7.8291e+00
7.8071e+01	-8.9044e+01	-7.2702e+01	-8.3855e+01	-8.5556e+00
-3.2832e-01	-5.9329e+00	-4.0260e+00	-1.4661e+02	1.1159e+00
9.8153e+00	-9.4011e+00	-1.7763e+01	-8.7322e+00	-1.3177e+02

```
bcgf =

  -1.0822e+01  -2.7878e+00
   6.8583e-01  -4.1887e+00
  -4.7724e+01  -2.8286e+01
   3.6012e+02   8.5027e+01
   4.7115e+02   1.4656e+02
  -6.4500e+01   2.1242e+01
   7.1903e+01   6.8206e+01
  -6.4391e+01   6.4952e+00
   6.4582e+00   1.9540e+01
  -1.7025e+01   2.2886e+00
   1.8515e+00   7.2405e+00
   1.2428e+00   8.3604e-01
   3.1364e+00   1.3847e+00
  -1.3148e+00   1.0517e-01
  -1.1379e-01  -1.8892e-01
  -2.1182e-01  -1.4546e-01
   8.7699e-01   6.0226e-01
  -7.4043e-01  -5.0848e-01
  -2.6335e-01  -1.8086e-01
   2.7014e-01   1.8552e-01
  -6.9940e-01  -4.8031e-01
   2.4769e-02   1.7010e-02
   1.8978e-01   1.3033e-01
  -1.5582e-01  -1.0700e-01
   2.3802e-01   1.6346e-01
  -4.7719e-02  -3.2771e-02
  -3.1925e-02  -2.1924e-02
  -3.5525e-03  -2.4397e-03
  -3.9408e-03  -2.7063e-03
```

```
ccgf =

  Columns 1 through 6

         0         0         0         0         0         0
         0         0         0         0         0         0

  Columns 7 through 12

         0         0         0         0         0         0
         0         0         0         0         0         0

  Columns 13 through 18

         0         0         0  -8.4999e-01  -1.5173e-01  -5.4154e-02
         0         0         0  -1.2095e-01   1.8226e+00   1.8269e+00

  Columns 19 through 24

  -3.7507e-02  -3.8748e-01   6.6203e-03   4.5526e-02  -5.1326e-02  -1.4025e-01
  -8.6488e-01  -8.4670e-02   8.7789e-01  -2.7117e-01   2.5437e-01  -1.4015e-01

  Columns 25 through 29

  -6.3435e-03   1.5178e-02  -3.9105e-02  -2.5113e-02  -1.5979e-03
   2.9992e-01  -5.7504e-02  -6.9062e-03   9.1004e-03  -4.6205e-03


dcgf =

     0     0
     0     0
```

Closed loop state space representation of the H_∞ limited-performance X-29 (unbalanced plant used in calculations).

acgflim =

Columns 1 through 6

-1.0402e-02	-5.8688e-05	-1.0935e-01	1.0846e-03	9.5729e-02	-2.1473e-02
4.7514e-05	-1.0127e-02	-2.2341e-02	2.5275e-01	7.5480e-02	-6.2276e-02
-1.0953e-01	1.7080e-02	-2.1014e+01	-2.1657e+01	2.9586e+01	-8.7074e+00
1.1830e-01	4.6756e-03	5.4776e+01	-4.9923e+01	2.0305e+01	2.4992e+01
1.0112e-01	2.5760e-02	3.0471e+01	-9.6706e+01	-7.0361e+01	5.0851e+01
-7.0719e-03	7.5703e-02	-2.4741e+00	-1.8064e+00	-2.0296e+01	-1.8520e+01
-1.1890e-02	-4.0375e-03	-4.3794e+00	9.4786e+00	1.5457e+01	3.0890e+00
3.5848e-02	-9.2905e-03	1.3787e+01	-2.9232e+01	-5.0189e+01	1.1314e+01
7.8006e-03	1.6081e-02	2.7372e+00	-6.6157e+00	-1.1414e+01	-7.6888e+00
6.9880e-03	-1.4086e-02	2.7883e+00	-5.6558e+00	-8.4502e+00	8.3607e+00
3.6963e-03	-2.3286e-03	1.4203e+00	-3.0586e+00	-4.8787e+00	1.8586e+00
9.8035e-04	-2.6757e-03	3.9874e-01	-7.6819e-01	-1.1181e+00	1.4626e+00
-9.9671e-04	-1.2236e-03	-3.6218e-01	8.6485e-01	1.4612e+00	3.7979e-01
4.9526e-04	-6.0858e-04	1.9331e-01	-4.0393e-01	-6.2616e-01	3.8745e-01
9.9360e-05	-1.1607e-04	3.8715e-02	-8.1164e-02	-1.2611e-01	7.4870e-02
0	0	0	0	0	0
0	0	0	0	0	0
0	0	0	0	0	0
0	0	0	0	0	0
0	0	0	0	0	0
0	0	0	0	0	0
0	0	0	0	0	0
0	0	0	0	0	0
0	0	0	0	0	0
0	0	0	0	0	0
0	0	0	0	0	0
-5.5647e+03	-2.5519e+03	-3.2170e+04	3.2203e+04	3.5087e+04	-1.3450e+04
-5.6119e+03	2.5455e+03	-2.7388e+04	-3.1437e+04	1.6463e+04	1.9671e+03
-1.9979e+05	9.0622e+04	-9.7503e+05	-1.1191e+06	5.8610e+05	7.0029e+04

Columns 7 through 12

-4.0275e-03	-2.6915e-02	3.4546e-03	5.3706e-04	-3.6531e-03	1.0496e-03
-2.4278e-02	5.1044e-02	2.2025e-02	-2.0440e-02	2.5551e-03	2.5566e-03
-1.7350e+00	-9.6190e+00	1.5835e+00	-1.1432e-01	-1.3381e+00	4.3285e-01
8.9719e+00	-1.8751e+01	-8.5052e+00	8.1165e+00	-9.6598e-01	-1.0186e+00
8.5586e+00	2.7161e+01	-8.5873e+00	3.9686e+00	4.1757e+00	-1.9185e+00
-1.2731e+01	1.4809e+00	1.1718e+01	-7.8909e+00	-1.2714e+00	1.6320e+00
-7.5102e+00	-1.1428e+01	1.0646e+01	-1.2192e+01	-2.8839e-01	1.8363e+00
4.9757e+01	-1.1776e+02	4.7311e+01	5.8958e+01	-2.1270e+01	-5.3409e-02
5.8087e+00	-8.6183e+01	-1.2232e+01	2.1820e+01	4.0286e-01	-3.2960e+00
8.8626e+00	-6.3838e+01	-6.7146e+00	-3.6223e+01	2.1952e+01	8.7173e+00
4.3397e+00	-2.3127e+01	-4.3150e+00	-3.3307e+01	-1.7274e+01	6.0655e+00
9.4872e-01	-7.3025e+00	3.8876e-01	-1.1983e+01	-1.1844e+01	-6.8722e+01
-1.3423e+00	6.0171e+00	2.5122e+00	2.5206e+00	7.0285e+00	1.3970e+01
5.5179e-01	-3.4240e+00	-3.5627e-01	-4.1849e+00	-4.9408e+00	-5.8083e+01
1.1123e-01	-6.8505e-01	-7.5761e-02	-8.2576e-01	-9.9156e-01	-9.0062e+00
0	0	0	0	0	0
0	0	0	0	0	0
0	0	0	0	0	0
0	0	0	0	0	0
0	0	0	0	0	0
0	0	0	0	0	0
0	0	0	0	0	0
0	0	0	0	0	0
0	0	0	0	0	0
0	0	0	0	0	0
-4.1178e+03	-7.6282e+02	3.6829e+03	-2.4198e+03	-6.5185e+02	5.9980e+02
1.9746e+03	-1.3742e+04	-1.8474e+03	2.7284e+03	-1.3132e+03	-3.8383e+01
7.0297e+04	-4.8921e+05	-6.5768e+04	9.7131e+04	-4.6750e+04	-1.3665e+03

Columns 13 through 18

8.3492e-04	-5.3511e-04	-8.1760e-05	-5.2019e+00	-1.1241e+00	0
-1.6840e-03	-4.2833e-04	-1.6786e-04	-5.0395e-01	2.3744e+00	0
2.8897e-01	-2.0766e-01	-3.3253e-02	-2.7401e+01	-7.7266e+00	0
6.5715e-01	1.7396e-01	6.7004e-02	2.9927e+01	4.7994e+00	0
-7.0494e-01	7.8492e-01	1.4255e-01	2.6073e+01	2.2229e+00	0
-1.4062e-01	-4.9365e-01	-1.1507e-01	1.2523e-01	-9.1880e+00	0
-5.8267e-01	-4.5585e-01	-1.2596e-01	-3.0793e+00	-1.5243e-01	0
7.5075e+00	-1.7408e+00	-5.7699e-02	8.7351e+00	2.9843e+00	0
1.0924e+00	8.0532e-01	2.2536e-01	2.3598e+00	-1.4722e+00	0
-6.3426e+00	-1.2524e+00	-5.5502e-01	1.3920e+00	2.0218e+00	0
9.2730e+00	-3.9489e+00	-4.7442e-01	8.6600e-01	4.6904e-01	0
-8.7804e-02	5.6209e+01	9.7762e+00	1.7759e-01	3.6550e-01	0
-1.3039e+02	1.4771e+01	1.1042e+00	-2.8039e-01	9.0399e-02	0
5.3211e+01	-4.0347e+01	-1.4513e+01	1.0853e-01	9.7591e-02	0
1.3336e+01	-1.5833e+01	-1.4561e+02	2.1926e-02	1.8874e-02	0
0	0	0	-4.1810e-01	9.9600e-01	-2.2690e-02
0	0	0	5.4740e+00	-3.4240e-01	2.5850e+00
0	0	0	0	0	0
0	0	0	0	0	0
0	0	0	0	0	0
0	0	0	0	0	0
0	0	0	0	0	0
0	0	0	0	0	0
0	0	0	0	0	0
0	0	0	0	0	0
0	0	0	0	0	0
1.1078e+01	-1.9609e+02	-4.2799e+01	3.5657e+00	1.3365e+00	-1.4790e+03
4.3911e+02	-9.0974e+01	-9.6295e-01	3.7297e+02	1.3980e+02	0
1.5632e+04	-3.2387e+03	-3.4281e+01	1.3278e+04	4.9769e+03	0

Columns 19 through 24

0	0	0	0	0	0
0	0	0	0	0	0
0	0	0	0	0	0
0	0	0	0	0	0
0	0	0	0	0	0
0	0	0	0	0	0
0	0	0	0	0	0
0	0	0	0	0	0
0	0	0	0	0	0
0	0	0	0	0	0
0	0	0	0	0	0
0	0	0	0	0	0
0	0	0	0	0	0
0	0	0	0	0	0
0	0	0	0	0	0
0	0	0	0	0	0
-1.2130e-01	-1.9480e-02	-9.4930e-04	4.4270e-05	-6.7120e-05	1.4510e-06
-1.3860e+00	-1.0580e+00	3.8980e-03	-1.1640e-02	-6.3970e-03	-2.5090e-04
0	0	1.0000e+00	0	0	0
0	0	0	1.0000e+00	0	0
0	0	0	0	1.0000e+00	0
0	0	0	0	0	1.0000e+00
0	0	0	0	0	0
0	0	0	0	0	0
0	0	0	0	0	0
0	0	0	0	0	0
0	0	0	0	0	0
0	0	-1.1430e+02	0	0	-2.5290e+00
-1.4910e+03	0	0	-1.1490e+02	0	0
0	-5.3020e+04	0	0	-1.8160e+03	0

Columns 25 through 29

0	0	0	0	0
0	0	0	0	0
0	0	0	0	0
0	0	0	0	0
0	0	0	0	0
0	0	0	0	0
0	0	0	0	0
0	0	0	0	0
0	0	0	0	0
0	0	0	0	0
0	0	0	0	0
0	0	0	0	0
0	0	0	0	0
0	0	0	0	0
0	0	0	0	0
-2.1620e-05	-3.5400e-06	0	0	0
-5.3620e-04	-2.9120e-04	0	0	0
0	0	0	0	0
0	0	0	0	0
0	0	0	0	0
0	0	0	0	0
1.0000e+00	0	0	0	0
0	1.0000e+00	0	0	0
0	0	1.0000e+04	0	0
0	0	0	1.0000e+04	0
0	0	0	0	1.0000e+04
0	0	-2.6970e+02	0	0
-2.5360e+00	0	0	-2.7010e+02	0
0	-1.7900e+01	0	0	-6.0530e+02

```
bcgflim =

   5.2019e+00   1.1241e+00
   5.0395e-01  -2.3744e+00
   2.7401e+01   7.7266e+00
  -2.9927e+01  -4.7994e+00
  -2.6073e+01  -2.2229e+00
  -1.2523e-01   9.1880e+00
   3.0793e+00   1.5243e-01
  -8.7351e+00  -2.9843e+00
  -2.3598e+00   1.4722e+00
  -1.3920e+00  -2.0218e+00
  -8.6600e-01  -4.6904e-01
  -1.7759e-01  -3.6550e-01
   2.8039e-01  -9.0399e-02
  -1.0853e-01  -9.7591e-02
  -2.1926e-02  -1.8874e-02
            0            0
            0            0
            0            0
            0            0
            0            0
            0            0
            0            0
            0            0
            0            0
            0            0
  -3.5657e+00  -1.3365e+00
  -3.7297e+02  -1.3980e+02
  -1.3278e+04  -4.9769e+03
```

```
ccgflim =

  Columns 1 through 12

     0     0     0     0     0     0     0     0     0     0     0     0
     0     0     0     0     0     0     0     0     0     0     0     0

  Columns 13 through 24

     0     0     0     1     0     0     0     0     0     0     0     0
     0     0     0     0     1     0     0     0     0     0     0     0

  Columns 25 through 29

     0     0     0     0     0
     0     0     0     0     0

 dcgflim =

     0     0
     0     0
```

REFERENCES

1. Doyle, J. C. and Stein, G., **Multivariable Feedback Design: Concepts for a Classical/Modern Synthesis**, IEEE Transactions on Automatic Control, Vol. AC-26, No. 1, pp. 4-16, February 1981.

2. Safonov, M. G., **Stability and Robustness of Multivariable Feedback Systems**, p. 68, The MIT Press, 1980.

3. Safonov, M. G., Laub, A. J., Hartman, G. L., **Feedback Properties of Multivariable Systems: The Role and use of the Return Difference Matrix**, IEEE Transactions on Automatic Control, Vol. AC-26, No. 1, pp. 47-65, February 1981.

4. McFarlane, A. G. J., **Return Difference and Return-Ratio Matrices and Their Use in Analysis and Design of Multivariable Feedback Control Systems**, Proceedings IEE, Vol. 117, No. 10, pp. 2037-2049, October 1970.

5. Lehtomaki, N. A., **Practical Robustness Measures in Multivariable Control System Analysis**, Ph.D. Dissertation, Massachusetts Institute of Technology, Cambridge, Massachusetts, May 1981.

6. Gordon, V. C., **Utilization of Numerical Optimization Techniques in the Design of Robust Multi-Input Multi-Output Control Systems**, Ph.D. Dissertation, Naval Postgraduate School, Monterey, California, September 1984.

7. Chiang, R. Y., and Safonov, M. G., **Robust-Control Toolbox, User's Guide**, pp. R4-R33, RR9, RR10-RR11, RR26-RR30, The Mathworks, Inc., June 1988.

8. Postlethwaite, I., and others, **H∞ Control System Design: A Critical Assessment**, International Federation on Automatic Control, Vol. 8, pp. 328-333, 1987.

9. Kwaakernaak, H., and Sivan, R., **Linear Optimal Control Systems**, John Wiley and Sons, Inc., 1972.

10. Alphatech, Inc., Technical Report 121, **Multivariable Stability Margins for Vehicle Flight Control Systems**, by Sandell, N., and others, December 1981.

11. Ogata, K., **Modern Control Engineering**, Prentice-Hall, Inc., 1970.

12. Safonov, M. G., and Chiang, R. Y., **CACSD Using the State Space L∞ Theory: A Design Example**, IEEE Transactions on Automatic Control, Vol. 33, No. 5, pp. 477-479, May 1988.

13. Francis, B. A., **A Course in H∞ Control Theory, Lecture Notes in Control Information Sciences**, Vol. 88, Springer-Verlag, 1987.

14. Doyle, J. C., and others, **State Space Solutions to Standard H_2 and H∞ Control Problems**, Proceedings American Control Conference, Vol. 2, pp. 1691-1696, 1988.

15. **Jane's All the World's Aircraft 1987-1988**, pp. 399-400, Jane's Information Group Limited, 1988.

INITIAL DISTRIBUTION LIST

		No. Copies
1.	Defense Technical Information Center Cameron Station Alexandria, Virginia 22304-6145	2
2.	Library, Code 0142 Naval Postgraduate School Monterey, California 93943-5002	2
3.	Chairman, Code 67 Department of Aeronautics Naval Postgraduate School Monterey, California 93943-5002	1
4.	Professor D. J. Collins Code 67Co Department of Aeronautics Naval Postgraduate School Monterey, California 93943-5002	5
5.	Professor J. P. Hauser Code 67Ha Department of Aeronautics Naval Postgraduate School Monterey, California 93943-5002	1
6.	Professor A. Schoenstadt Code 53Zh Department of Mathematics Naval Postgraduate School Monterey, California 93943-5002	1
7.	Mr. Tor W. Jensen Code 6013 Naval Air Development Center Warminster, Pennsylvania 18974	1
8.	Mr. Joe Gera NASA Dryden Flight Research Center P.O. Box 273 Mail Code OFDC Edwards, California 93523	1
9.	Mr. Thomas Momiyama AIR 931 Naval Air Systems Command Washington, D.C. 20361-0001	1

10. Mr. George Derderian 1
AIR 931E
Naval Air Systems Command
Washington, D.C. 20361-0001

11. LCDR Walt Rogers 2
AIR 546D
Naval Air Systems Command
Washington, D.C. 20361-0001